TRANSGENIC EXPRESSION OF HUMAN ALPHA-L-IDURONIDASE IN MOUSE AND CHARACTERIZATION OF THE LONG TERM PATHOPHYSIOLOGY OF MURINE ALPHA-L-IDURONIDASE DEFICIENCY

By

Christopher Spencer Russell

B.Sc., University of British Columbia, 1993

A THESIS SUBMITTED IN PARTIAL FULFILLMENT OF
THE REQUIREMENTS FOR THE DEGREE OF

DOCTOR OF PHILOSOPHY

In

THE FACULTY OF GRADUATE STUDIES

Department of Medical Genetics

We accept this thesis as conforming to the required standard

THE UNIVERSITY OF BRITISH COLUMBIA

December 2003

Abstract

Mucopolysaccharidosis type I (MPS I) is an autosomal recessive genetic disorder resulting from deficiency of alpha-L-iduronidase (IDUA), a lysosomal hydrolase required in the catabolism of heparan and dermatan sulfate glycosaminoglycans (GAGs). MPS I presents as a clinical spectrum of disease ranging from a severe multisystem disease with associated death in the first decade (Hurler syndrome) to milder forms of MPS I which are compatible with a normal lifespan (Scheie syndrome).

Towards a better understanding of MPS I, I have characterized the long term pathophysiology of murine IDUA deficiency. Skeletal manifestations represent the earliest clinical finding in MPS I mice with histologic analysis of growth plate and cortical bone revealing evidence that significant early pathology is present. Analysis of the central nervous system has revealed the novel finding of progressive neuronal degeneration within the cerebellum. In addition, brain tissue from MPS I mice show increased levels of GM_2 and GM_3 gangliosides. While persisting to adulthood and capable of mating, the IDUA deficient mouse most closely resembles severe MPS I in humans or Hurler syndrome.

While many efforts are directed towards solving the problems of long term therapeutic gene expression, it remains to be determined if gene therapy will have the desired curative effects on the host of MPS I symptoms, and, additionally, whether expression of therapeutic genes in an unregulated manner will disrupt normal cellular metabolism, *i.e.* inducing disease. I have successfully generated murine strains which have the potential to express human IDUA in a conditional transgenic approach. In addition to genetic crosses into the IDUA deficient strain to address the benefit of IDUA

expression in specific tissues at defined time points, these transgenic mice lines can provide a source of human IDUA expressing cells for use in transplantation studies. Finally, the phenotype of transgenic human IDUA expression, if any, can be determined. It is hoped that these mouse strains will be useful in determining levels, locations, and time points important to the efficacy and safety of gene therapy for MPS I.

Table of Contents

Abstract ii

Table of Contents iv

Table of Figures vii

Table of Tables ix

List of Abbreviations x

CHAPTER 1: INTRODUCTION 1

1.1 Thesis Focus and Chapter Overview 1

1.2 MPS I 4
1.2.1 Clinical Presentation of MPS I 4
1.2.2 Glycosaminoglycans and proteoglycans 7
1.2.3 Secondary storage in MPS I 12
1.2.4 The MPS family of disorders 13
1.2.5 Genetics 14
1.2.7 IDUA protein synthesis and transport to the lysosome 21

1.3 Therapies for MPS I 23
1.3.1 Rationale 23
1.3.2 MPS animal models 26
1.3.3 Bone Marrow Transplantation for MPS I in humans 29
1.3.4 Bone marrow transplantation in MPS animal models 30
1.3.5 Cellular transplantation in MPS animal models 31
1.3.6 Gene therapy for MPS I 32
1.3.7 Gene therapy in animal models of MPS disorders 33
1.3.8 Enzyme replacement therapy for human lysosomal disorders 37
1.3.9 Enzyme replacement in animal models of MPS 38
1.3.10 Generation of a murine model of MPS I 39

1.4 Thesis objectives and supporting hypotheses 45

CHAPTER 2: MATERIALS AND METHODS 46
2.1 Polymerase chain reaction 47
2.2 Preparation of the human IDUA cDNA 47
2.3 Construction of the myeloid-specific transgene constructs. (CD11B-IDUA and CD11B-reporter gene) 48
2.4 Construction of the myeloid-specific transgene constructs with a selection cassette for selection in ES cells. (CD11B-IDUA and CD11B-reporter gene) 48
2.5 Construction of a ubiquitous IDUA expressing transgene construct. (CMV-IDUA) 49
2.6 Construction of a ubiquitous IDUA expressing transgene construct with a selection cassette for selection in ES cells. (pFlox-IDUA) 50
2.7 Construction of a ubiquitous IDUA expressing transgene construct with a selection cassette for selection in ES cells. (pCAGGS-IDUA) 50
2.8 Construction of a conditional Cre regulated transgene construct with a selection cassette for selection in ES cells (pCCALL2-IRES-IDUA) 52
2.9 Histopathology 52

2.10 Radiography 53
2.11 Thin Layer Chromatography of Gangliosides 53
2.12 Colorimetric Assay of Glycosaminoglycans 54
2.13 Embryonic stem cell growth and electroporation 54
2.14 Transfection of ES cells with Cre plasmid 55
2.15 IDUA enzyme assay 55
2.16 Beta-galactosidase staining of ES cells and tissue fragments 56
2.17 Alkaline phosphatase staining of ES cells 56
2.18 Alkaline phosphatase staining ear punches and tissue fragments 57
2.19 DNA Isolation 58
2.20 Transformation 59
2.21 Southern blotting 59
2.22 Animals 59

CHAPTER 3: CHARACTERIZATION OF THE LONG TERM PATHOPHYSIOLOGY OF MURINE MPS I 61

3.1 Abstract 62

3.2 Introduction 62

3.3 Results 64
3.31 Clinical Features 64
3.32 Life span of MPS I mice 66
3.33 Growth Profiles 67
3.34 Radiographic Examination 70
3.36 Glycosaminoglycan Excretion 72
3.37 Gangliosides 73
3.38 Bone Histopathology 74
3.39 Neuropathology 77

3.4 Discussion 80

CHAPTER 4: PRONUCLEAR AND EMBRYONIC STEM CELL ATTEMPTS AT GENERATION OF MURINE TRANSGENIC LINES WITH UBIQUITOUS OR MYELOID SPECIFIC EXPRESSION OF HUMAN IDUA 89

4.1. Introduction 90
4.1.1 A model of *in utero* bone marrow transplantation 93
4.1.2 Widespread high level IDUA expression 95
4.1.3 The use of the human IDUA cDNA 97
4.1.4 The generation of transgenic mice 99

4.2 Results 103
4.2.1 Pronuclear injection approach for the generation of myeloid specific, and ubiquitous, IDUA expressing transgenic mice 103
4.2.2 Embryonic stem cell approach for the generation of myeloid specific and ubiquitous IDUA expression 111

4.3 Discussion 120

CHAPTER 5: CONDITIONAL TRANSGENIC EXPRESSION OF HUMAN ALPHA-L-IDURONIDASE IN A MURINE MODEL TO ESTABLISH EFFECTIVE AND TOLERABLE LIMITS FOR GENE THERAPY FOR MPS I 121

5.1 Introduction 122
5.1.1 Conditional transgene regulation systems 123
5.1.3 Experimental Approach 130

5.2 Results 137

5.3 Discussion 151

CHAPTER 6: SUMMARY AND CONCLUSIONS 155

6.1 Characterization of the long term pathophysiology of murine MPS I 156

6.2 Future work: 157

6.3: Generation of transgenic murine strains expressing human IDUA 157

6.4 Future work 163

REFERENCES 164

Table of Figures

Figure 1.1: Heparan sulfate exodegradation 8
Figure 1.2: Dermatan sulfate exodegradation 10
Figure 1.3: Organization of the human IDUA gene locus 15
Figure 1.4: The human IDUA cDNA 16
Figure 1.5: Endogenous and exogenous pathways for transport of lysosomal enzymes including IDUA to the lysosomes 22
Figure 1.6: Routes for the introduction of therapeutic IDUA 24
Figure 1.7: Targeted inactivation of the murine Idua gene 41
Figure 1.8: Clinical feature of Idua -/- mice at 12 weeks of age 43
Figure 1.9: Electron micrographs from 8 week old Idua -/- and control mice 44
Figure 3.1: Phenotype of MPS I mice 65
Figure 3.2: Life span of affected animals 67
Figure 3.3A: Growth curves of male Idua -/- mice relative to normals 68
Figure 3.3B: Growth curves of female Idua -/- and control mice 69
Figure 3.4: Radiographic examination of Idua -/- and control mice 70
Figure 3.5: Skulls of Idua -/- and normal male mice at 70 weeks of age 71
Figure 3.6: Glycosaminoglycan excretion in male Idua -/- and normal mice 73
Figure 3.7: Thin layer chromatogram of brain lipids 74
Figure 3.8: Proximal tibial growth plates 76
Figure 3.9: Polarized light microscopy of cortical bone samples 77
Figure 3.10: PASD staining of the Purkinje cell layer of cerebellum 79
Figure 4.1: Identity between human and murine Idua exon II 99
Figure 4.3: Embryonic stem cell approach for the generation of transgenic mice 101
Figure 4.4 Transgenic construct for myeloid specific expression 104
Figure 4.5: A map of the backbone CD11b-hgh vector for myeloid transgene expression 105
Figure 4.7: The pEGFP-C2 plasmid for expression of enhanced green flourescent protein 106
Figure 4.8: Analysis of 18 samples from co-microinjection of CD11b-IDUA and CD11b-LacZ constructs 107
Figure 4.9: Analysis of 11 samples from co-microinjection of CD11b-IDUA and CD11b-EGFP contructs 108
Figure 4.10: Ubiquitous Transgene Construct CMV-IDUA 109
Fig 4.11: Analysis of samples from microinjection of ubiquitous IDUA construct CMV-IDUA 110
Figure 4.12: pFLOX-CMV-IDUA-EGFP 112
Figure 4.13: The Flox vector used for ES selection of the ubiquitous IDUA and EGFP expressing construct used previously for pronuclear injection 113
Figure 4.14: Ubiquitous Transgene Construct pCAGGs-IDUA 114
Figure 4.15: pCAGGs vector for high level eukaryotic expression 115
Figure 4.16: The pGT1.8IresBgeo vector 116
Figure 4.17: CD11b-LacZ reporter construct integrates into ES clones after co-electroporation with the CD11b-IDUA-Neo construct 117
Figure 4.18: Representation of ES clones screened for beta-galactosidase staining intensity 118

Figure 5.1: Cre/loxP recombination 128
Figure 5.2: Schematic of the selection and screening for desirable ES clones 132
Figure 5.3: pCCALL2-IRES-hAP/cg parent construct 133
Figure 5.4: Schematic of the pCCALL-IDUA construct 134
Figure 5.5: Recombination and the expression of human IDUA 136
Figure 5.6: Rearrangement check on pCCALL2 construct. 137
Figure 5.7: PCR detection of bacterial clones containing pCCALL2 ligated with the human IDUA cDNA. 138
Figure 5.8: Pst I restriction digest of plasmid from ligation of pCCALL2 construct with human IDUA cDNA to determine orientation. 139
Figure 5.9: Restriction digestion to identify clones with correctly inserted and unrearranged hIDUA cDNA into pCCALL2 139
Figure 5.10: Analysis of large scale plasmid isolation of pCCALL-IDUA. 140
Figure 5.11: LacZ staining of ES colonies demonstrating expression variability. 141
Figure 5.13: Southern blot analysis of 48 ES clones with good reporter gene expression for single copy integrates. 143
Figure 5.14: Alkaline phosphatase staining of ES cells containing single copy integrations of pCCALL-IDUA. 145
Figure 5.15: Overall Pedigree 150
Figure 5.16: Schematic of the selection and screen for desired ES clones 152

Table of Tables

Table 1.1: Representative proteoglycan..... 12

Table 1.2: Strategies for the introduction of therapeutic IDUA..... 25

Table 1.3: Therapies for MPS I assessed on MPS model..... 34

Table 2.1: PCR primers..... 46

Table 4.1: Summary of Pronuclear Microinjection attempts at generation of transgenic lines..... 110

Table 4.2: Blastocyst injection of engineered ES clones produces only low level chimeras..... 118

Table 5.1: Representative Cre expressing mice..... 124

Table 5.2: Summary of ES clone analysis..... 145

List of Abbreviations

AGU	aspartylgycoasminuria
beta-geo	neomycin and beta-galactosidase fusion gene
BMT	bone marrow transplantation
CD-MPR	cation dependent mannose-6-phosphate receptor
cDNA	complementary DNA
CHO	chinese hamster ovary cells
CI-MPR	cation independent mannose-6-phosphate receptor
CMV	cytomegalivirus
CNS	central nervous system
Cre	causes recombination recombinase
CRM	cross reactive material
CS	chondroitin sulfate
DMSO	dimethyl sulfoxide
DNA	deoxyribonucleic acid
Dox	doxycycline
DS	dermatan sulfate
EC	extracellular space
EE	early endosome
EGFP	enhanced green flourescent protein
ER	endoplasmic reticulum
ERT	enzyme replacement therapy
ES	embryonic stem cell
ES	embryonic stem (cell)
G	golgi
GAG	glycosaminoglycan
GM	ganglioside
GT	gene therapy
GUS	beta-glucuronidase
H & E	haematoxylin and eosin stain
hAP	human alkaline phosphatase
HD	huntington
HLA	human leucocyte antigen
HS	heparan sulfate
HSC	hematopoietic stem cells
i.v.	*intra venous*
IDUA	alpha-L-iduronidase enzyme, cDNA, or mRNA
IDUA	alpha-L-iduronidase gene, human
Idua	alpha-L-iduronidase gene, mouse
IE	immediate early
IRES	internal ribosome entry site
kDA	kilo Daltons
KS	keratan sulfate
L	lysosome

LacZ	beta-galactosidase
loxP	locus of crossover
LSD	lysosomal storage disease
M-6-P	mannose-6-phosphate
MPRs	mannose-6-phosphate receptors
MPS	mucopolysaccharidosis
mRNA	messenger RNA
pA	polyadenylation signal
PAS	periodic-acid schiff with diastase stain
PBS	phosphate buffered saline
PCR	polymerase chain reaction
PGK	phospho-glycerate kinase
PM	plasma membrane
RER	rough endoplasmic reticulum
RNA	ribonucleic acid
SAT-1	sulfate transporter-1 gene, human
Sat-1	sulfate transporter-1 gene, mouse
SAT-1	sulfate transporter-1 protein, cDNA, or mRNA
SRP	signal recognition particle
TetR	tetracycline responsive
TSP	tissue specific promoter
V	vesicle

Chapter 1: Introduction

1.1 Thesis Focus and Chapter Overview

This thesis describes the long term characterization of murine IDUA deficiency and the generation of transgenic murine strains conditionally expressing human IDUA. Severe MPS I in humans is a multisystem, progressive disease with a characteristic phenotype, however the pathological and biochemical alterations which underlie the development of overt symptoms in MPS I are not well understood and difficult to study in humans. Using a mouse model of IDUA deficiency, I have studied specific features of IDUA deficiency and provide new observations and insights on the pathophysiological progression of IDUA deficiency in mouse, and, likely, humans. Importantly, IDUA deficiency in the mouse is found to most closely resemble severe IDUA deficiency in humans, with multisystem progressive involvement of most tissues including skeletal and neurologic systems.

The second objective of this work was the generation of mouse strains conditionally expressing human IDUA for use in determining the outcome of specific therapeutic reconstitution of IDUA in a background of complete IDUA deficiency. This will allow for the assessment of different therapy approaches for MPS I, which, along with a number of other members of a larger group of genetic disorders called lysosomal storage diseases (LSDs), are some of the only genetic diseases to have reached the point of gene product therapy. For MPS I, therapy is presently in the form of cell transplantation using bone marrow, or enzyme replacement using recombinant human IDUA protein enzyme, however approaches using gene therapy are also considered suitable.

The structure of the thesis is as follows:

Chapter 1 provides background information relevant to this thesis, describes the objectives of the thesis, and presents hypotheses explored in the thesis. The current understanding of human MPS I is presented, including the biochemical basis of MPS, the genetics of the disease including the presence of an overlapping sulphate transporter gene (*SAT-1*), and the normal production and delivery of IDUA enzyme to the lysosome. The potential for therapy of MPS I is then discussed, including various routes and methods for correction of IDUA deficiency. A discussion of animal models of MPS disorders and attempts at correction of enzyme deficiency provides an up to date review of therapeutic approaches for the MPS disorders. The objectives and supporting hypotheses of the thesis are then presented.

Chapter 2 details the materials and methods used in this project.

Chapter 3 is an examination of the long term clinical, biochemical, and pathological course of murine IDUA deficiency. One of the major goals of the characterization of murine IDUA deficiency is to establish the breadth of IDUA deficiency in mouse and place it on the spectrum of human IDUA deficiency. In addition, the progression of IDUA deficiency in critical tissue systems can be determined thus leading towards a better understanding of the pathophysiology of IDUA deficiency. Finally, characterization of murine IDUA deficiency may establish markers of disease useful in the assessment of therapies for IDUA deficiency. Important findings include the presence of early pathology in the growth plates of bones, the presence of secondary accumulations in brain similar to those described in human MPS I, and the presence of neurologic disease including dysmorphology of Purkinje cells in the cerebellum. The

observations are important as they confirm the utility of the *Idua -/-* mouse, and provide a better understanding of the pathology occurring over time in tissues not yet responsive to therapy.

Chapter 4 describes the attempted production of transgenic mouse lines expressing human IDUA either ubiquitously, or in the myeloid hematoipoietic lineage, for use in transplantation studies as well as genetic crosses into IDUA deficient line. The myeloid specific transgenic would address the maximum potential of bone marrow derived cells for the correction of IDUA deficiency. Using both a pronuclear injection approach and an embryonic stem cell approach, attempts at generation of germline transmissible founders or chimeras were unsuccessful.

Chapter 5 documents the successful generation of transgenic lines expressing human IDUA, employing a conditional transgenic approach involving Cre-mediated activation of human IDUA expression. This approach includes a dual reporter system indicating the state of transgene recombination. Initial mating into a widespread Cre-expressing line produced double transgenic offspring, some of which express human IDUA and the reporter gene alkaline phosophatase. These mice can be used to express human IDUA specifically in a wide variety of tissues and can fulfill the dual objectives of chapter 4, namely marrow derived IDUA expression to represent bone marrow transplantation, and ubiquitous IDUA expression for transplantation experiments and to determine the phenotype of IDUA overexpression.

Chapter 6 is a discussion of the results from the thesis. Briefly, the observations described here on the long term pathophysiology of IDUA deficiency in the mouse improve our understanding of the cellular events underlying the development of overt

symptoms in human MPS I. The IDUA-deficient mouse model of MPS I represents all major aspects of human IDUA deficiency so far examined, including significant involvement of the neurologic and skeletal compartments. Secondary accumulations of toxic gangliosides associated with morphology changes and inappropriate cell death are found in the IDUA-/- mouse as they are in human IDUA deficiency. Finally, the generation of transgenic murine lines expressing human IDUA will help determine effective therapeutic approaches for MPS I and determine the phenotype of transgenic expression of IDUA.

1.2 MPS I

1.2.1 Clinical Presentation of MPS I

Deficiency of the lysosomal enzyme α-L-iduronidase (IDUA) underlies mucopolysacchardosis type I (or MPS I), which can result in a wide range of clinical symptoms. MPS I represents the most common severe MPS subtype, occurring with a frequency of approximately 1/100,000 in most populations (Lowry *et al.,* 1990) Three forms of MPS I are recognized, differing in onset, system involvement, and overall severity, with Hurler syndrome (MPS IH) the most severe, Scheie syndrome (MPS IS) involving a much milder course, and Hurler-Scheie syndrome (MPS IH/S) representing an intermediate phenotype. MPS I therefore presents as a spectrum of disease phenotypes (Roubicek *et al.,* 1985). Historically the differentiation between MPS I phenotypes was based on clinical symptom criteria, however molecular characterization of the *IDUA* gene encoding a-L-iduronidase and its mutations increasingly allows genotyping of patients, useful in prognosis based on established genotype-phenotype

correlations. All forms of MPS I share in common excessive urinary excretion of heparan and dermatan sulphate and absence of alpha-L-iduronidase activity.

Most often born with no obvious phenotype, patients with the most severe form of MPS I (MPS IH -Hurler) usually present clinically before age 2 with developmental delay, coarse facial features, enlargement of the spleen and liver, skeletal deformities, a prominent forehead, and joint stiffness. Symptoms rapidly become more severe and diagnosis of MPS IH typically occurs between 6 and 30 months of age (Colville and Bax, 1996). Developmental delay is a precursor to developmental decline, with a maximum functional age of 2 to 4 years obtainable followed by progressive deterioration. Limited language skills result from a combination of mental handicap, tongue enlargement, airway obstruction, and possible hearing loss. Corneal clouding is progressive and may result in blindness. Hydrocephalus resulting from increased intracranial pressure is common and, again, progressive. Skeletal deformities are widespread and progressive and include the skull, dentition, vertebrae, phalanges and the long bones among others, leading to the term dysostosis multiplex (Fields *et al.*, 1994). Shortened stature and very coarse features are seen with MPS IH. Obstructive airway disease, respiratory infection, and cardiac complications are the most common causes of death, which usually occurs before age 10.

The mild form of MPS I, Scheie syndrome (MPS I S) presents at a later age than MPS I H with clinically significant symptom development usually after 5 years of age with diagnosis normally between 10 and 20 years of age, depending on severity. MPS I S is characterized by joint stiffness, back pain, aortic valve disease, and corneal clouding, while intelligence and stature are normal. While progressive, the acceleration in disease

severity observed in MPS I H is not seen in Scheie syndrome. Survival into late adulthood is normal, however cardiac complications may result in death before middle age (Scheie *et al.,* 1962).

Intermediate forms of MPS I (Hurler-Scheie or MPS I H/S) have a clinical phenotype between Hurler and Scheie syndromes. Typically, progressive dysostosis multiplex is present, however little or no intellectual dysfunction is observed. Other somatic features of MPS I, including corneal clouding, joint stiffness, deafness and cardiac disease, are usually present. Symptom development occurs between the ages of 3 and 8 and survival into adulthood is common. Clinical mortality normally results from cardiac involvement and airway obstruction (McKusick and Neufeld, 1983).

The diagnosis of MPS I in patients is confirmed by measurement of enzyme activity in leukocytes, plasma, or fibroblasts. Routinely the enzyme activity is measured with the use of a flurogenic substrate 4-methylumbelliferyl-alpha-iduronide (Hopwood and Muller, 1982). Samples used in the diagnosis of MPS I include cultured fibroblasts, plasma, or serum, and cultured cells derived from amniotic fluid for prenatal diagnosis. Chorionic villus biopsies are used for diagnosis for a number of MPS disorders including II, III A, III B, III C, and IV A, however it has been reported that the low level of IDUA activity in villi makes diagnosis of MPS I more difficult (Poenaru, 1987). The advent of molecular diagnosis coupled with the extensive characterization of mutations in the *IDUA* gene play an increasing role in diagnosis as well as well as prognosis and will be discussed later.

1.2.2 Glycosaminoglycans and proteoglycans

Deficiency of IDUA in MPS I results in the accumulation of undegraded mucopolysaccharides, commonly called glycosaminoglycans (GAGs). GAGs are sulfated, linear carbohydrates consisting of repeating sugar groups, and include heparan sulphate (HS), dermatan sulphate (DS), keratan sulphate (KS), and chondroitin sulfate (CS). GAGs are normally found linked to a protein core as part of macromolecules termed proteoglycans, to which they impart functional properties. As MPS I involves accumulation of HS and DS the role of these GAGs and their associated proteoglycans will be discussed here. HS consists of uronic acid residues alternating with alpha-linked glucosamine residues (Hopwood, 1989). The uronic acid may be glucuronic or iduronic acid, and may be sulphated. The glucosamine may be N-sulphated or N-acetylated, and may also be 3- or 6-sulphated. Different permutations of modifying sulphation and acetylation on a carbohydrate backbone, which itself varies in sugar group representation, impart GAGs with their unique functional properties and provides for huge complexity and biological diversity within each type of GAG.

Degradation of HS and other GAGs begins with proteolysis in the early endosomes producing liberated chains of GAG (approx. 30kDa). Endoglycosidases then cleave GAG chains into oligosaccharides (approx. 5kDa), which are targeted to the lysosome for stepwise exodegradation (reviewed in Hopwood *et al.*, 1989). The structure of a hypothetical HS oligosaccharide and the enzymes required for its lysosomal endodegradation are pictured in Figure 1.1.

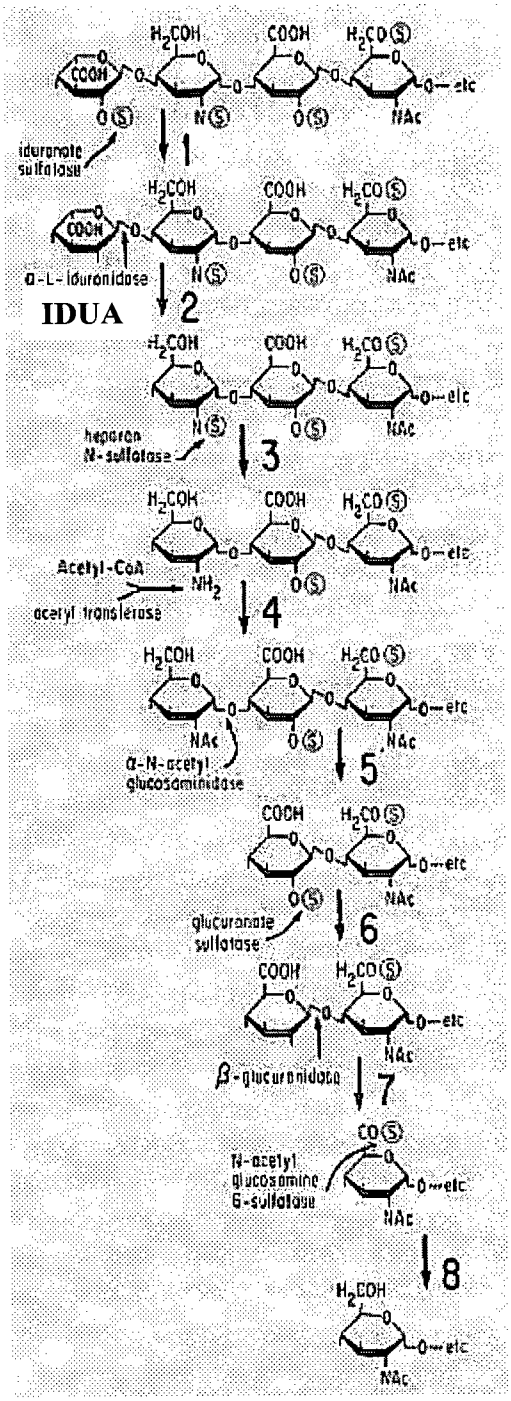

Figure 1.1: Heparan sulfate exodegradation

IDUA hydrolyzes removal of terminal desulfated iduronic acid residues, step 2 above. This produces free iduronic acid and leaves a terminal glucosamine for further exodegradation. 9 enzymes are required for HS degradation. Not shown: glucosamine-3-sulphatase. From Scriver *et al.*, 1989.

The lysosomal exodegradation of HS oligosaccharides requires at least nine enzymes, with deficiency of any single enzyme resulting in blockage of the entire pathway and accumulation of partially degraded HS chains. These enzymes include glycosidases such as IDUA, sulphatases, and include a biosynthetic enzyme that adds an acetyl group required for subsequent enzymatic degradation. As shown in Figure 1.1, alpha-L-iduronidase (IDUA) acts on terminal desulfated iduronic acid residues producing free iduronic acid and a terminal glucosamine residue for further degradation. The degradation of GAGs releases monosaccharides and sulfate which exit from the lysosome for recycling in biosynthetic reactions (Hopwood *et al.,* 1989).

Dermatan sulfate (DS) consists of iduronic acid, which may be C-2-sulphated, and glucuronic acid residues alternating with beta-linked N-acetylgalactosamine, which may be sulphated (Roden, 1980). As for HS, degradation of DS containing proteoglycans includes proteolysis followed by endoglycosidase activity, producing DS oligosaccharides. The structure of a hypothetical DS oligosaccharide and the enzyme required for its exodegradation are shown in Figure 1.2. As for HS catabolism, deficiency of any single enzyme in the pathway results in accumulation of undegraded DS oligosaccharides. As for HS oligosaccharides, IDUA recognizes and cleaves terminal desulfated iduronic acid residues from DS chains, leaving on DS chains terminal N-acetylgalatosamine residues for further enzymatic degradation. In IDUA deficiency, HS and DS oligosaccharides would be expected to accumulate with terminal iduronic acid residues. The demand for lysosomal degradation of GAGs varies in tissues according to GAG and proteoglycan content and turnover. Proteoglycans, the form in which GAGs are

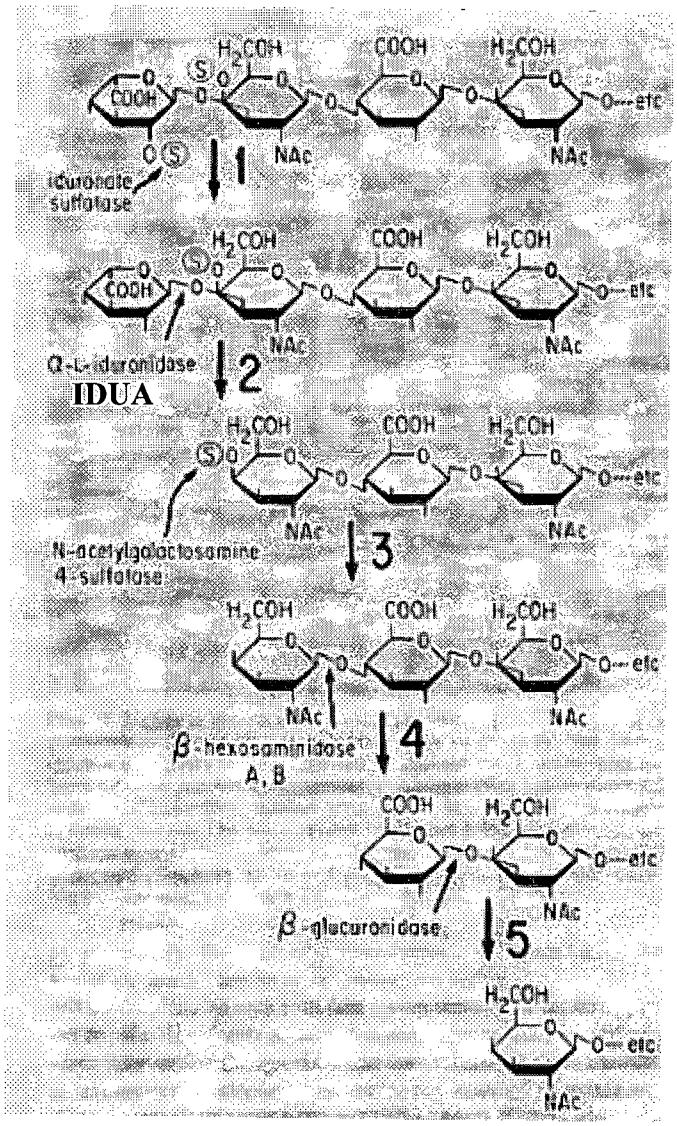

Figure 1.2: Dermatan sulfate exodegradation

IDUA hydrolyzes removal of terminal desulfated iduronic acid residues, step 2 above. This produces free iduronic acid and leaves a terminal N-acetylgalactosamine for further exodegradation. From Scriver *et al.*, 1989.

functional, are proteins containing glycosaminoglycan carbohydrate chains. Typically, a protein core has one to hundreds of covalently attached GAG chains. Proteoglycans range greatly in the ratio of protein to GAG carbohydrate, and in GAG composition. Proteoglycans are dynamic molecules, with expression and composition, including GAG content, changing during development. Proteoglycans do not share a unifying functional feature, playing diverse roles such as forming components of the extracellular matrix, in cell communication, and in ligand-receptor interactions.

Understanding the functions of heparan and dermatan sulfate containing proteoglycans, and the locations where they function, provides some insight into the sites of GAG accumulation in MPS I. Cell surface heparan sulfate, attached to transmembrane proteins, modulates the actions of a large number of extracellular ligands. The structural heterogeneity of HS chains allows binding of a diverse repertoire of proteins under physiological conditions (reviewed in Bernfield *et al.*, 1999). The HS chains provide cells with a mechanism to mediate interactions with a wide variety of extracellular effectors without requiring multiple novel binding proteins. While found on a variety of cell surface proteins, HS chains are consistently found on members of two major families of membrane-bound proteoglycans, the syndecans and the glypicans. These heparan sulfate proteoglycans immobilize and regulate the turnover of ligands that act at the cell surface, by binding to ligands and enhancing formation of their receptor-signalling complexes. The extracellular domains of syndecans and glypicans can be shed from the cell surface, producing soluble HS proteoglycans that act as HS proteoglycan antagonists, and cells that are less responsive to ligand stimulation. The ligand affinities of the syndecans and glypicans include ligands involved in morphogenesis and wound repair, consistent with

the regional and temporal expression patterns of specific members of these HS proteoglycans. Internalization of basic fibroblast growth factor at the mouse blood-brain barrier involves perlecan, a heparan sulfate proteoglycan (Deguchi *et al.,* 2002). Dermatan sulfate (DS) proteoglycans are less widespread than HS proteoglycans but likewise show regional and temporal expression patterns consistent with functions in morphogenesis. DS proteoglycans in the adult are found in tissues such as cartilage and bone (Roughley and Lee, 1994). Table 1.1 describes some common proteoglycans, their functional location, and their GAG content.

Name	Location	Function	GAGs	Reference
perlecan	basement membrane	cell adhesion	HS	Groffen *et al.*, 1999
glypican	cell surface	regulate growth factors	HS	Song and Filmus, 2002
decorin	connective tissue, cartilage	matrix assembly	DS, CS	Roughley and Lee, 1994
aggrecan	cartilage	osmotic compressive properties	CS, KS	Roughley and Lee, 1994
neurocan	extracellular matrix of CNS	matrix assembly	CS	Rauch *et al.*, 2001

Table 1.1: Representative proteoglycans

GAGs=glycosaminoglycans, HS=heparan sulfate, DS=dermatan sulfate, CS=chondroitin sulfate, KS=keratan sulfate, CNS=central nervous system.

1.2.3 Secondary storage in MPS I

Somewhat unique to some of the lysosomal storage disorders is the potential for storage of compounds not related to the pathway which is biochemically deficient. This may be attributed to inhibition of pathways by storage of primary substrates. Secondary

accumulation of gangliosides including GM_2 and GM_3 have been noted in human, canine, and murine, IDUA deficiency, as well as other storage disorders unrelated to primary defects of glycosphingolipid metabolism (Constantopoulos & Dekaban 1978, Constantopoulos *et al.*, 1985). The role that ganglioside accumulation plays in the pathogenesis of MPS I disorders is unknown but may be important. Defects in the catabolism of GM_2 ganglioside in Tay-Sachs and Sandhoff disease results in neurodegenerative disease. Gangliosides including GM_2 have been implicated in neuronal apoptosis, and GM_2 has been postulated to underlie the generation of ectopic dendrites in pyramidal neurons in both Tay-Sachs as well as other generalized lysosomal storage disorders (Walkley 1995).

1.2.4 The MPS family of disorders

At least 10 enzymes required for GAG catabolism have been identified, primarily as a result of studying enzyme deficiency in the MPS syndromes. All of the MPS associated enzymes are unable to mediate endodegradation; that is, only terminal substrates are cleavable. Therefore deficiency of any single enzyme required for GAG degradation blocks the degradation pathway, resulting in storage in the lysosome and excretion in the urine. Differences in the type of GAG and their terminal residues accumulated in the different MPSs result in the distinguishing pathophysiology of the MPSs. MPS I, with accumulation of HS and DS, includes, in severe forms, visceral, skeletal, and neurological involvement, consistent with representation of HS and DS GAGs in these tissue systems. MPS II, sharing with MPS I accumulation of both HS and DS, has a phenotype similar to MPS I, involving both somatic and CNS systems. Interestingly, MPS VI, with accumulation of DS only, involves skeletal disease but

normal neurological function, while MPS III A, B, C, and D, with accumulation of HS only, involves severe mental deterioration, but only mild somatic symptoms and no skeletal disease. This suggests the skeletal disease observed in severe MPS I, similar to the phenotype of MPS VI, likely results from accumulation of DS, while the neurological degeneration and CNS involvement observed in severe MPS I likely results primarily from accumulation of HS, as observed with MPS III. The role of KS in the skeletal system is highlighted in MPS IV B, where accumulation of KS is associated with a phenotype of severe skeletal disease.

1.2.5 Genetics

MPS I results from deficiency of alpha-L-iduronidase, encoded by the *IDUA* gene. In humans, the *IDUA* gene is located on the short arm of chromosome 4 close to the telomere (4p16.3) in the same region as the Huntington disease (*HD*) gene (Scott *et al.*, 1990). The *IDUA* gene contains 14 exons spanning 19 kb, organized as two clusters of exons: exon I and II separated by an intron of 566 bp, a large intron II of 13 kb, and remaining exons III to XIV clustered in a 4.5 kb region (Scott *et al.*, 1991, 1992). Intron 2 of the human *IDUA* gene contains an Alu repetitive element and an 86 bp highly polymorphic VNTR repeat (D4S111) used in the diagnosis of HD (Scott *et al.*, 1992, MacDonald *et al.*, 1991). Contained entirely within the *IDUA* gene, on the opposite strand to IDUA, is the Sulphate transporter-1 gene, *SAT-1* (see Figure 1.3)(Clarke *et al.*,, unpublished data). The *SAT-1* gene will be discussed further later.

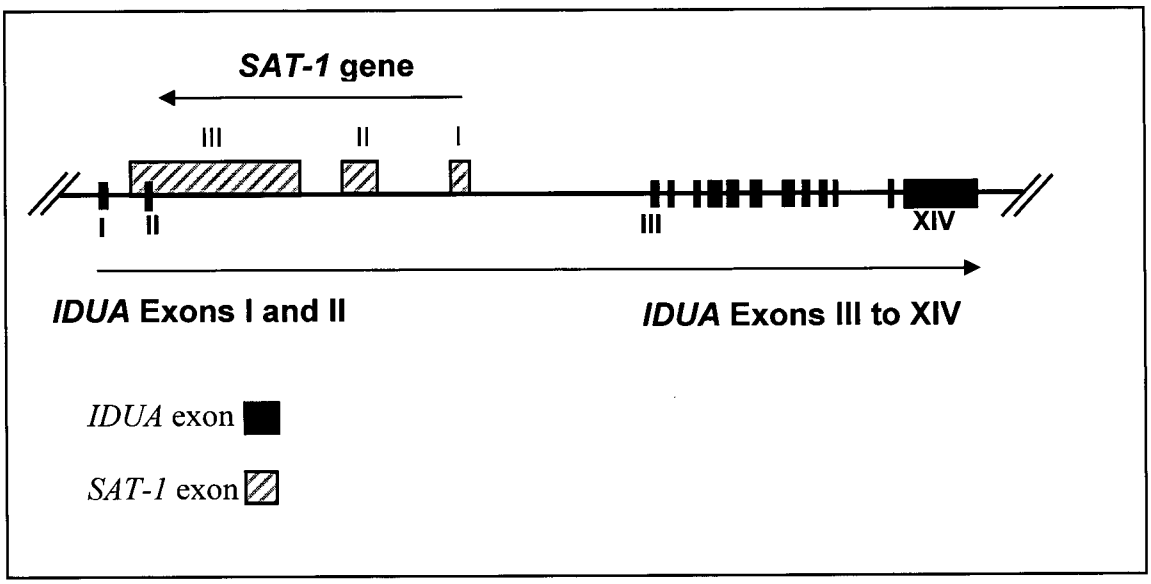

Figure 1.3: Organization of the human IDUA gene locus
Arrows indicate the direction of transcription the *IDUA* gene (with black exons) and the *SAT-1* gene (checkered exons). The human *IDUA* gene spans 19 kb, including intron 2 (13 kb) containing most of the *SAT-1* gene, which is encoded on the opposite strand to *IDUA* and includes a 3' untranslated region that overlaps *IDUA* exon II, a coding exon.

In humans the *IDUA* gene produces a predominant transcript of 2.3 kb at a low level of transcription as determined by Northern blot analysis (Scott *et al.*, 1992). Alternate spicing of *IDUA* exons II, the overlapping exon, and exon IV, has been observed (Scott *et al.*, 1991). As shown in figure 1.4, the human IDUA cDNA includes an open reading frame of 1959 bp, encoding a peptide of 653 amino acids (Scott *et al.*, 1991). In addition to the human IDUA cDNA, murine and canine IDUA cDNAs have been sequenced (Clarke *et al.*, 1994, Menon *et al.*, 1992). The architecture of the *Idua* gene is conserved in all three species, and the *Sat-1* sequence and genomic organization has been detailed in mouse and found to be similar to the human *IDUA* locus. The entire region of human chromosome 4p16.3 containing *IDUA* is syntenic with a region of mouse chromosome 5

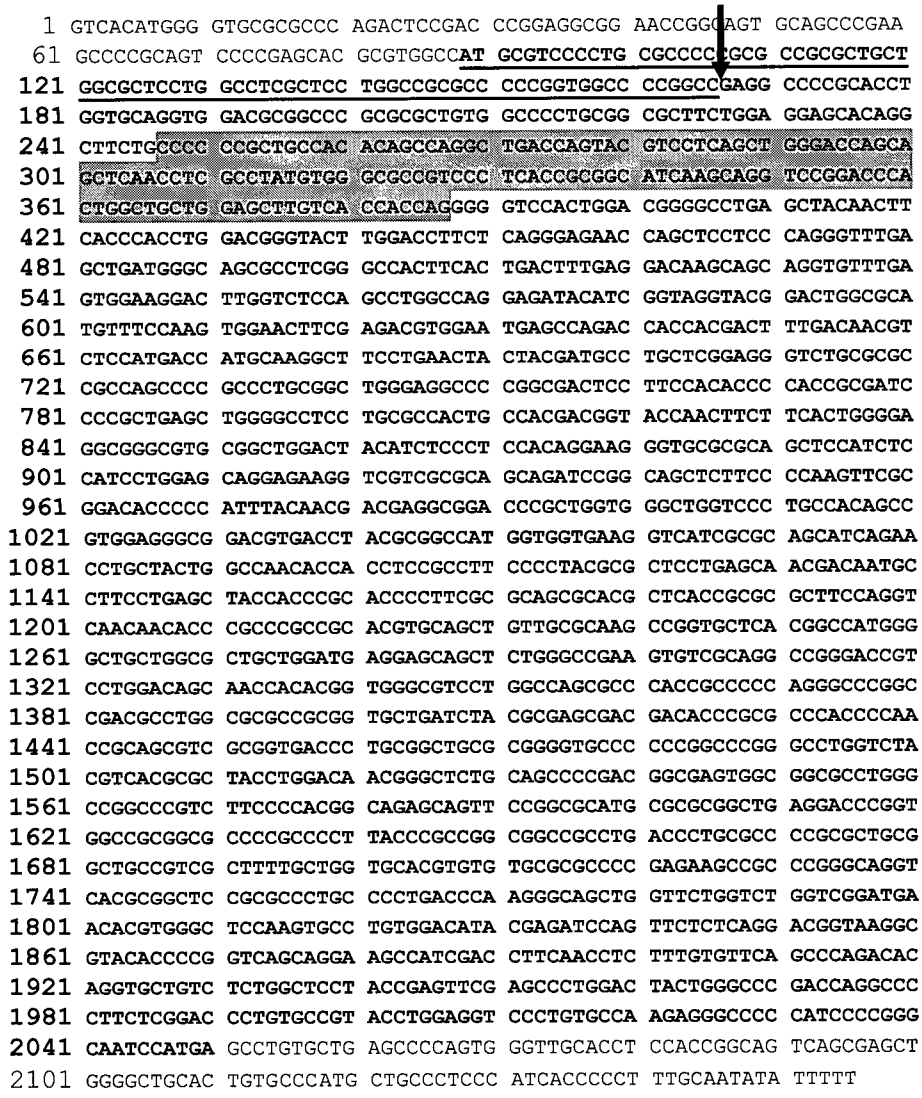

Figure 1.4: The human IDUA cDNA

The 2155 bp cDNA has an open reading frame, bold, of 1959 bp encoding a polypeptide of 653 amino acids. A signal peptide of 26 amino acids, underlined, is cleaved at the site indicated by the arrow, leaving a mature polypeptide of 627 amino acids. Exon II of *IDUA*, complementary to the 3'UTR of the SAT-1 cDNA, is shaded.

(Grosson *et al.*, 1994), including the presence of the HD gene. Comparison of the cDNA across species shows the canine and human cDNA and protein show 82% homology (Stoltzfus *et al.*, 1992), while the murine cDNA and protein show 78% and 77% homology with the human cDNA and protein, respectively (Scott *et al.*, 1995).

Expression of *Idua* appears to be limited at numerous points during transcription.

The postulated promoter of the human *Idua* gene has only a GC box-type consensus sequences, and no obvious TATA box, consistent with a housekeeping gene. In human, murine, and canine, intron 11 contains an apparently conserved GC/AG exception in the donor splice site, which is associated with reduced splicing efficiency and gene expression. The overlapping *Sat-1* gene in human and mouse, and most likely the canine *Idua* gene locus, encodes an mRNA transcript complementary to *Idua*, and this could further regulate *Idua* expression via antisense interactions. Together, these features of the *Idua* gene contribute to the low level of expression observed from the *Idua* gene.

With almost 75 distinct mutations already described in *IDUA*, the clinical spectrum of MPS I is explained in part by the myriad of genotypes possible which combine alleles that may encode low levels of IDUA activity, or, for null alleles, no IDUA at all (Human Gene Mutation Database). Mutations occur throughout the *IDUA* gene including exon II, the exon overlapping with a portion of *SAT-1* 3' untranslated sequence. These mutations include nonsense, missense, and splice site mutations, minor deletions, insertions, and complex rearrangements (reviewed in Scott *et al.*, 1995). Eight nonsense mutations have been described, including W402X, one of the most common mutations in Caucasians, and all result in a total lack of IDUA function and are associated with severe phenotypes when found in homozygosity. Interestingly, some nonsense mutations are associated with lower levels of IDUA mRNA transcripts, as determined by Northern blot analysis, indicating detection and deletion of nonsense mutation containing transcripts (Scott *et al.*, 1992, Bach *et al.*, 1993). Twenty-one missense mutations have been described in *IDUA*. Missense mutations are more likely than nonsense mutations to permit some enzymatic function, and many missense mutations are associated with mild

or intermediate phenotypes when found in homozygosity. Three splice site mutations have been described in *IDUA*, with two of them resulting in inclusion of introns in the IDUA mRNA. Splice site mutations are associated with both mild and severe phenotypes when found in homozygosity. Seven small deletions (1 to 12 bp) and six small insertions (1 to 12 bp) have been described in the *IDUA* gene (Bunge *et al.*, 1994, 1995). 30 non pathogenic polymorphisms have been detected in *IDUA*.

Siblings carrying identical MPS I alleles can have significantly different clinical outcomes, indicating modifier genes or the environment can influence disease progression (McDowell *et al.*, 1993, Scott *et al.,* 1993, Neufeld, 1991). This is also seen in mouse models of MPS VII, where the phenotype of enzyme deficiency varies with strain including viability, life span, and reproductive success (Casal and Wolfe, 1998). In humans, a pseudodeficiency *IDUA* allele with exceedingly low activity levels has been described which produces no clinical phenotype in homozygotes for the allele, but that encodes such a low level of IDUA enzymatic function that homozygotes appear completely IDUA deficient in standard IDUA enzyme assays and heterozygotes appear as MPS I carriers, complicating biochemical screening for carriers (Whitley *et al.*, 1996).

1.2.6 The *Sat-1* gene

Discussion of the *Sat-1* gene is relevant to this thesis as the overlap region shared by the genes could impact disease or therapy. The genomic architecture of *Sat-1* is similar in human and mouse, and is shown in figure 1.3. In both species, *Sat-1* spans approximately 6 kb and includes 4 exons (Lee *et al.*, 2003, Regeer *et al.*, 2003). Exons I to III are embedded in intron 2 of *Idua*, while a 141 bp region of the 3' untranslated region of *Sat-1* overlaps the entirety of *Idua* exon II. The two genes are encoded on

opposite strands of DNA and are transcribed in opposite directions. The *Sat-1* gene encodes a 74 kd protein including 12 predicted transmembrane domains. Northern blot analysis indicates SAT-1 is widely expressed in human tissues as a 4.4 kb transcript, with placenta showing an additional, presumably alternatively spliced transcript of 6.0 kb. In contrast, SAT-1 mRNA expression in mouse is selective with a transcript of 4.0 kb observed in liver and kidney, and weaker but detectable signals observed in lung, spleen, and brain. IDUA mRNA expression in both human and mouse is widespread but at low levels (Clarke *et al.*, unpublished data).

The function of the SAT-1 protein is only partially characterized. Bissig *et al.*, cloned the SAT-1 cDNA from rat liver using a functional expression assay designed to identify transporters of sulfate and characterized SAT-1 as the primary canalicular sulfate transporter (Bisseg *et al.*, 1994). Markovich *et al.*, have shown that SAT-1 is responsible for the majority of sodium-independent sulfate transport in the kidney (Markovich *et al.*, 1994), and SAT-1 has been localized to the basolateral membrane of the proximal tubule by immunohistochemistry (Karniski *et al.*, 1998). SAT-1 is expressed in brain and functions as the main transporter of sulphate, at least in rat (Lee *et al.*, 1999). No diseases have been mapped to the human *SAT-1* gene. Abnormalities in sulfate transporter genes related to *SAT-1* in humans have been implicated in 5 diseases resulting from mutations in 3 genes, *DRA* (Congenital Chloride Diarrhea) (Moseley *et al.*, 1999), *DTDST* (Diastrophic Dysplasia) (Hastbacka *et al.*, 1996) and *PDS* (Pendred Syndrome)(Everett *et al.*, 1997). *DTDST* encodes a sulfate transporter that is deficient in an allelic series of 3 clinically distinct chondrodysplasias; diastrophic dysplasia, atelosteogenesis type II, and achondrogenesis type IB. All 3 disorders result from deficient sulfation of cartilage

proteoglycans, which may limit binding with, and activation of, stimulatory signals crucial to chondrocyte function and normal skeletal development. Mutations in *DRA* underlie Congenital Chloride deficiency, a debilitating and potentially fatal disease resulting from disruption of colon chloride anion homeostasis. *PDS* encodes a sulfate transporter deficient in Pendred syndrome, a form of nonsyndromic deafness with associated goiter. These seemingly unrelated disorders share in common mutations in genes related to *SAT-1*. To further understand the function of *SAT-1*, the Clarke group has generated a mouse line with targeted disruption of the murine *Sat-1* gene (Clarke, unpublished data). Homozygote *Sat-1* knockouts are viable and await further characterization.

The unusual architecture of the *Sat-1* and *Idua* genes, and the apparent concomittant expression of their mRNA transcripts, indicates antisense mediated regulation of the genes may occur as a result of the complementary 141 bp overlapping region. If the transcripts from the two genes interact, mutations that destabilize one transcript might lead to changes in expression of the other partially complementary transcript. For example, mutations in *Idua* that destabilize the IDUA transcript might alter SAT-1 expression, which could contribute to the disease phenotype. Another consequence of the *Sat-1* and *Idua* overlap is the potential for altering SAT-1 expression by overexpressing complementary IDUA transgenes. This potential for regulation of SAT-1 expression has been recognized in efforts to develop a mouse expressing human IDUA, and as will be discussed led to the use of the human, rather than murine, IDUA cDNA.

1.2.7 IDUA protein synthesis and transport to the lysosome

Processing of IDUA includes translation, post-translational modification, and delivery to the lysosome. Transport and processing are important to this discussion as they play a role in disease but also as these processes are important for the successful therapeutic introduction of IDUA. Figure 1.5 depicts transport of lysosomal enzymes. Lysosomal enzymes, membrane proteins, and proteins destined for secretion, are translated on endoplasmic reticulum-bound ribosomes and include a hydrophobic signal sequence which, *via* interaction with a signal recognition particle (SRP), mediates translocation of the developing hydrophilic protein into the lumen of the endoplasmic reticulum (ER) (Gorlich and Rapoport, 1993). The signal peptide is not present in the mature protein. In the ER the IDUA polypeptide is folded and processed, including the addition of high mannose oligosaccharides critical to targeting the enzyme to the lysosome. After transfer to the *cis*-golgi, mannose oligosaccharides are modified by the addition of a mannose-6-phosphate marker by the action of two enzymes. With the addition of the mannose-6-phosphate residues, IDUA and other proteins targeted for the lysosome are recognized by either of two mannose-6-phosphate receptors (MPRs). The first of these MPRs, the cation independent MPR (CI-MPR), mediates transfer of mannose-6-phosphate containing proteins that are either newly synthesized, or produced exogenously and found in the extracellular environment, to the lysosome. The cation dependent MPR (CD-MPR) mediates lysosomal transfer of newly synthesized enzyme only and is not involved in endocytosis of exogenous proteins. As will be discussed later, overexpression of a protein with the mannose-6-phosophate marker has resulted in

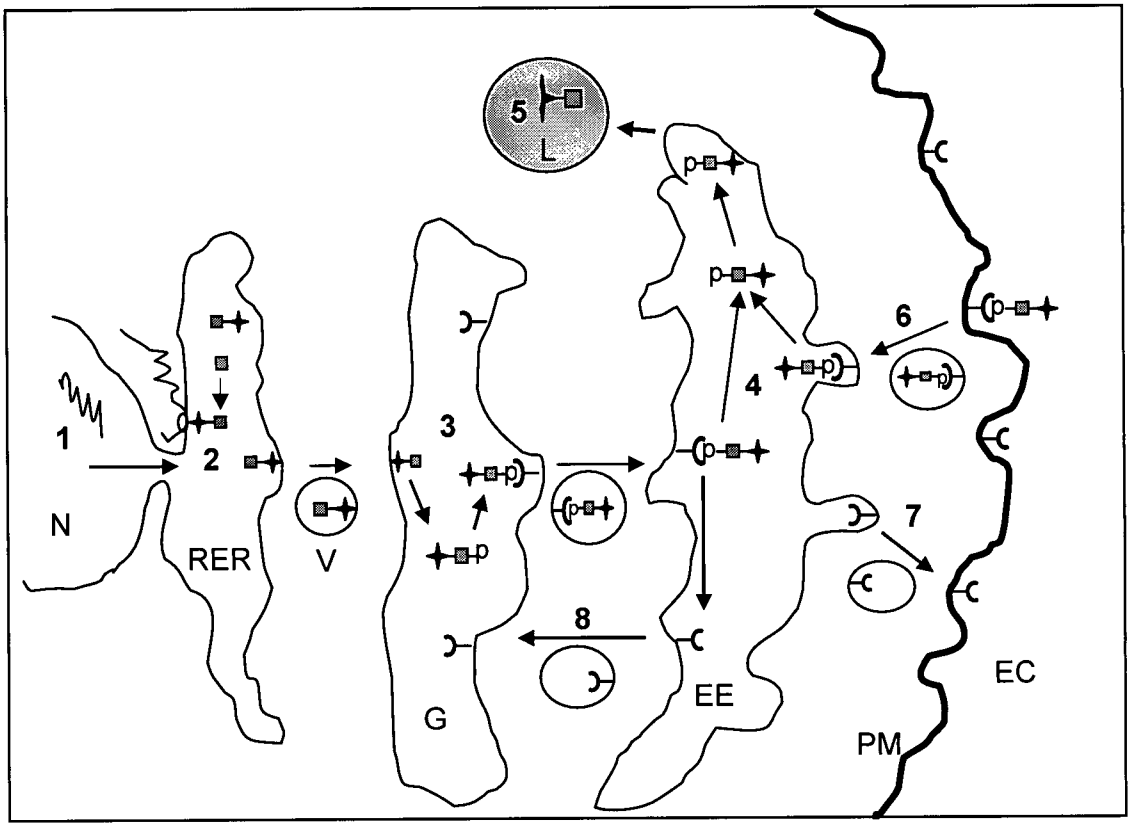

Figure 1.5: Endogenous and exogenous pathways for transport of lysosomal enzymes including IDUA to the lysosomes

(1) mRNA trancripts encoding lysosomal enzymes include signal sequences directing translocation of the synthesized protein into the lumen of the rough endoplasmic-reticulum (RER), where (2) post-translational modifications including addition of high mannose oligosaccharides occurs. Vesicular (V) delivery to the golgi (G) is followed by (3) phosphorylation of oligosaccharides (p), which mediates binding to mannose-6-phosphate receptors (MPRs) in the golgi. Phosphorylated enzymes bound to MPRs are then transported to early endososmes (EE), where (4) acid pH dissociates the enzyme-receptor complex which is then delivered to the lysosome (L), completing the endogenous pathway for lysosomal targeting (5). Exogenously produced lysosomal enzymes are targeted to lysosomes (6) by way of cell surface MPRs, delivered to the plasma membrane (PM) from the EE (7). (8) Recycling of MPRs to the golgi. N=nucleus, EC=extracellular space. Figure based on Kornfeld 1987.

apparent overwhelming of the MPR mediated delivery of lysosomal proteins, resulting in reduced levels of other lysosomal proteins in the lysosome and increased levels of lysosomal proteins in the extracellular environment (Anson *et al.*, 1992). Proteins bearing

the mannose-6-phosphate marker bind MPRs and are directed to early endosome compartments, where under the influence of low pH, the proteins dissociate from the receptors. Freed receptors are recycled to the golgi for reuse. Proteins destined for the lysosome, including IDUA, are transported in an endosome like vesicle that fuses with or becomes a lysosome.

1.3 Therapies for MPS I

1.3.1 Rationale

MPS I, and other lysosomal storage disorders, are somewhat unique in that multiple strategies for therapeutic reconstitution are possible. The rationale for therapy for the MPS disorders is based on two observations. First, cross correction of IDUA deficient fibroblasts occurs with co-cultivation of fibroblasts from patients with other forms of MPS disorders. The corrective factor has been determined to be the lysosomal enzyme itself, which can be secreted by one cell for uptake and delivery to the lysosome of another, deficient cell (Barton and Neufeld, 1971). This means in contrast with disorders requiring endogenous production of therapeutic proteins for correct function, IDUA and other lysosomal enzymes bearing the MPR phosphate residue can be introduced in protein form, rather than requiring direct gene therapy approaches. Second, patients expressing only low level IDUA levels, as low as 0.13% of normal IDUA protein levels, undergo a dramatically different disease course including no significant central nervous system disease and mild skeletal disease (Scott *et al.*, 1993). This suggests that the successful introduction of even low levels of IDUA activity could improve important features of MPS I currently not fully addressed. Figure 1.6 depicts the routes for delivery

of therapeutic enzyme to the lysosome. Transplanted cells are a source of enzyme with bone marrow transplantation (BMT), which delivers enzyme to diseased lysosomes *via*

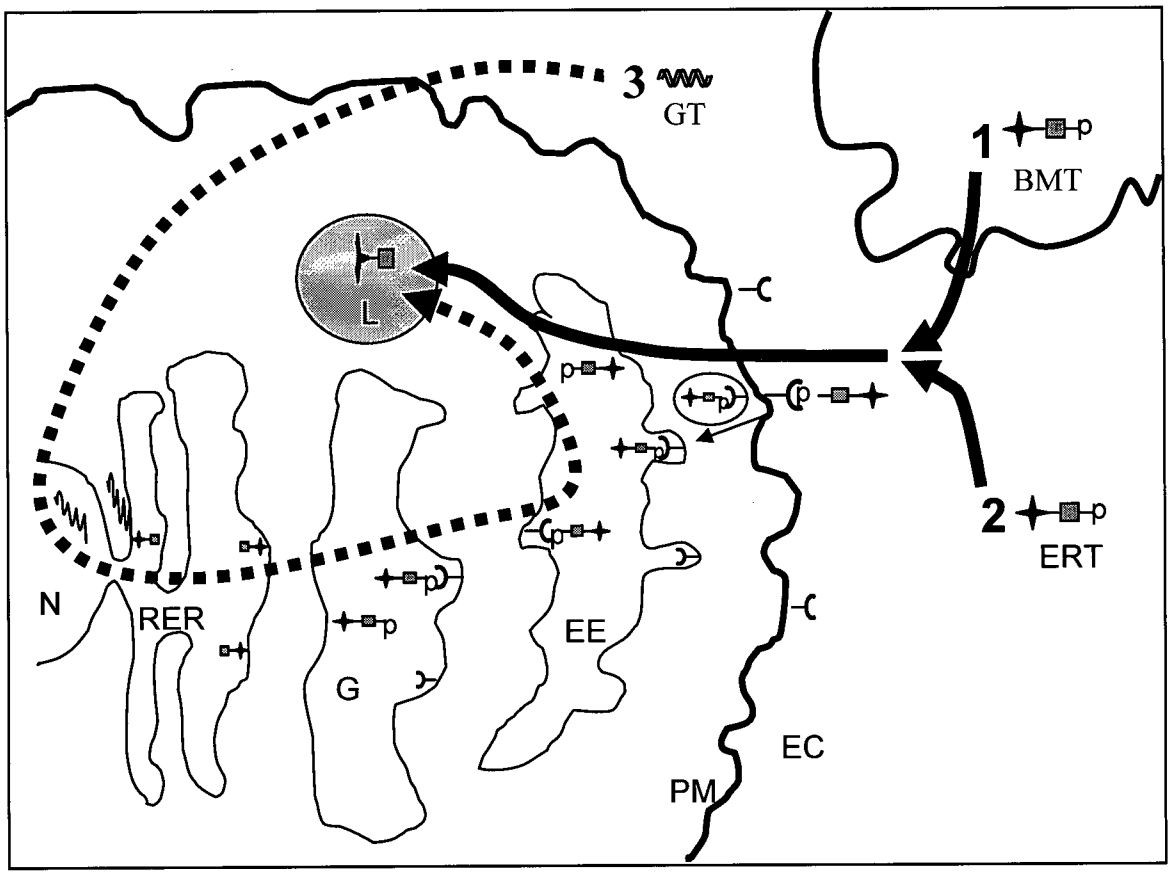

Figure 1.6: Routes for the introduction of therapeutic IDUA

Therapeutic IDUA can be produced by numerous strategies. (1) transplanted tissue, exemplified by bone marrow transplantation (BMT), and (2) enzyme replacement therapy (ERT), both involving delivery of exogenously produced enzyme (solid lines) to lysosomes via cell surface MPRs. (3) Gene therapy (GT), requires delivery of agents to the nucleus (dotted line) resulting in endogenously produced enzyme. N=nucleus, RER=rough endoplasmic reticulum, G=golgi, EE=early endosome, L=lysosome, PM=plasma membrane, EC=extracellular space, MPRs=mannose-6-phosphate receptors.

cell surface MPR receptors. Using the same route enzyme replacement therapy (ERT) can likewise provide therapeutic enzyme. Gene therapy (GT) differs from BMT and ERT as the therapeutic enzyme is produced internally and is targeted to the lysosome via both

Strategy	Target sites	Outcome	Limitations	Species and references
Bone marrow trans-plantation (BMT)	Bone marrow and bone marrow derived cells including widespread cells of the monocyte/macro-phage lineage	Reduction in urinary GAG excretion Somatic improvement Stabilization of neurologic complications	Compatible donors Transplantion complicatons, engraftment Limited benefit to central nervous system Limited benefit to skeletal system	Human Pearson, 1986 Shapiro *et al.*, 1995 Dog Constantopoulous *et al.*, 1989
Enzyme replacement therapy (ERT)	Plasma, cells	Reduction in urinary GAG excretion Somatic improvement Stabilization of neurologic complications	Limited benefit to central nervous system Limited benefit to skeletal system Immunologic response	Dog Kakkis *et al.*, 1996 Cat Kakkis *et al.*, 2001 Human Kakkis *et al.*, 2001
Gene therapy (GT)	Not yet defined; Somatic, central nervous system, and skeletal system	unknown	unknown; delivery, expression, persistence, immunologic response	Dog Shull *et al.*, 1996 Meertens *et al.*, 2002 Lutzko *et al.*, 1999

Table 1.2: Strategies for the introduction of therapeutic IDUA

the endogenous route and for neighboring cells, the exogenous route. Gene therapy approaches, including *ex vivo* gene therapy, have suffered from poor transduction efficiencies, short-term or silenced gene expression *in vivo*, and the difficulty of delivering therapeutic protein to target cells, but have shown some remarkable results in animal models of MPS disorders.

As summarized in table 1.2, different approaches to therapy offer specific therapeutic benefits, however no therapy is complete. A unique therapy may be of benefit to a subset of MPS I patients which have premature stop mutations. In this strategy, aminoglycosides are used that suppress premature nonsense stop mutations. MPS I fibroblasts heterozygous for *IDUA* stop mutations Q70X and W402X, common *IDUA* mutations, showed a restoration of almost 3% of normal IDUA activity levels when treated with gentamicin. Gentamicin treatment reduced GAG accumulation in MPS I cells to a normal level for at least 2 days after discontinuing treatment, and produced a reduction in lysosomal storage as shown by flourescent microscopy (Keeling *et al.*, 2001). This treatment could have applications for numerous disorders resulting from premature stop mutations but the *in vivo* effectiveness and tolerance has not yet been shown.

1.3.2 MPS animal models

Animal models of human disease are useful both in understanding disease pathophysiology as well as assessment of therapies. Naturally occurring animal models for a number of MPS disorders have been identified, including alpha-L-iduronidase deficiency (MPS I) in cat (Haskins *et al.*, 1979) and dog (Shull *et al.*, 1982), aryl

sulfatase deficiency (MPS VI) in cat (Jezyk *et al.*, 1977), and beta-glucuronidase deficiency (MPS VII) in dog (Haskins *et al.*, 1984) and mouse (Birkenmeier *et al.*, 1989).

Examination of these naturally-occurring models indicates they represent well the disease pathology and course observed in the corresponding human MPS disorder. In the MPS I cat, a three basepair deletion leads to the predicted loss of a single aspartate residue from the feline IDUA polypeptide (He *et al.*, 1999). The level of residual IDUA activity expressed from the three basepair deletion allele is uncertain, but transient overexpression of the cDNA including the mutation produced no detectable IDUA activity. The phenotype of MPS I in the cat includes somatic, neurological, and skeletal involvement similar to intermediate or severe MPS I in humans.

The MPS I dog model shares with the MPS I cat an intermediate to severe course involving somatic, neurologic and skeletal systems, and has been used extensively in the assessment of treatment protocols for MPS I. Secondary accumulations of GM_2, GM_3, and gangliosides have been detected in canine MPS I as observed in humans. The organization of the canine *Idua* gene has been determined and the cDNA has been sequenced. The basis of IDUA deficiency in the MPS I dog has been found to result from a G-to-A transition in the donor splice site in intron 1 of the canine *Idua* gene, leading to inclusion of intron 1 in the mRNA and the creation of a premature termination codon at the exon-intron junction (Menon *et al.*, 1992). The MPS I dog is believed to produce no IDUA activity and may further have a cross reactive material (CRM) negative status, which models those severe human MPS I cases with no generation of immunogenic protein. This has important implications for therapies which introduce potentially immunogenic IDUA protein or nucleic acid encoding IDUA to patients that

have not been exposed to IDUA antigens, and thus the MPS I dog models the challenges encountered in CRM negative MPS I patients.

The most dramatic therapeutic success has been demonstrated in another MPS model, the MPS VII mouse. A naturally occurring mouse model of complete beta-glucuronidase (GUS) deficiency (MPS VII, Sly disease) has been identified (Birkenmeier *et al.*, 1989). In addition to HS and DS stored in MPS I, MPS VII includes accumulation of KS GAGs, and in humans complete GUS deficiency results in a phenotype similar to severe MPS I, with involvement of somatic, skeletal and, to a lesser extent than MPS I, neurologic impairment. A number of factors contribute to the utility of the MPS VII mouse, in addition to the advantages of mouse models in general discussed, including 1) the availability of a genetically well-defined, inbred population of MPS VII carrier and affected mice, 2) the clinical, pathologic, and biochemical characterization of MPS VII mice, 3) availability of recombinant GUS enzyme, 4) a detailed understanding of the normal enzyme, including structure and important modificatons relevant to function has been developed, and 5) the generation of histochemical markers to identify *in-situ* the location of functional GUS enzyme. Important novel findings have been made with the MPS VII mouse that may apply to the MPS disorders in general. MPS VII mice have defects in immune function including an impaired T-cell proliferation response and decreased antibody production after immunization with foreign antigens (Daly *et al.*, 2000). These defects are thought to result from the inhibition of proteases required for antigen processing by lysosomal GAGs. Fetal lysosomal storage in MPS VII mice is evident very early, by 15.5 days of gestation, and can be detected in brain as early as 3 weeks of age (Casal and Wolfe, 2000). The phenotype of MPS VII is different when the

identical mutant allele is expressed in different mouse strains, including differences in vigor, fertility, and longevity, indicating the importance of modifying genes (Casal *et al.*, 1998).

1.3.3 Bone Marrow Transplantation for MPS I in humans

Bone marrow transplantation is used as a therapy for MPS and other lysosomal storage disorders with limited success. Bone marrow is used as a source of tissue for transplantation as it undergoes extensive proliferation, offers long term expression stability, and generates circulating effecter cells that permeate the entire body. Bone marrow transplantation carries a high risk of mortality and morbidity from graft versus host disease and other complications. In a group of 23 MPS patients treated with BMT, a mortality rate of 30% was observed when HLA-identical sibs were used as donors and even higher rates occurred with noncompatible donors (Pearson, 1986). While effective for the somatic features of MPS I such as hepatosplenomegaly, corneal clouding, and joint mobility, BMT is of limited benefit to the neurologic and skeletal complications of MPS I. Skeletal abnormalities do not appear to be reversible, though complications can be partially prevented if transplantation occurs very early in the course of disease. Likewise neurologic degeneration may be stabilized or partially prevented when BMT is performed before significant neurologic dysfunction is present (Shapiro *et al.*, 1995). This highlights the need for early diagnosis and intervention for MPS I. The limited availability of suitable marrow donors, the mortality associated with the procedure, and the limited effect on critical neurologic and skeletal features of MPS I make BMT a less than ideal treatment.

1.3.4 Bone marrow transplantation in MPS animal models

Bone marrow transplantation (BMT) of allogeneic normal marrow into myeloablated MPS I dogs has been performed with partial success (Breider *et al.*, 1989, Shull *et al.*, 1987, Constantopoulous *et al.*, 1989). BMT decreases urinary excretion of GAGs and leads to significant improvement of somatic tissues including liver, spleen, and kidney. Modest improvement was noted in the CNS, where low levels of IDUA activity were detected after transplantation, producing a decrease in brain GAG levels and decreased neuronal vaculation (Shull *et al.*, 1987), but considerable CNS pathology persists after BMT. Corneal opacity was largely alleviated by BMT (Contantopoulos *et al.*, 1989), however skeletal disease showed only limited improvement or was delayed in progression (Shull *et al.*, 1988). This is similar to the limited benefit obtained with BMT in humans, where somatic tissues show significant improvement while CNS and skeletal features of MPS I remain problematic, and confirms the utility of the MPS I dog for evaluation and refinement of BMT for human MPS I.

Similar to the findings from BMT in human and canine MPS I, BMT in young adult MPS VII mice is of limited benefit to the skeletal and CNS manifestations of MPS VII (Birkenmeier *et al.*, 1991). The limited success of BMT is believed to result from the presence of irreversible features of disease and the closing of windows for therapeutic intervention, stimulating the investigation of therapy earlier in the course of murine MPS VII. BMT in newborn MPS VII mice treated with conditioning irradition showed improvement in somatic systems as expected from previous results but, importantly, significant improvement was shown in bone growth and structure. Neuronal storage and behavioural abnormalities were not affected. While promising, early BMT was not

successful in correcting storage in all tissues and the irradiation treatment required for engraftment induced dysplasia in brain, bone, and other tissues (Sands *et al.*, 1993, Bastedo *et al.*, 1994). This prompted investigation of early, non toxic approaches to therapy. Without preconditioning such as marrow ablation, a large dose (10^7) of bone marrow cells was introduced by *i.v.* injection to 3 day old MPS VII mice, where it is was hoped they would engraft resulting in chimeric recipients. Long-term multilineage engraftment was established and positive outcomes included prolonged life, improved bone structure, and generally reduced storage, but no reduction in neuron lysosomal storage was observed (Soper *et al.*, 2001). As described earlier, the fetal environment offers unique advantages for therapy. Transplanation of fetal donor tissue into diseased fetal recipients offers further advantages, as graft versus host disease is limited because of both the immune tolerance of the fetal recipient and the immune incompetence of the fetal donor cells, and additionally fetal tissue should contain a higher proportion of stem cells than older tissues. Transplantation of allogenic, transgenic fetal liver cells overexpressing human GUS enzyme into fetal recipients showed early clinical improvement at 2 months of age but no improvement at 7 months (Casal *et al.*, 2001). Low engraftment levels were assumed to limit therapeutic benefits, however the non-toxic, early approach clearly shows promise.

1.3.5 Cellular transplantation in MPS animal models

Specifically targeting the CNS manifestations of MPS VII, transplantation of neuronal progenitor cells into the cerebral ventricles of newborn mice resulted in long term engraftment and increased GUS activity in the CNS and decreased lysosomal storage in neurons and glia (Snyder *et al.*, 1995), an encouraging result for CNS therapy.

Another transplantation approach assessed on the MPS VII mouse is the implantation of neo-organs consisting of normal or overexpressing fibroblasts encapsulated in a matrix designed to limit immune destruction of internal GUS-expressing fibroblasts. Introduction of microcapsules overexpressing GUS into the peritioneal cavity of MPS VII mice reduced liver, spleen and general visceral storage but failed to increase GUS activity in the brain, and appeared to invoke an anti-GUS antibody response which limited GUS level (Ross *et al.*, 2000), while introduction of the microencapsules into the cerebral ventricles reversed local brain storage and resulted in increased brain GUS activity and more normal behavior (Ross *et al.*, 2000).

1.3.6 Gene therapy for MPS I

Gene therapy for human MPS I has not yet been attempted. Challenges facing GT approaches include maintaining therapeutic levels of gene expression, delivery of gene constructs to critical tissues like the brain and bone, and immune response to novel proteins or delivery agents. The attraction of gene therapy is the possibility of a universal treatment, without ongoing infusion. A number of groups have investigated the early stage of autologous marrow transplantation with retrovirally transduced patient tissue. Fairbairn *et al.* constructed a retroviral vector with the full length cDNA for IDUA and used it to transduce bone marrow from patients with MPS I. They showed successful gene transfer into desired CD34+ cells and enzyme expression in the resulting progeny cells (Fairbairn *et al.*, 1996). The enzyme produced was able to correct the lysosomal distention in MPS macrophages, confirming that the enzyme is functional and localizes to the lysosome by both the endogenous and exogenous routes as desired. No human trials using this approach have yet been attempted.

Animal studies on models of MPS disorders have shown improvement to critical organ systems not addressed in human therapy. Most impressive are the results from adeno-associated virus, or AAV, used to directly transduce diseased tissue *in vivo*. Most importantly, it remains to be determined what amount of correction of skeletal and neurologic systems is possible in MPS I, and how to achieve this. Specifically, the cellular targets, and timing of introduction, critical to the successful correction of all complications of MPS is not yet known.

1.3.7 Gene therapy in animal models of MPS disorders

The MPS disorders are single gene disorders with obvious, easily detectable pathologic involvement and as such are considered good models for gene therapy. The main issues limiting improvement of the CNS and skeletal features of MPS I after BMT or ERT are believed to relate to limited delivery to these tissues and/or the presence of irreversible pathology before the introduction of therapy. Ideally, therapies would correct all aspects of MPS I and be widely available. Gene therapy offers the potential for delivery to many cell types and wide spread availability. Numerous gene therapies have been assessed on the MPS I dog (see table 1.3). Direct intramuscular injection of plasmid encoding the alpha-L-iduronidase cDNA resulted in no detectable enzyme production (Shull *et al.*, 1996). A further attempt at muscle derived IDUA expression used myoblasts grown *in vitro* from muscle biopsies transduced with a retroviral vector containing the canine gene under control of the muscle creatine kinase enhancer. While transduced myoblasts showed several hundred fold overexpression of IDUA *in vitro*, enzyme

Species	Therapy	Outcome	Reference
Dog	Bone marrow transplantation	Benefit to somatic storage Improved mobility Continued skeletal disease Some IDUA activity in brain	Breider *et al.*, 1989, Shull *et al.*,1987, Constantopoulous *et al.*, 1989
Dog	Enzyme replacement therapy. Intravenous infusion of human recombinant IDUA	Benefit to somatic storage Some IDUA activity in brain No improvement to cartilage Immune response	Kakkis *et al.*, 1996
Dog	Adult transfer of retrovirus transfected myoblasts	Immune response No amelioration of disease	Shull *et al.*, 1996
Dog	In-utero injection of IDUA encoding retrovirus	Short term expression in multiple tissues No amelioration of disease course	Meertens L *et al.*, 2002
Dog	In-utero transfer of iduronidase-transduced autologous HSCs	Immunotolerance to IDUA protein Low level engraftment No amelioration of disease course	Lutzko *et al.*, 1999
Cat	ERT Intravenous infusion of human recombinant IDUA	Reduced lysosomal distention Limited delivery to brain Immune response	Kakkis *et al.*, 2001
Mouse	ERT Intravenous infusion of human recombinant IDUA	Reduced lysosomal distention Continued skeletal disease Limited delivery to brain	Clarke *et al.*, unpublished

Table 1.3: Therapies for MPS I assessed on MPS I models

production declined rapidly following reintroduction of the cultured cells in to MPS I dogs. Antibodies specific to IDUA and inflammation at sites of myoblast injection were detected (Shull *et al.*, 1996).

Host immune response likewise appears to limit the benefit of autologous transplantation of retrovirally transduced hematopoietic stem cells into nonmyeloablated recipients. Even with high level transduction and overexpression at 10 to 200 fold normal levels in long-term marrow cell cultures, and evidence of engraftment persisting after 2 to 3 years post-infusion, albeit at low levels of 0.01 to 1% in blood and marrow leukocytes, no IDUA enzyme or transcripts encoding IDUA were detected in any recipient dog (Lutzko *et al.*, 1999a). Examination of immune responses revealed humoral responses to IDUA, and cellular responses were detected against IDUA transduced, but not control, cells (Lutzko *et al.*, 1999b).

The prenatal environment may be immunogically naïve and provide for the introduction of therapeutic levels of enzyme before the formation irreversible features of MPS I. To evaluate HSC gene therapy for canine MPS I in the preimmune fetal environement, *in utero* adoptive transfer of IDUA transduced MPS I LTMCs was performed on fetal nonmyeoloablated MPS I pups. (Lutzko *et al.*, 1999) Again, only low level (1%) engraftement was observed, and no IDUA activity or IDUA transcripts were detected in recipients. All recipients died of MPS disease with no evidence of improvement from the therapy, however, in contrast with post-natal transplanatation, no evidence of a humoral response against IDUA was detected. The low levels of engraftment observed, coupled with poor maintenance of proviral IDUA expression, at present limit the utility of this approach for MPS I. Direct injection of a retrovirus vector into the developing fetus showed successful transduction of numerous cells types, and, while gene expression and IDUA activity were detected in the liver and kidney of a deceased pup, IDUA activity was not detected in adult tissues of surviving pups

(Meertens *et al.*, 2002). This again may be the result of deficiency in long term expression from proviral vectors. None of the gene therapy approaches yet assessed in a model of MPS I produce significant improvement to all tissue systems although the benefit of early intervention is clear.

Gene therapy approaches have also produced some exciting results in the MPS VII mouse. Reversal of pre-existing storage in neurons and glia was observed with implantation of retrovirally transduced fibroblasts overexpressing GUS into the neocortex of adult MPS VII mice (Taylor *et al.*, 1997). However, expression of the transgene was lost with time. Stable integration into the host genome and efficient transduction of non dividing cells makes lentivirus mediated therapy attractive. Intraparenchymal injection of lentivirus encoding GUS into the brains of adult MPS VII mice produced stable cell transduction and GUS expression over the 16 weeks of the study, and lead to a marked reduction in lysosomal storage in neurons, glia, and perivascular cells distant from the site of injection (Bosch *et al.*, 2000).

Perhaps the best results of any approach have come with use of adeno-associated (AAV) virus vectors. AAV vectors can infect nondividing cells and may lead to integration into the host genome. A single intravenous injection of AAV carrying the human GUS cDNA in newborn mice resulted in long-term expression of GUS, persisting at least 4 months, in multiple tissues and a dramatic reduction in lysosomal storage in multiple organ systems, including the brain. Almost complete clearage of lysosomal storage was observed in neurons, glia, and meninges (Daly *et al.*, 1999). Follow-up a year after the single injection showed treated mice had superior survival rates, bone lengths, and weight than untreated MPS VII mice (Daly *et al.*, 2001). These promising results

indicate the neurologic and skeletal features of MPS disorders can be dramatically influenced with therapy, and highlights the importance of early intervention.

1.3.8 Enzyme replacement therapy for human lysosomal disorders

Enzyme replacement therapy (ERT) is well established for Gaucher disease type I, where clinical trials have shown reversal of the liver, spleen, and bone marrow complications of this disorder (Barton *et al.*, 1991). The skeletal pathology that may be present in Gaucher type I showed little improvement with ERT. As bone marrow transplantation does not appear to significantly alter the course of central nervous system disease observed in other forms of Gaucher disease with neurologic involvement (types II and III), ERT is not considered suitable for these forms of Gaucher disease. Important to the success of ERT for Gaucher was modification of the enzyme to target uptake to critical cells. With Gaucher as a model system, ERT has been developed for other lysosomal storage diseases including Pompe disease (Reuser *et al.*, 2002) and Fabry disease (Breunig and Wanner, 2003).

Recently, clinical trials determining the safety and efficacy of IDUA ERT for MPS I have been performed. Recombinant IDUA enzyme was used to treat 10 patients with varying severity of MPS I at a dose of 125,000 units per kg of body weight given intravenously once weekly for 52 weeks (Kakkis *et al.*, 2001). Significant improvement was noted including decreased hepatosplenomegaly with normalization of the size of the liver after 26 weeks in eight of the patients. Improved flexibility and decreases in urinary GAG were also found. Immune reaction to the enzyme can be problematic, and 4 patients had detectable serum antibodies to IDUA. It is clear the blood brain barrier

limits the delivery of intravenously injected IDUA to the brain. It is not yet known what impact long term ERT will have on skeletal complications of MPS I, but it is clear that early intervention has a greater impact on disease progression as found with BMT. ERT has important advantages relative to BMT including reduced mortality and morbidity, and is not limited by donor compatibility. With improvements in delivery and optimization of therapeutic regimes, ERT may become the preferred therapy for MPS I, as it has for non-neurologic forms of Gaucher disease.

1.3.9 Enzyme replacement in animal models of MPS

Enzyme replacement therapy (ERT) was attempted in canine MPS I in anticipation of human trials (Kakkis *et al.*, 1996, Shull *et al.*, 1994). While the large size of the dog makes trials prohibitive, human recombinant IDUA was produced in Chinese hamster ovary cells and purified for intravenous injection. Injected enzyme was found to clear from the blood quickly and was taken up primarily by the liver. Dramatic improvement in lysosomal storage in both hepatocytes and Kupffer cells were noted after a short trial of 12 days. MPS I dogs treated for 3 months showed normal levels of IDUA activity in liver and spleen, lower levels in kidney and lung, and barely detectable (less than 5% of normal) levels in brain, heart valves, and cartilage. Pathologic findings mirrored enzyme activity levels, with improvement in somatic tissues but no improvement noted in brain or heart valves (Shull *et al.*, 1994). In a long term, higher dose trial, an MPS I dog was treated for 13 months. While the brain showed detectable IDUA activity, and decreased lysosomal GAG storage, histologic improvement of the brain was not evident. In addition, no improvement in cartilage and heart valve was demonstrated with high dose long term ERT (Kakkis *et al.*, 1996). Thus ERT shares with

BMT limitations in the therapeutic benefit these options offer to the CNS and skeletal systems, and these limitations are faithfully revisited in the MPS I dog. As BMT involves replacement of the recipient's immune system, immune recognition of foreign IDUA protein is not an issue with BMT. In both short term and long term ERT trials, complement-activating antibodies against human IDUA were generated, which may be associated with immune complex deposition of therapeutic protein, disease, and reduced therapeutic efficiency. These may be partially relieved with slow infusion of enzyme and premedication, as described in the MPS I dog (Shull *et al.*, 1994).

ERT has been assessed extensively in the mouse model of MPS VII. When performed early as suggested by previous BMT trials, ERT results in delivery of detectable GUS activity to critical tissues including bone and brain and lead to a widespread reduction in storage (Vogler *et al.*, 1996). If performed before 14 days of age, ERT produced 31% of normal GUS activity in the brain and resulted in reduced neuronal storage (O'Connor *et al.*, 1998, Vogler *et al.*, 1999). This early window for CNS improvement indicates either the immature blood brain barrier allows access of intravenous proteins, or, storage after this time point is irreversible. This was the first demonstration of significant impact on the CNS and skeletal disease for an MPS disorder.

1.3.10 Generation of a murine model of MPS I

Gene targeting in embryonic stem cells was used to generate a murine model for MPS I with complete deficiency of IDUA (*Idua*-/-) which forms the centerpiece of this thesis (Clarke *et al.*, 1997). An interruption type knock out construct was designed to introduce the neomycin antibiotic resistance selection cassette into exon VI of the murine

Idua locus as shown in Fig 1.7. Care was taken to avoid the *Sat-1* gene and its possible

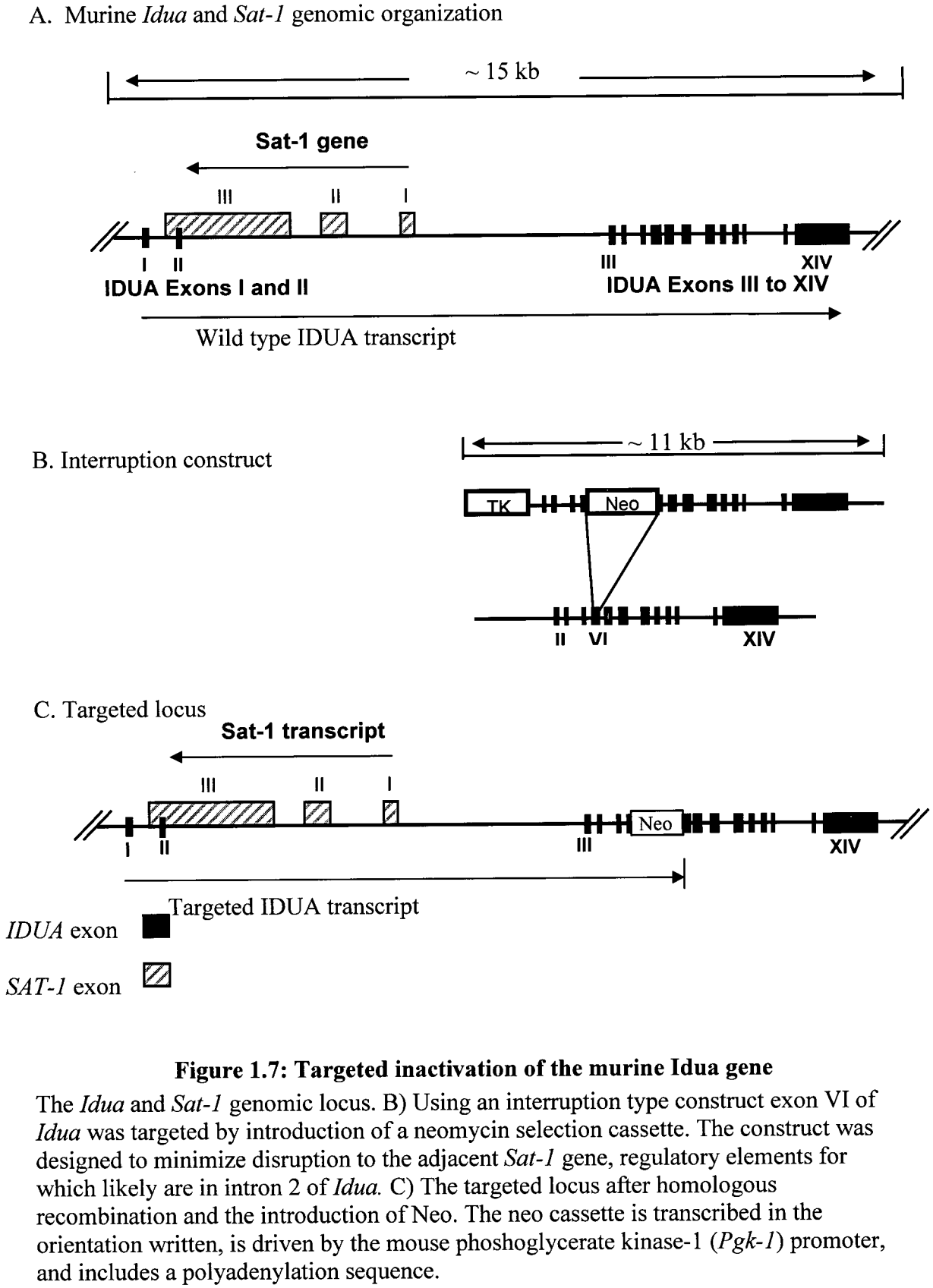

Figure 1.7: Targeted inactivation of the murine Idua gene

The *Idua* and *Sat-1* genomic locus. B) Using an interruption type construct exon VI of *Idua* was targeted by introduction of a neomycin selection cassette. The construct was designed to minimize disruption to the adjacent *Sat-1* gene, regulatory elements for which likely are in intron 2 of *Idua.* C) The targeted locus after homologous recombination and the introduction of Neo. The neo cassette is transcribed in the orientation written, is driven by the mouse phoshoglycerate kinase-1 (*Pgk-1*) promoter, and includes a polyadenylation sequence.

regulatory elements and an interruption construct rather than a deletion construct was used for IDUA inactivation. Analysis of *Sat-1* expression by Northern blot analysis indicated SAT-1 expression was not altered in *Idua* -/- mice, while RT-PCR analysis confirmed a complete absence of IDUA mRNA expression. Homozygous *Idua* -/- mice have no detectable IDUA enzyme activity and have increased urinary GAGs levels.

Normal appearing at birth, MPS I mice develop a characteristic phenotype first discernable at 3 weeks of age and including a flattened profile, thickening of the digits, and coarseness of the coat as seen in Fig 1.8. No obvious growth deficiency or mortality is seen within the first 20 weeks of life, but as discussed in Chapter 3, MPS I mice have a shortened life span. Skeletal disease in the MPS I mouse includes anterior flaring of the ribs and thickening of the facial bones as early as 4 weeks of age. Pathological evidence of disease was found at 4 weeks of age as lysosomal storage observed in limited tissues including cells of the reticuloendothelial system such as Kupffer cells, splenic sinusoidal lining cells, and glial cells. At 8 weeks of age, more widespread lysosomal storage is noted in hepatocytes, chondrocytes, and neurons, as seen in Fig 1.9.

While *Idua* -/- mice live to adulthood in contrast with humans with complete deficiency of IDUA, the severe skeletal, neurologic, and somatic disease observed in the *Idua* -/- mice is representative of the severe form of MPS I or Hurler syndrome. Chapter 3 is a study of the long term pathophysiology of IDUA deficiency in this murine model of MPS I. The generation of transgenic models of therapy for use in conjunction with the *Idua* -/- mouse strain is the focus of Chapters 4 and 5.

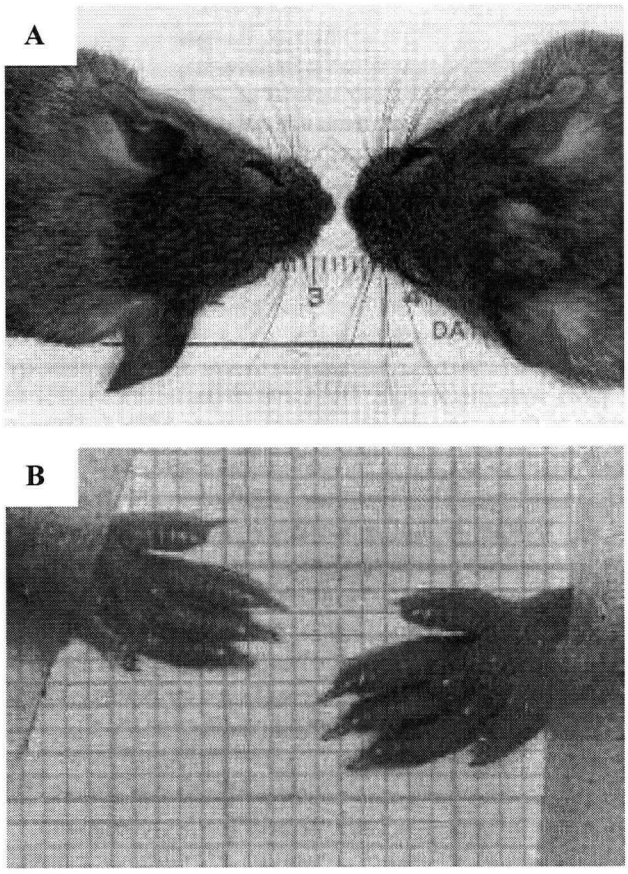

Figure 1.8: Clinical feature of Idua -/- mice at 12 weeks of age

A: Facial dysmorphic features of *Idua* -/- mouse (on the right) compared with *Idua* +/+ mouse (left). Note the shortness to the snout in the *Idua* -/- mouse with a loss of the fine taper to the face. B: Photograph of the hind paws of the same mice noting the broadness and thickness to the digits of the *Idua* -/- mouse, right. As published Clarke *et al.*, 1997.

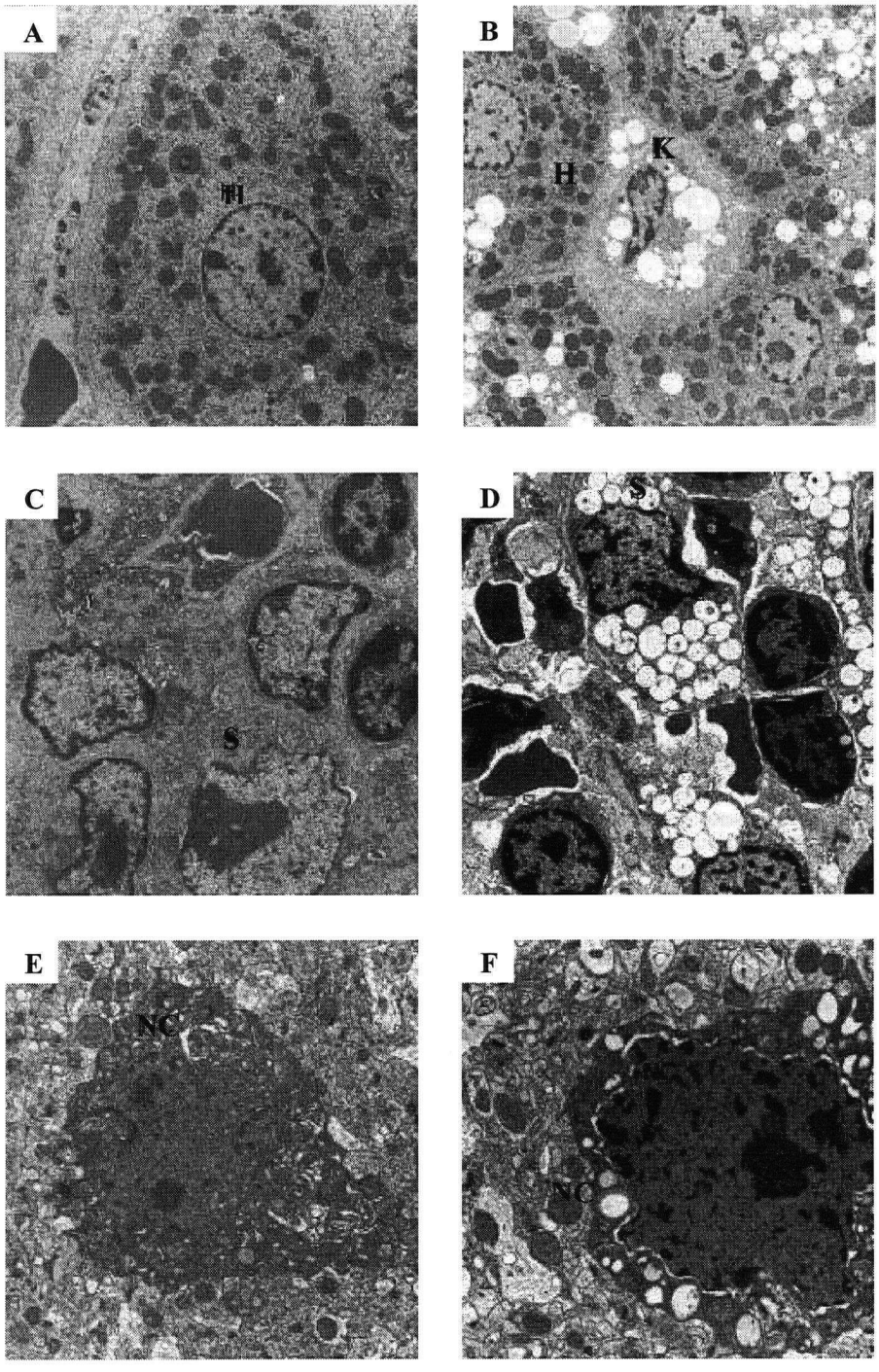

Figure 1.9: Electron micrographs from 8 week old Idua -/- and control mice

A, B: Liver, magnification 4175X. **A**: *Idua* +/+ mouse hepatocyte (H). **B**: *Idua* -/- mouse, note vaculated hepatocytes (H), and vacoulated central Kupffer cell (K). **C,D**:Spleen, magnification 5400X. **C**: *Idua* +/+ mouse, sinusoidal cell (S). **D**: *Idua* -/- mouse, note the highly vacoulated sinusoidal cell (S). **E,F**: Cerebral cortical neuron, magnification 9000X. **E**: *Idua* +/+ mouse. **F**: *Idua* -/- mouse, note the prominent neuronal cytoplasmic vacuolation (NC). All magnifications are approximate. As published Clarke *et al.*, 1997.

1.4 Thesis objectives and supporting hypotheses

Objective:

Characterization of the long term pathophysiology of the MPS I mouse.

Hypothesis:

IDUA deficiency in the mouse will result in a progressive disease course similar to severe MPS I in humans.

Objective:

Generation of a conditional transgenic mouse line with the potential to express human IDUA.

Hypotheses:

Above a certain level, expression of the human cDNA encoding IDUA is toxic and will produce a unique phenotype, while low level transgenic expression of IDUA will be tolerated in a normal background.

Low level transgenic expression of human IDUA will be corrective for all aspects of murine MPS I.

Chapter 2: Materials and Methods

2.1 Polymerase chain reaction

Primer ID	Purpose	Primer Sequence 5 prime to 3 prime	Product size in basepairs	Conditions
Neo A PrimerB	ES clone and mouse knockout	GGAAGACAATAGCAGGATGCT AAGATGGCTTGTCACCTGTCTTCAC	1200	58 c anneal 35 cycles
HID1F HID4R	Human IDUA detection	CGCTTCTGGAGGAGCACAGG CTGGAGACCAAGTCCTTCCACTC	340	62 c anneal 35 cycles 2% DMSO
HID3F HID7R	Human IDUA detection	CTGAGCTACAACTTCACCCACCTG CTCGTCGTTGTAAATGGGGGTGTC	580	68 c anneal 30 cycles
HID4F HID6R	Human IDUA detection	GACTTTGAGGACAAGCAGCAGGTG CTTCCTGTGGAGGGAGATGTAGTC	370	62 c anneal 35 cycles

Table 2.1: PCR primers

Isolated genomic DNA was used in PCR reactions. PCR primers used in this thesis are shown in table 2.1. Typical conditions were 1mM $MgCl_2$, 0.8 um each primer, 0.1 mM dNTP, 0.5 U of Taq DNA polymerase (Gibco BRL), and 1X PCR buffer in a final volume of 25 to 50 µl. PCRs were initiated at 94 C for 2 minutes and then cycled through annealing and elongation for 30 to 40 cycles as indicated.

2.2 Preparation of the human IDUA cDNA

The 2100 basepair sequence enoding the human IDUA cDNA, (a gift from Dr. John Hopwood, Women's and Children's Hospital, Adelaide Australia), was removed

from vector backbone with an *EcoRI* and *HindIII* co-digestion. Using partial digestion with *TspR1*, the native IDUA polyadenylation signal was removed. In preparation for ligation into assorted constructs, the *EcoRI/HindIII* fragment was Klenow blunted.

2.3 Construction of the myeloid-specific transgene constructs. (CD11B-IDUA and CD11B-reporter gene)

The 6891 bp CD11b.HGH (D736).gck vector (a gift from Frank Jirik, published in Back *et al.*, 1995) was opened at a unique *BamHI* site for introduction of either the human IDUA cDNA or one of two reporter genes, beta-galactosidase or enhanced green fluorescent protein. The CD11b vector was then blunted and the 5'terminal phosphate residues were removed to reduce self ligation using calf alkaline phosphatase (CAIP) (BRL). CAFP and residual enzyme were removed in preparation for ligation. Finally the human IDUA cDNA, or one of the reporter genes, was blunted and ligated with the vector backbone. The final constructs were linearized, and mixed for pronuclear co-injection.

2.4 Construction of the myeloid-specific transgene constructs with a selection cassette for selection in ES cells. (CD11B-IDUA and CD11B-reporter gene)

To the CD11B-IDUA construct described above, a PGK-NEO selection cassette was added which allows for selection of ES clones that have integrated, and are capable of expressing, the transgene construct. The CD11B-reporter gene constructs did not have a selection cassette added and would be expected to be found in only a subset of Neo resistant clones after co-integration of the constructs following electroporation into ES cells.

2.5 Construction of a ubiquitous IDUA expressing transgene construct. (CMV-IDUA)

The pEGFP-C2 mammalian expression vector (Clontech) was used a source of a promoter for driving high level, ubiquitous human IDUA expression, as well as a source of the enhanced green flourescent protein (EGFP) gene. This vector includes a 600 bp human cytomegalovirus (CMV) immediate early promoter which was removed with sequential *Ase1* and *Nhe1* digests. The promoter was then blunted and ligated with a *Cla1* digested and blunted pBS-IDUA vector, placing the promoter in front of the IDUA cDNA. Orientation was checked with restriction digestion. The polyadenylation sequence and terminal non-coding 3 exons of the human growth hormone gene (HGH) was then removed from the CD11b parent vector, described earlier, to increase expression levels of IDUA. This 2.2 kb *EcoRI/EcoRI* hgh fragment was cloned into an existing *EcoR1* site. This completed the CMV-IDUA portion of the construct. A reporter construct was then isolated from pEGFP-C2, consisting of the CMV promoter and the EGFP gene as well as a polyadenylation sequence. First, a *BglII* and *BamHI* digest on pEGFP-C2 removed a multiple cloning site which included restriction sites that would make downstream isolation of the final construct difficult. After removal of the multiple cloning site, the modified pEGFP-C2 was self ligated. The CMV-EGFP 1.4 kb fragment without the internal multiple cloning site was then isolated using an *AseI/MluI* digestion, blunted, and ligated into the CMV-IDUA vector at an *EcoRI* site downstream of the CMV-IDUA fragment. The final construct, called CMV-IDUA, was prepared for pronuclear injection with an *XhoI/Bam HI* digest.

2.6 Construction of a ubiquitous IDUA expressing transgene construct with a selection cassette for selection in ES cells. (pFlox-IDUA)

For selection in ES cells, the isolated CMV-IDUA construct described above, including the EGFP reporter, was introduced into pFlox, a parent vector including both the neomycin resistance gene and the thymidine kinase gene (Marth, unpublished). The thymidine kinase gene was not required for this project but this vector contained convenient cloning sites relative to other neomycin encoding constructs.

2.7 Construction of a ubiquitous IDUA expressing transgene construct with a selection cassette for selection in ES cells. (pCAGGS-IDUA)

A second construct intended to drive high level, ubiquitous human IDUA expression was generated using a vector proven to result in high level expression in transgenic murine lines, pCAGGs (a gift from Dr. Jun-ichi Miyazaki, published in Niwa *et al.*, 1991). pCAGGs features a proven ubiquitously strong promoter based on the chicken beta-actin promoter as well as the CMV-IE enhancer. Other features of this vector include the rabbit beta-globin gene polyadenylation sequence for efficient post transcriptional processing, and splicing to increase expression levels. In order to generate a single construct that encodes both human IDUA as well as a reporter gene, I chose to use an internal ribosome entry site (IRES) which allows for expression of two distinct proteins from a single RNA transcript. By physically linking IDUA and reporter gene expression, cells positive for reporter gene expression are likely to express IDUA. The generation of pCAGGs-IDUA was intended to express human IDUA and the beta-geo fusion protein encoding neomycin resistance for selection in ES cells, as well as the reporter gene beta-galactosidase. A vector described earlier was used which included the human IDUA cDNA with no polyadenylation site in a pBS backbone. This vector was

digested with *XbaI*, and a 4.5 kb *XbaI/XbaI* insert containing an IRES site and linked beta-geo fusion gene were then ligated. This linked the IDUA cDNA to the IRES beta-geo sequences. Next, the IDUA-IRES-beta-geo fragment was isolated with a *SalI* and partial *NotI* digest, and the 6.7 kb fragment was isolated in preparation for ligation into the parent pCAGGS vector. However for later isolation of the completed construct, a *SalI* site had to be introduced into pCAGGs, which would allow eventual isolation of the completed transgenic construct with a single, complete *SalI* digestion. An oligo was designed which includes the *SalI* site and has a flanking *HindIII* site, and which would in solution form a duplex that would allow ligation with *HindIII* sites. The sequence for this oligonucleotide is 5'-AGCTGTCGAC-3'. After ligation of the *SalI* site into *HindIII* digested pCAGGs, the amplified vector was *EcoRI* digested to remove an undesired EGFP sequence, and a linker allowing sticky ligation with the 6.7 kb IDUA-IRES-beta-geo fragment was engineered. The linker was generated by producing two oligonucleotides which, as a duplex, would have exposed *EcoRI* sticky ends and contain both *NotI* and *XhoI* sites. The sequences of these oligos are: oligo #1: 5'-AATTCTCGAGGCGGCCGC-3', oligo # 2: 5'-AATTGCGGCCGCCTCGAG-3'. After addition of the *NotI* and *XhoI* sites, the vector was digested with *NotI/XhoI*, and the *SalI/NotI* 6.7 kb IDUA-IRES-beta-geo fragment would allow sticky ligation, as *XhoI* and *SalI* sites are compatible, however the junction formed is subsequently not recognized by *SalI*. Finally, a complete *SalI* digestion allows for the isolation of an approximately 9.4 kb transgene construct for electroporation into ES cells.

2.8 Construction of a conditional Cre regulated transgene construct with a selection cassette for selection in ES cells (pCCALL2-IRES-IDUA)

The pCCALL2-IRES-hAP/cg plasmid was opened at a unique *XhoI* site, blunted, and the terminal 5 prime phosphate group was removed to limit self-ligation. The blunted human IDUA cDNA, with no polyadenylation signal, was ligated with the construct. Plasmid clones with the IDUA insert were identified by PCR, and orientation of the IDUA insert was determined by restriction analysis.

2.9 Histopathology

Animals were sacrificed by cervical dislocation and tissues obtained within 20 minutes of death. The cerebrum and cerebellum of mutant and control mice were removed at autopsy and grossly examined and weighed. The cerebrum was sectioned coronally and the cerebellum horizontally. Sections were fixed in 10% neutral buffered formalin, snap frozen in liquid nitrogen and fixed in 4% gluteraldehyde. The paraffin embedded sections of cerebrum and cerebellum were sectioned at 5 microns, stained with haematoxylin and eosin (H & E), and periodic-acid schiff with diastase (PAS + diastase). Sections of the cerebral hemispheres and cerebellum were histologically examined by light microscopy. The hind limbs were disarticulated from the hips, cleared of soft tissue and fixed overnight in 10% neutral formalin. The bones were decalcified in 22% formic acid for 18 hours and bisected longitudinally. Paraffin embedded sections were then cut at 5 microns and stained with H & E. The growth plate, cortical and trabecular bone was examined histologically with both light and polarizing microscopy.

2.10 Radiography

Animals were anesthetized with methoxyflurane and X-rayed at 200 MAS and 50 KVP at a distance of 980 mm from the source using a General Electric portable X-ray machine.

2.11 Thin Layer Chromatography of Gangliosides

Total lipid was extracted from brain and partitioned with the method of Folch *et al.*, (1957), as modified by Suzuki (1965). Brain tissue from normal and mutant mice was weighed and then homogenized for 5 min. with 19 vol. chloroform-methanol (2:1, v/v). After filtration, the residue was extracted with 10 vol. chloroform-methanol (1:2, v/v) containing 5% H_2O. The filtered extracts were combined and chloroform was added to give a final concentration of chloroform-methanol of (2:1, v/v). The lipids were partitioned with the addition of 0.2 vol. of 0.8% KCl. The upper phase was removed and the lower phase was washed twice. The pooled upper phases were then dialyzed in Spectra/Por® tubing (Spectrum Medical Industries Co.) for 2 days at 4 °C against several changes of distilled H_2O and then lyophilized. The resulting gangliosides were resuspended with 200 µl of chloroform-methanol-water (10:10:3, by volume) and chromatographed on silica 60 Å plates (Whatman Inc.) with chloroform, methanol 60:40 and 0.2% calcium chloride for 8 hours. The volume loaded on each lane was normalized for a brain weight of 0.3 gms. The gangliosides were visualized by spraying with 2% resorcinol, followed by drying at 100 °C for 30 min.

2.12 Colorimetric Assay of Glycosaminoglycans

Urinary glycosaminoglycan and creatinine excretion was measured as described by Whitley *et al.* (1989). Urine samples from normal and affected mice were collected and stored at -70 °C until assayed. Heparan sulfate (Sigma Chemical Company) was used to generate a standard curve. Urine samples of 40 ul, diluted 2.5 times for normal mice and 8 times for mutant mice, were mixed with 500 µl of 35 µmol/L DMB reagent, sodium formate buffer, pH 3.5. Absorbancy at 535 nm was measured within 30 min. with a Beckman DU 640 spectrophotometer. Urinary creatinine was measured by the method of Folin using creatinine (Sigma Chemical Company) as a standard. 2 ul of urine was mixed with 8 ul of water followed by 500ul of picric acid solution. Absorbancy at 535 nm was measured after 20 minutes. Quantification of glycosaminoglycan and creatinine in the urine samples was done by comparing to the respective standard curves.

2.13 Embryonic stem cell growth and electroporation

R1 embryo stem cells (a gift from A. Nagy, Mount Sinai Hospital Research Institute, Toronto) at passage 13 were cultured on primary embryonic fibroblasts, according to conditions as described (Wurst and Joyner, 1993). ES cells were grown in Dulbecco's modified Eagle's medium with high Glucose (Gibco) supplemented with 15% fetal calf serum (Hyclone), 1 mM nonessential amino acids (Gibco), 1 mM sodium pyruvate (Gibco), 2 mM L-glutamine, 10-6 B-mercaptoethanol (Sigma) , and 1000 U/ml leukemia inhibitory factor (Gibco). ES and fibroblasts were cultured at 37 C with 5% CO2 in air with humidity. Electroporation of ES cells (1 X 10^7) at passage 14 or 15 was performed in a Bio-Rad Gene Pulser at 250 V, 500 uF. Immediately after electroporation ES cells were plated on gelatin (Sigma) coated plates at high dilutions to promote single

colony development. The next day neomycin selection using G418 (Gibco) at 200 ug/ml was commenced. After 7 to 10 days of selection individual ES colonies were picked, aggressively trypsinized (Gibco), and transferred to 96 well plates with embryonic fibroblasts for expansion. ES cells were grown for 2 to 3 days before passaging, involving trypsinization and transfer to 6 well plates with fibroblasts. ES cells were propagated on fibroblasts until sufficient numbers were attained for screening as desired and freezing. For freezing, log phase growth ES cells were trypsinized, counted and frozen in freezing media containing 50% Fetal calf serum, 10% DMSO, and 40% ES media (described above) at 5 million cells per ml in one ml cryovials.

2.14 Transfection of ES cells with Cre plasmid

Transfection of ES clones with Cre encoding plasmid (Joanne Fox, unpublished) was performed to identify clones capable of Cre recombination and expression of the human alkaline phosphatase reporter as well as transgenic IDUA enzyme activity. ES clones were seeded to achieve low density, rapidly growing clonal replica plates. Transfection was carried out as described using Lipofectamine (BRL Cat# 10964-013) in a 96 well plate format using 0.1 ug of plasmid DNA per well. ES clones were incubated with Cre plasmid for 3 hours, and clones were harvested 3 days later for reporter gene analysis and IDUA enzyme activity analysis.

2.15 IDUA enzyme assay

IDUA activity was measured using a sensitive fluorometric assay (Hopwood *et al.*, 1979). Tissues were homogenized in distilled water (25:1 volume to weight ratio) using a motor driven pestle in a chilled 10 ml glass tube. Enzyme assays were performed

in buffer consisting of 0.01 % formic acid, 77 mM NaCl, 7.7 mM sodium azide, 0.1 % Triton X-100 and 25 uM 4-methylumbelliferyl-(alpha-L-iduronide (Sigma) pH 3.5 in a final volume of 50 ul. Samples were incubated at 37C for 3-4 h for liver homogenates and cell culture samples, and 16 h for tail clippings. The reaction was stopped with 2 ml of 1 M glycine NaOH buffer, pH, 10.5. Fluorescence was measured with a Hoeffer Scientific Florometer (model TKO 100) and expressed in relation to protein mass as determined using the Lowry assay (Lowry *et al.*, 1951). Activity was expressed as nanomoles of 4-methyl-umbelliferone released per hour.

2.16 Beta-galactosidase staining of ES cells and tissue fragments

ES cells attached to plates were stained for LacZ by gentle fixation with 0.2% gluteraldehyde in 1X PBS for 5 minutes on ice. Cells were washed three times in wash buffer (2 mM $MgCl_2$, 0.01% deoxycholate, 0.02% Nonidet-P40, 100 mM $NaP0_4$, pH 7.3). Cells were then stained in wash buffer containing 1mg/ml X-gal, 6 mM potassium ferrocyanide, and 5 mM potassium ferricyanide. Staining was allowed to proceed overnight at 37 C, with staining often apparent within minutes to hours. Ear punches or sections of tail were stained for LacZ by placing in 96 well plates. Samples were washed three times in 1X PBS, then fixed for 10 to 30 minutes on ice in 0.2% gluteraldehyde in 1X PBS. Samples were then stained as described above, with staining apparent after 10 minutes.

2.17 Alkaline phosphatase staining of ES cells

ES cells bound to plates were fixed in 2% formaldehyde, 0.2% gluteraldehyde, in 1X Dulbecco's PBS with no Ca+ or Mg2+, for 5 to 10 minutes at 4 C. Cells were then

washed twice with 1X PBS at room temperature for 5 minutes each. Then 100 ul (for 96 well plate) of 1X PBS was added and plates were placed at 70 C for 30 minutes to inactivate endogenous alkaline phosphatase activity. Cells were then washed twice with 1X PBS at room temperature. Cells were then washed in alkaline phosphatase wash buffer, consisting of 100 mM Tris-HCl, pH 9.5, 100 mM NaCl, and 10 mM $MgCl_2$, for 10 minutes at room temperature. Cells were then stained with alkaline phosphatase NBT/BCIP stain (100 mM Tris-HCI, pH 9.5, 100 mM NaCl, 50 mM $MgCI_2$, 0.01% sodium deoxycholate, 0.02% NP-40, 337 ug/ml NBT (nitroblue tetrazolium salt; Boehringer Mannheim), and 175 ug/ml BCIP (5-bromo-4-chloro-3-indolyl phosphate, toluidinium salt; Boehringer Mannheim), well mixed, for 10 to 30 minutes at room temperature. Stain solution was then removed, cells washed gently twice with 1X PBS, and dehydrated with ethanol.

2.18 Alkaline phosphatase staining ear punches and tissue fragments

Tissues were fixed aggressively to allow penetration of the alkaline phosphatase substrate in 2% formaldehyde, 0.2% gluteraldehyde, 0.02% NP-40, and 0.01% sodium deoxycholate, in 1X Dulbecco's PBS with no Ca+ or Mg2+, for 5 to 10 minutes at 4 C. Tissues were then washed twice in 1X PBS, then a fresh volume of 1X PBS sufficient to completely cover tissues was added and endogenous alkaline phosphatases were heat inactivated at 70 C for 30 minutes. Tissues were again washed twice in 1X PBS, then washed in alkaline phosphatase buffer (100 mM Tris-HCI, pH 9.5, 100 mM NaCl, 10 mM $MgCl_2$) for 10 minutes, and stained with BM Big Purple alkaline phosphatase substrate (Boehringer Mannheim) at 4 C for 2 to 36 hours in the dark.

2.19 DNA Isolation

DNA was isolated from tissue (usually tail) or from cells using the same basic protocol. A suitable volume of lysis solution, containing 100 mM Tris-HCl pH 8.5, 5 mM EDTA, 0.2% SDS, and 200 mM NaCl, was added to samples. For a tail sample of 0.5 cm in length, 400 ul of lysis solution was used. Fresh proteinase K solution was added to a final concentration of 0.2 mg/ml from a 10mg/ml proteinase K stock. Samples were then incubated overnight at 56 C. An organic solvent extraction was then performed using a volume of chloroform equal to the volume of the digested sample, samples were mixed by inversion, then incubated at room temperature 5 minutes. Samples were then spun for 5 minutes at 12,000 rpm in a benchtop microcentrifuge and the upper aqueous phase containing DNA was transferred to a new microcentrifuge tube. A second choloroform extraction was performed using 400 ul choloroform, samples mixed, spun, and the aqueous phase transferred to a fresh tube. The final volume was estimated (usually slightly less than 400 ul) and twice the volume (approx 800 ul) of 95% ethanol was added to precipitate the DNA fraction. Samples were mixed gently by inversion and then spun at 12,000 rpm for 10 minutes. DNA pellets were then normally visible. The pellet was then washed twice by removing the aqueous phase, adding 400 ul of 70% ethanol, inverting, and spinning as above for 5 minutes. The ethanol was removed, the pellet was allowed to air dry no more than 5 minutes, and then the pellet was brought up in a suitable volume of autoclaved H_20 or Tris-EDTA, pH 7.5, for at least 3 hours to overnight at room temperature or 4 C. DNA concentration was determined by gel electrophoresis against standards of known concentration and/or by spectrophotometry.

2.20 Transformation

BRL DH5-alpha E. coli cells were used for all transformations. 50 ul of thawed cells were added to cooled tubes on ice containing 1 to 5 ul of plasmid DNA (or ligation reactions) and mixed gently by shaking. Cells were incubated on ice for 30 minutes and then heat shocked at 42 C for 30 seconds. Reactions were incubated on ice for 2 minutes before addition of 1ml of LB broth. Reactions were then incubated at 37 C at 200 rpm for 1 hour before plating on LB plates containing 50ug/ml ampicillin with or without X-gal (1% final) depending if color selection was applicable. Plates were then incubated overnight at 37 C and individual colonies analyzed for plasmid content.

2.21 Southern blotting

Genomic DNA was isolated as described and digested using suitable restriction enzymes. Digested DNA fragments were separated in agarose gels and the DNA was then transferred to Hybond –N nucleic acid transfer membrane (Amersham) overnight using standard transfer solutions (Southern, 1975). Suitable probe DNA was labeled with radioactive alpha-32P-dCTP (Amersham) using a random primer labeling system (Gibco BRL) and purified using a G-50 sephadex column. Hydridization was performed at 50 to 65 C in commercially available hybridization buffer (Clonetech). Washed membranes were exposed to Kodak X-OMAT scientific imaging film at -70 C for periods ranging from half a day to a week.

2.22 Animals

Animals were cared for under the guidelines set up by the Canadian Council on Animal Care. All animals used for these studies originated from a single founder and

were established by brother-sister mating. The mice were fed PMI Feeds autoclaved rodent diet 5010.

Chapter 3: Characterization of the long term pathophysiology of murine MPS I

Based on the paper "Murine MPS I: Insights into the pathogenesis of Hurler syndrome" Published in Clinical Genetics, 1998 Volume 53, pages 349-361.

Christopher Russell, Glenda Hendson, Gareth Jevon, Tina Matlock, Jessica Yu, Muktak Aklujkar, Kwok-Yu Ng, and Lorne A Clarke.

3.1 Abstract

A murine model which shows complete deficiency in alpha-L-iduronidase activity has been developed and shows phenotypic features similar to severe MPS I in humans. Here we report on the long-term clinical, biochemical, and pathological course of MPS I in mice with emphasis on the skeletal and central nervous system manifestations of disease. Affected mice show a progressive clinical course with the development of coarse features, altered growth characteristics and a shortened life span. Progressive lysosomal accumulation is seen in all tissues. Skeletal manifestations represent the earliest clinical finding in MPS I mice with histologic analysis of growth plate and cortical bone revealing evidence that significant early pathology is present. Analysis of the central nervous system has revealed the novel finding of progressive neuronal loss within the cerebellum. In addition, brain tissue from MPS I mice show increased levels of GM_2 and GM_3 gangliosides. This murine model clearly shows phenotypic and pathologic features which mimic those seen in severe human MPS I and should be an invaluable tool for the study of the pathogenesis of generalized storage disorders.

3.2 Introduction

The phenotype of IDUA deficiency or MPS I in humans is represented by a spectrum of clinical severity ranging from severely affected individuals, *i.e.* Hurler syndrome, to more mildly affected individuals *i.e.* Scheie syndrome. In the severe form, symptoms are recognizable in toddlers (age 1 to 3 years), clinical features progress rapidly, mental retardation becomes pronounced, and death occurs in the first decade. The milder form of the disease is associated with a later onset of symptoms, slower

disease progression, no mental degeneration, and life into adulthood. Features of MPS I common to both ends of the clinical spectrum include corneal clouding, dysostosis multiplex, joint involvement and visceral storage, however, in severe MPS I, the onset of these symptoms occurs earlier and become more pronounced than in milder forms of MPS I (Scheie *et al.*, 1962).

This clinical heterogeneity is reflected by the many mutations that have been identified at this locus (Clarke *et al.*, 1993 and 1994, Scott *et al.*, 1993, 1995). Mutations that permit some enzyme activity, as low as 0.13% of normal IDUA protein, are associated with a milder phenotype (Scott *et al.*, 1993). This finding indicates that small amounts of residual activity, particularly within the brain, can significantly alter the clinical phenotype, thus indicating the potential of gene therapy and enzyme replacement strategies for this group of disorders. Enzyme replacement in the form of bone marrow transplantation (BMT) in humans with MPS I, has shown that although visceral storage can be significantly reduced, there is a lesser effect on the CNS complications of disease and very little effect on the skeletal manifestations (Peters *et al.*, 1996, Field *et al.*, 1994). In addition, the response to BMT is related to the age of the patient at the time the procedure is performed (Shapiro *et al.*, 1995).

We previously reported the generation of a murine strain completely deficient in iduronidase by targeted disruption of the murine *Idua* gene. Early characterization revealed that these mice showed phenotypic, pathologic and biochemical features which resembled severe deficiency of IDUA in human MPS I (Clarke *et al.*, 1997). This chapter characterizes the long term clinical, pathological and biochemical features of this model with emphasis on the development of CNS and skeletal manifestations of IDUA

deficiency. Together it is hoped this will identify pathways altered in IDUA deficiency thereby suggesting targets for therapeutic intervention. As the IDUA deficient MPS I mouse model will be used in the assessment of therapies for MPS I, characterization of the *Idua* -/- mouse might also provide markers of disease useful in therapy trials.

3.3 Results

3.31 Clinical Features

At birth, IDUA deficient (-/-) mouse pups cannot be discerned from controls. By 4 weeks of age, male *Idua* -/- mice begin to present with a progressive facial phenotype including wide set eyes, broadening of the cranium, foreshortening of the snout, and protruding of the nasal bridge. The facial features present earlier in *Idua* -/- males than in *Idua* -/- females. By 8 weeks of age, affected mice have thickened digits with paws lacking in detailed relief pattern as compared with controls. There is slow progression in the degree of facial dysmorphology with the mice appearing quite coarse by 16 weeks of age, when affected mice of both sexes have facial coarseness reminiscent of human patients with Hurler's syndrome. The progression of these features is detailed in figure 3.1.

The coats of affected mice are tattered and thin relative to normal mice. Redundancy of the skin of the face and thickening of the perioccular tissues results in partial closure of the eyes in some affected mice. Slit lamp examination does not reveal evidence of corneal clouding even late in the progression of murine IDUA deficiency. While the eyes of some *Idua* -/- mice become encrusted with mucous, the chronic rhinitis often present in human MPS IH is not an obvious feature of murine IDUA deficiency.

3.1A

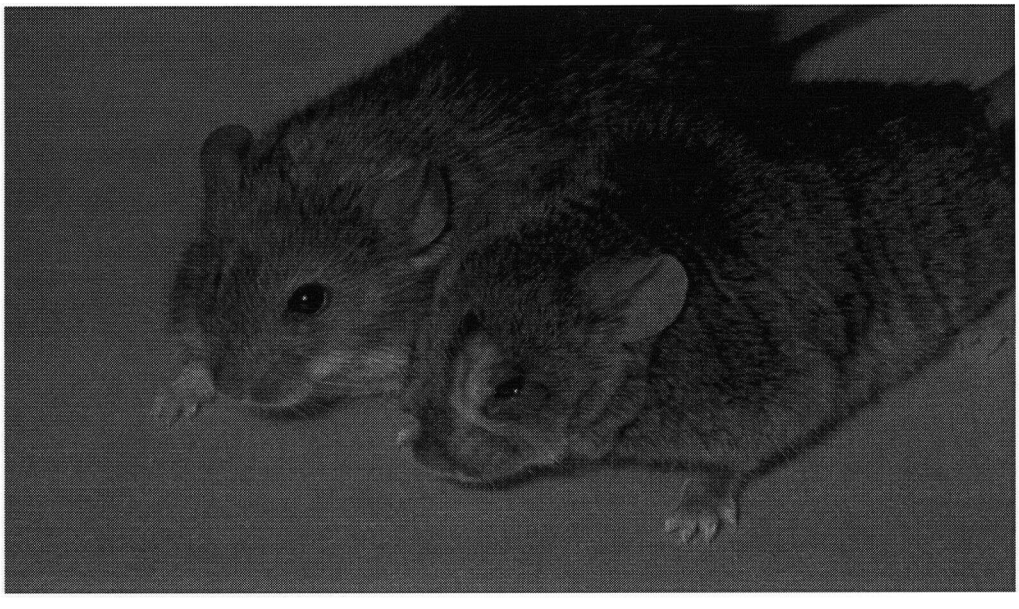

3.1B

Figure 3.1: Phenotype of MPS I mice

3.1A: Ages from left to right; 4, 16, 23, 45, and 54 weeks. Note the progressive development of coarse facial features and coarseness to the coat. 1B: Normal (left) and MPS I mice (right) at 40 weeks of age. MPS I mice develop severe folding of skin as observed over the entire body of the MPS I mouse, and which can obscure vision. Gibbous deformity is present in the MPS I mouse and mobility is limited. Note loss of hair is unrelated to IDUA deficiency.

Young affected mice are active and appear capable of a full range of movement, although, with age *Idua* -/- mice show a progressive decline in mobility. By 40 weeks of age, *Idua* -/- mice do not require anesthesia or restraint during examination, in marked contrast with controls. Many *Idua* -/- mice develop gibbous deformity which is resistant to flexion during examination under anesthesia or after death. Subluxation of the hips is apparent in some older *Idua* -/- mice and may further limit mobility. With age, many *Idua* -/- animals have a severely abnormal gait, with dragging of the hindquarters during forward locomotion.

3.32 Life span of MPS I mice

Figure 3.2 highlights the life span of *Idua* -/- animals within this colony. The average age of death of affected mice is approximately 48 weeks, with the earliest death occurring at 25 weeks of age. No affected animals have lived past 85 weeks of age. Amongst control litter mates approximately 5% die of natural causes within the first 90 weeks, and mice typically live over 2 years. The immediate causes of death in affected mice are not readily apparent, however, autopsy has revealed evidence of congestive heart failure in some mice.

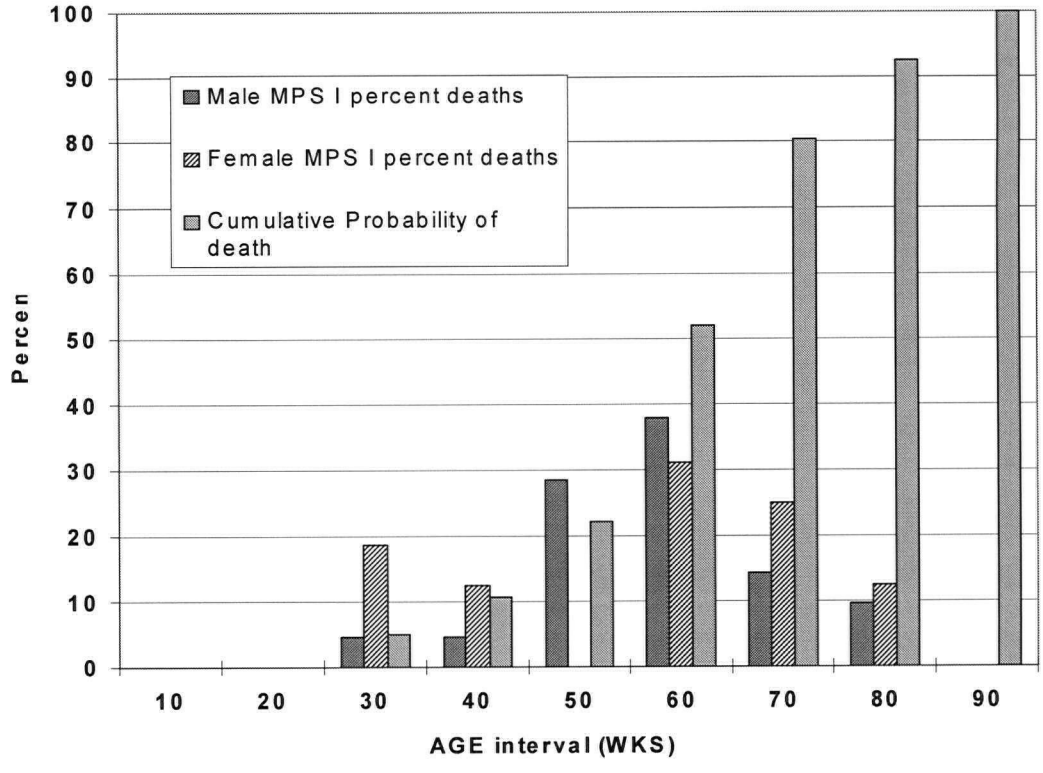

Figure 3.2: Life span of affected animals

The percent of natural deaths occurring per each weekly time interval was calculated by dividing natural deaths in that interval by the total number of natural deaths (total natural deaths MPS I male mice=21, females=16). The cumulative probability of death was calculated taking into consideration all animals that persisted through prior time intervals, and thus includes in addition to natural deaths, animals that were sacrificed as well as animals that were still alive at the time of analysis. A total of 138 MPS I mice were used in the calculation of cumulative probability of death.

3.33 Growth Profiles

Weekly weights were recorded on all mice, including those with genotypes MPS I *Idua* -/-, *Idua* +/- heterozygotes, and *Idua* +/+ wild type homozygotes, to generate weight curves as an indication of growth. *Idua* +/- and +/+ were used as controls to generate growth curves of normal mice. The genetic background of the *Idua* -/- and normal mice is a mix of C57bl/6 and CBA strains. Figure 3.3 depicts the growth profiles for both male (a) and female (b) mice within the colony.

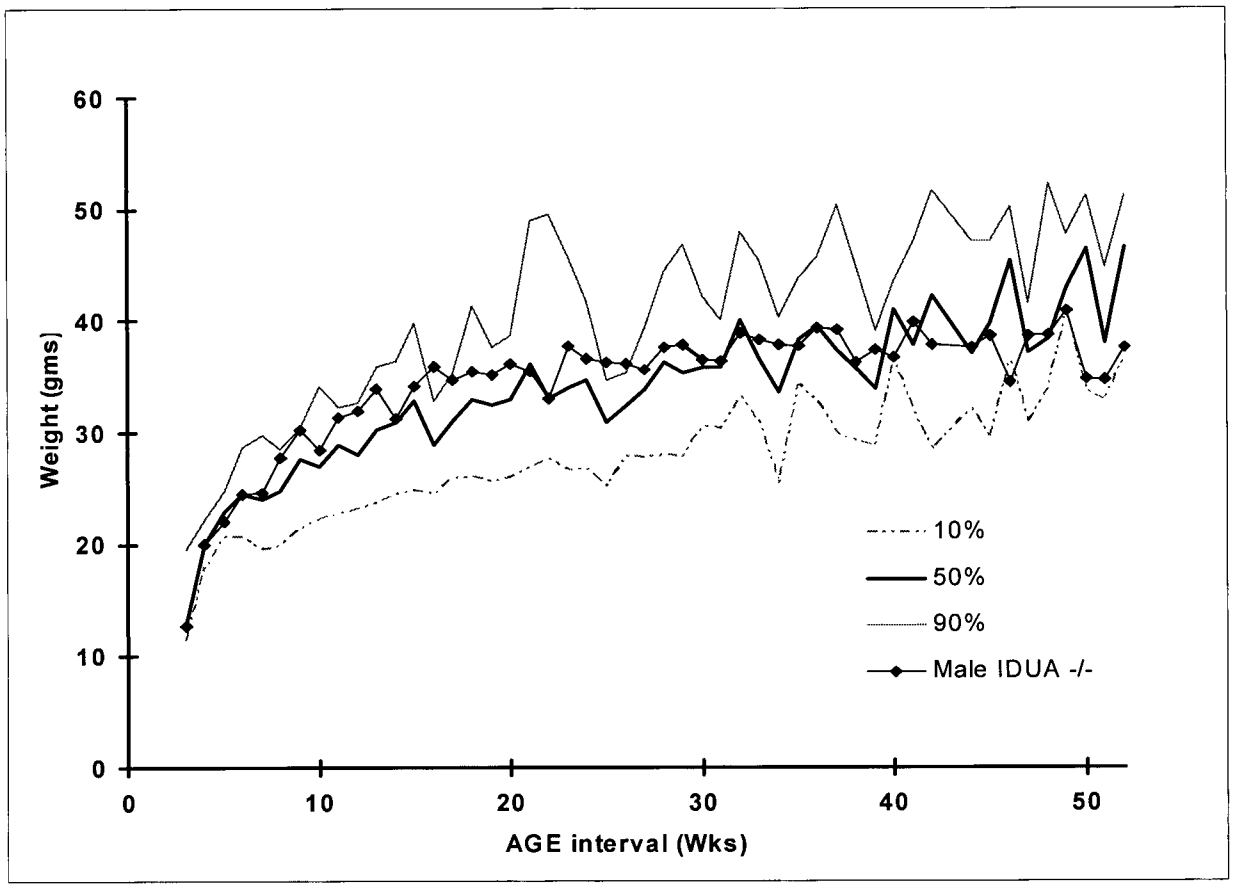

Figure 3.3A: Growth curves of male Idua -/- mice relative to normals

Weights were monitored as an index of growth. 10, 50, and 90th percentile weekly interval growth curves were established for normal animals. The median weight of mutant mice at each time interval is plotted against the normal curves. M. Aklujkar gathered animal weights.

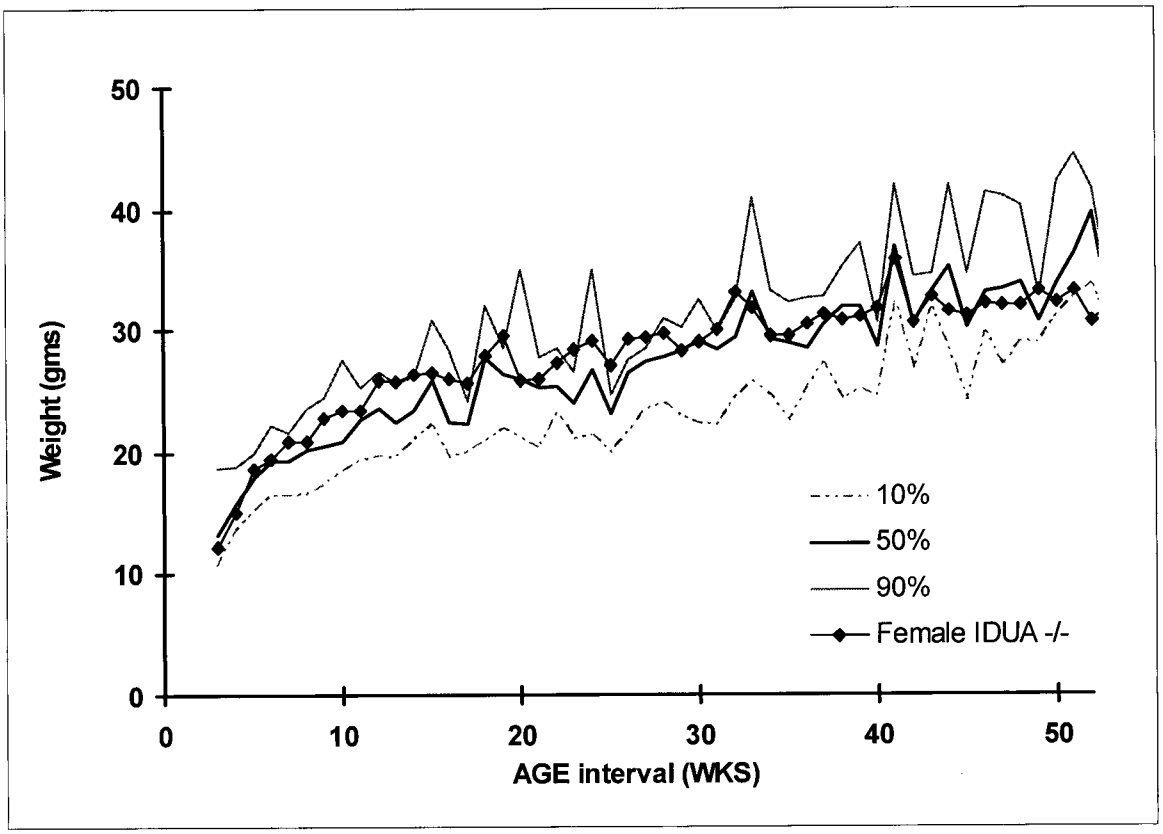

Figure 3.3B: Growth curves of female Idua -/- and control mice

Female *Idua* -/- mice have a similar pattern of growth as *Idua* -/- males. Young *Idua* -/- females (3-30 weeks) are consistently heavier than normals. M. Aklujkar gathered animal weights.

A total of 1300 separate weights were used to profile the growth of normal mice (757 male, 543 female) and 875 weights were used for the mutant data points (494 males, 381 females). The weights of control animals are expressed as percentiles for each weekly interval and the weights for the same interval of mutant animals are expressed as the median (50th percentile). Males and females differ significantly in weight and so are graphed separately; however the general growth pattern of *Idua* -/- males and females is similar. Large fluctuations in the control growth profiles of the normal animals reflect

the variation in sample size for each interval. *Idua* -/- mice of both sexes consistently grow at or above the 50th percentile from 8 weeks to approximately 25 weeks of age. However, by 30 weeks growth of the mutant mice appears to plateau, crossing the 50th percentile curve of the normal mice. By 50 weeks, mutant mice have weights well below the 50th percentile of controls.

3.34 Radiographic Examination

Figure 3.4 reveals the radiographic changes discernible at 57 weeks in *Idua* -/- animals.

Figure 3.4: Radiographic examination of Idua -/- and control mice
Idua -/- mice on the left, control same sex littermate on the right. Mice are 57 weeks of age. The *Idua* -/- mouse shows evidence of severe dysostosis multiplex, including widened ribs, vertebral abnormalities, and craniofacial foreshortening and thickening.

At 4 weeks of age, *Idua* -/- mice show evidence of foreshortening of the premaxillary bones and enlargement of the cranium. The squamosal, zygomatic and malar process

appear denser and smaller. While control mice have a pronounced tapering of the vertebrae spanning the length of the pelvis, the vertebrae in this region in MPS I mice are wider and do not taper relative to adjacent vertebrae.

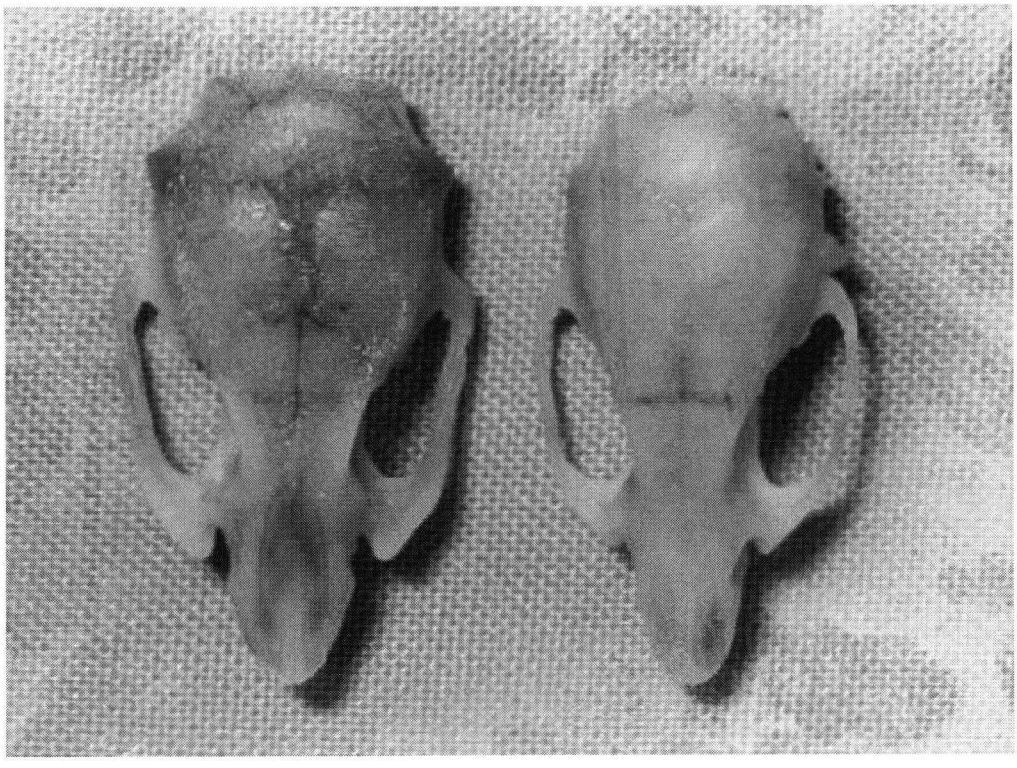

Figure 3.5: Skulls of Idua -/- and normal male mice at 70 weeks of age
On left, the *Idua* -/- skull , on right, normal. The *Idua* -/- skull has a thickened zygomatic arch, frontal bossing, and widened cranium and nasal bones.

This difference in vertebral morphology is evident by 4 weeks and persists for the life span of MPS I mice. The proximal tibial metaphysis of young MPS I mice appear to be less ossified as determined by radiodensity, than noted in control animals. With age, general thickening of the diaphysis of long bones becomes evident and widening of the malar processes and zygomatic arch becomes exaggerated. The ribs of affected mice become wider than in controls and flare at their anterior ends similar to the oar shaped ribs seen in human MPS IH. Late in MPS I (57 weeks) there is evidence of thoracic

vertebral kyphosis. Figure 3.5 demonstrates the thickened skulls of MPS I mice relative to normal controls.

3.36 Glycosaminoglycan Excretion

Urinary glycosaminoglycan (GAG) levels were analyzed in 114 MPS I and 112 control male mice and plotted in figure 3.6. MPS I males excrete 2 to 3 times the total urinary GAG of controls at all time points ranging from 3 weeks to 60 weeks. Similarly, MPS I female mice excrete 2 to 3 fold greater urinary GAG levels than female controls. Female MPS I mice excrete approximately 60 to 70% of the urinary GAG of male MPS I mice, a difference also observed between female and male control mice. No obvious change in the level of GAG excretion is apparent over the assessed time course (3 weeks to 60 weeks) in either MPS I affected mice or control mice, though tracking individual mice (control or MPS I) over time revealed that individual animals did have wide variations in the excretion of total GAGs.

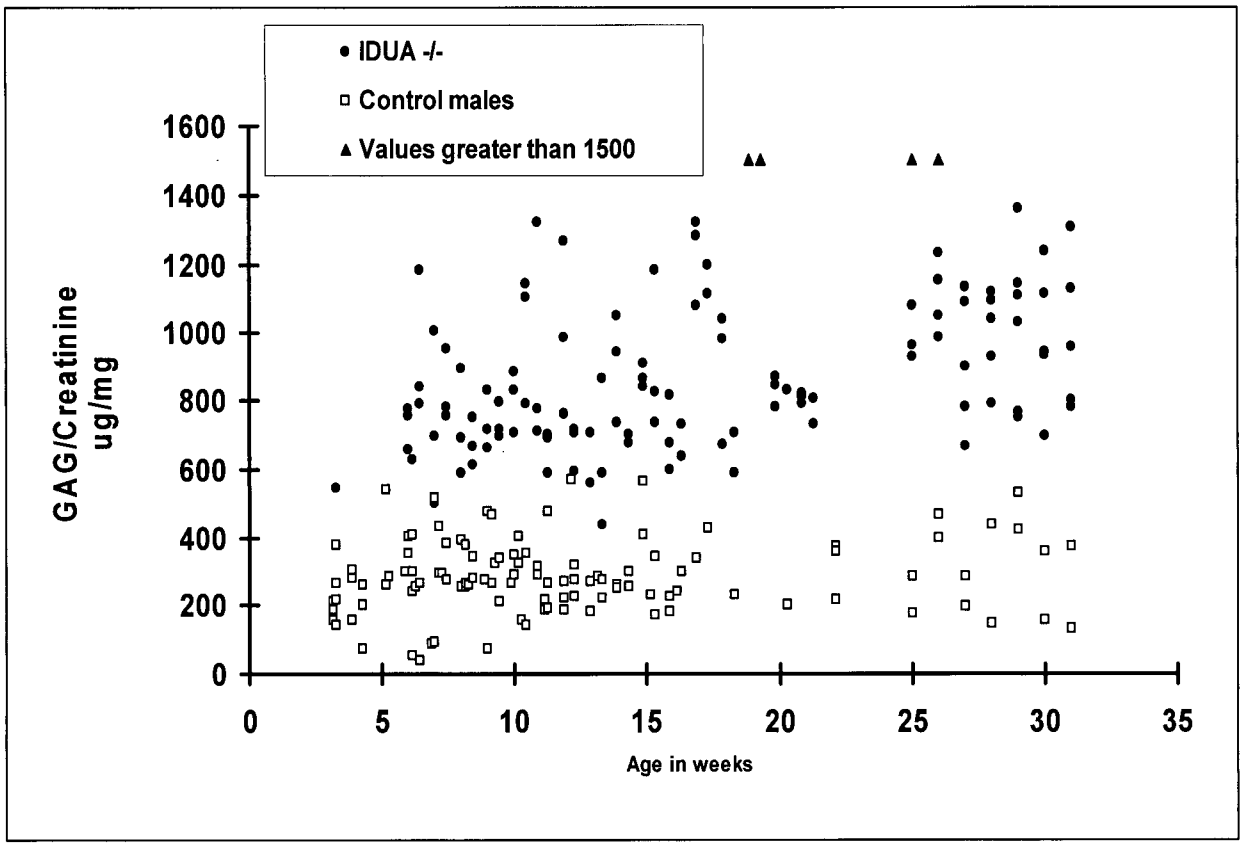

Figure 3.6: Glycosaminoglycan excretion in male Idua -/- and normal mice
Total urinary GAG levels are expressed as a ratio to creatinine excretion. 112 normal and 115 mutant data points are shown. *Idua* -/- male mice consistently excrete higher levels of urinary GAG than control male mice, with only rare overlaps. M. Aklujkar gathered urine for GAG chemical analysis by J. Yu.

3.37 Gangliosides

Figure 3.7 shows a thin-layer chromatogram of gangliosides extracted from the total brain of 4 *Idua* -/- and 4 control mice. Brain extracts from affected mice contain increased amounts of gangliosides with the mobility of GM_2 and GM_3 gangliosides.

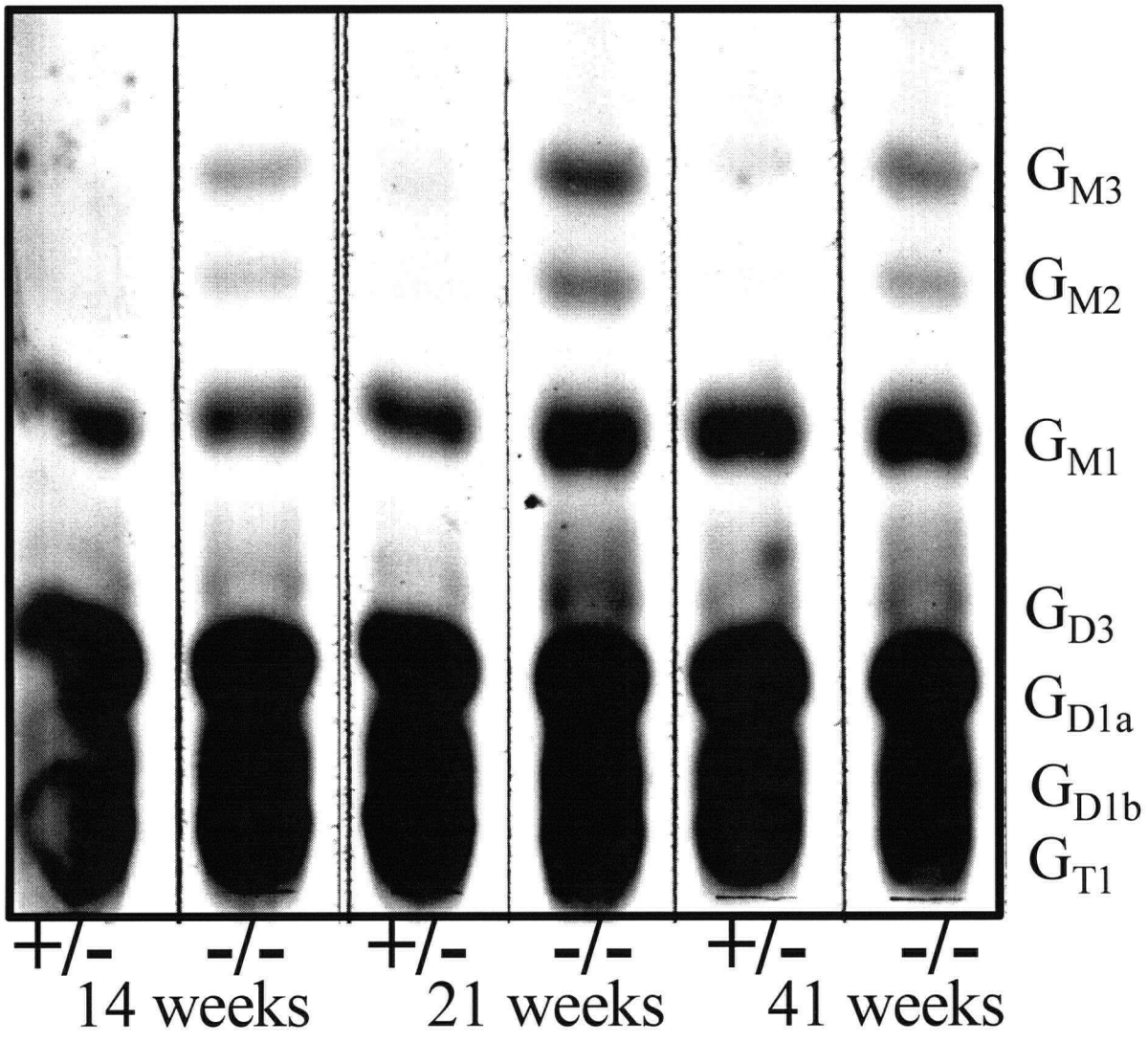

Figure 3.7: Thin layer chromatogram of brain lipids

Lipids were isolated from equivalent masses of brain tissue from control and mutant animals and separated by thin layer chromatography positions of ganglioside standards are listed. Note the increase in gangliosides with mobility of GM_2 and GM_3 in mutant mice relative to same aged controls. While attempts were made to load equal sample volumes, not all lanes contain equal sample volumes. K.Y. Ng performed ganglioside chromatography.

3.38 Bone Histopathology

Figure 3.8 shows the histopathologic changes of the proximal tibial growth plate at various ages. The growth plate at 6 weeks (fig. 3.8 a, b) is thickened and contains increased numbers of chondrocytes showing normal resting and proliferative zonal organization. The cells are swollen with increased fibrillary or vacuolar contents, especially prominent in the resting zone. The hypertrophic zone, although hypercellular, shows disorganization with a haphazard horizontal arrangement of cells. Most of the chondrocyte nuclei in the zone of hypertrophy appear degenerate. The junction between the zone of provisional calcification and the primary spongiosa appears irregular and disorganized with loss of the normal hill and valley pattern. The primary calcification zone is also increased in size. The longitudinal arrangement of the primary trabecula is abnormal with the trabeculae increased in number, thick, and containing a marked increase of cartilage surrounded by woven bone. Osteoblasts appear to be increased in number, especially in the proximal intertrabecular spaces, but do not appear swollen. Blood vessels appear normal histologically. The growth plates at 14 and 19 weeks show much more disorganization of the growth plate stacks with almost complete loss of the normal columnar arrangement of cells. There are irregular primary trabecula with scalloped margins and obvious retained cartilage within the ossified bone.

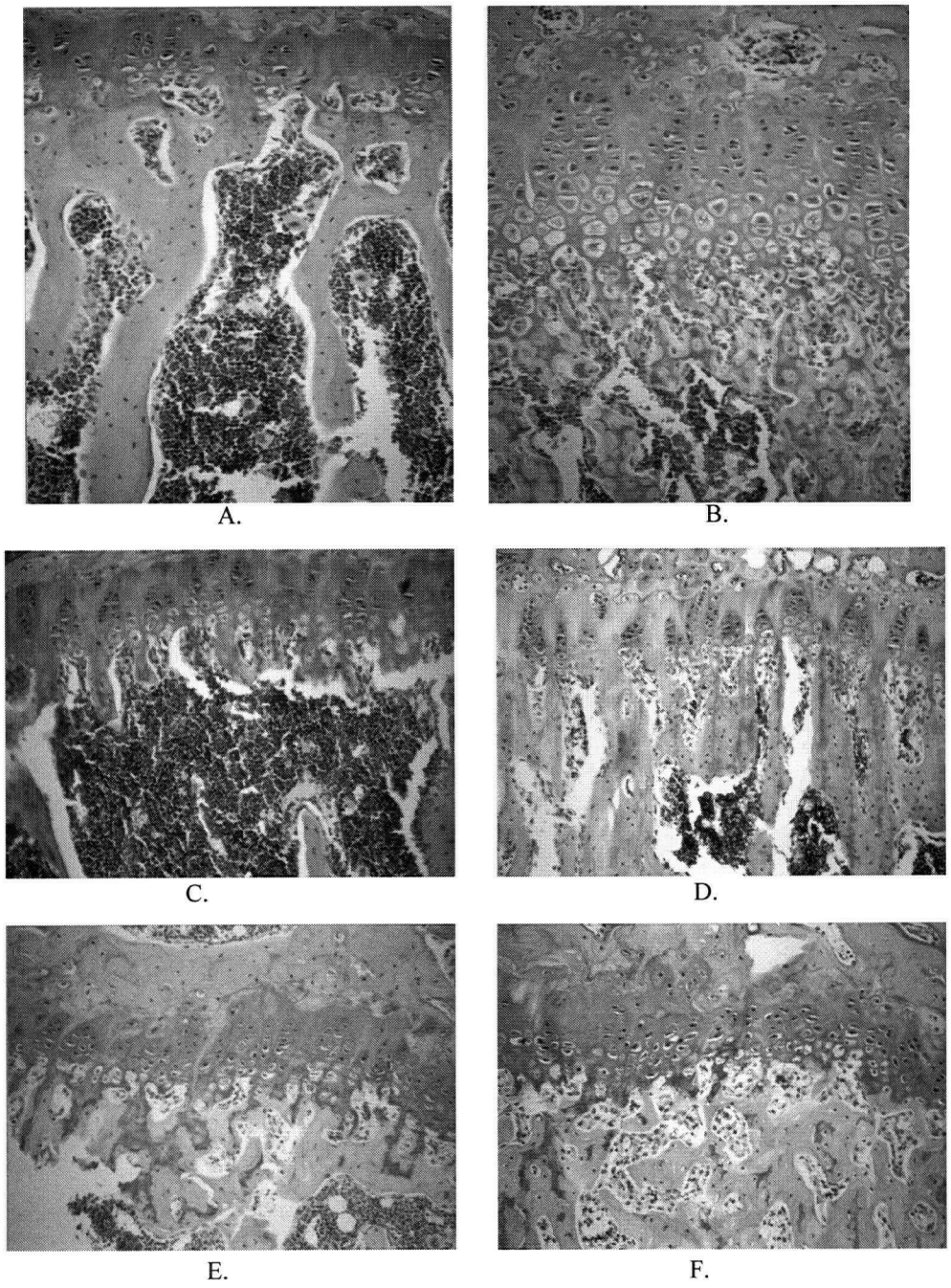

Figure 3.8: Proximal tibial growth plates

Tibias were fixed overnight in formalin, decalcified, bisected, and embedded in paraffin for examination. **A, B:** Growth plates at 6 weeks, control and mutant. **C, D:** Growth plates at 14 weeks, control and mutant. **E, F:** Growth plates at 19 weeks, control and mutant. (H&E staining, original mag. 100X). Results based on observations from 2 mutant and 2 control samples minimum for each time point. Pathology by G. Jevon.

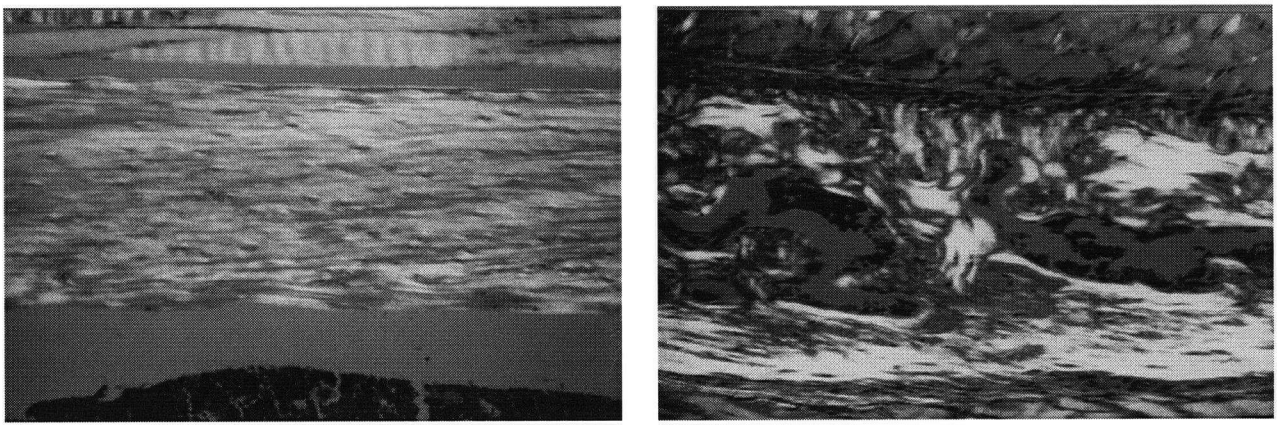

Figure 3.9: Polarized light microscopy of cortical bone samples
A: Control cortical bone with lamellar, parallel organization. **B:** MPS I cortical bone with gross disorganization. (H&E staining, original mag. 100X). Pathology by G. Jevon.

Figure 3.9 represents polarized light microscopy of tibial cortical bone at 14 weeks of age. The polarized light views reveal a loss of the parallel order of the bone matrix with loss of the concentric arrangement of lamellae or haversian system formation. The cortex is thickened in affected mice and has a heterogeneous appearance comprised of cartilage-staining (purple) material intermixed with mineralized compact bone (pink) in contrast to the homogenous pink of control compact bone. The osteocytes have clearly increased cytoplasmic volumes.

3.39 Neuropathology

Gross examination of brain tissue revealed no difference in the cerebrum or cerebellum between control and mutant mice. Figure 3.10 represents sections through the cerebellum revealing evidence of progressive loss of Purkinje cells. Controls at all ages

were found to contain well populated Purkinje cell layers. In contrast, mutant mice had progressive Purkinje cell dropout evident as early as 19 weeks. The Purkinje cell dropout increased with increase in age in the mutant mice with the distance between Purkinje cells becoming greater. PAS staining of the cerebellum revealed increased PAS positive material in the Purkinje cells of mutant mice relative to controls. This difference became pronounced with increasing age and was noticeable from the age of 8 weeks. PAS + diastase staining of the cerebrum revealed increased amounts of PAS positive material and increased size of neurons in the caudate nucleus in mutant mice relative to controls. The amount of PAS positive material in the neurons increased with increase in age and was noticeable from the age of approximately 18 weeks. H&E staining of cerebrum revealed no obvious differences between control and mutant mice.

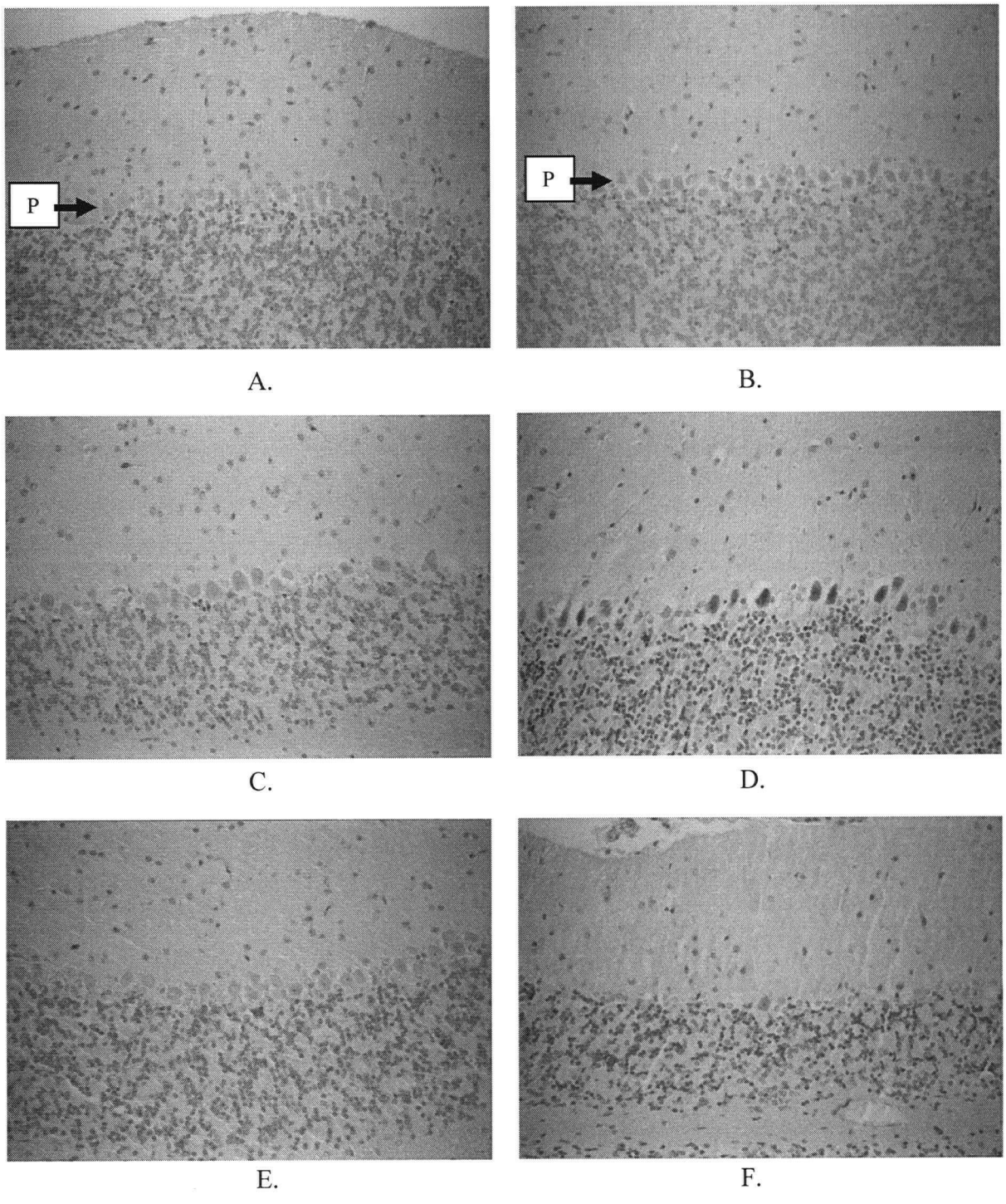

Figure 3.10: PASD staining of the Purkinje cell layer of cerebellum

A, B: Control and MPS I mice at 6 wks, respectively. **C, D:** Control and MPS I mice at 19 wks. **E, F:** Control and MPS I mice MPS I at 41 wks. (PAS and diastase staining, original mag. 250X). The region containing Purkinje cells is identified in A and B above with the letter P and an arrow. Results based on observations from 2 mutant and 2 control samples minimum for each time point. Pathology by G. Hendson.

3.4 Discussion

This chapter describes the long-term clinical, biochemical, and pathological features of an iduronidase deficient (-/-) mouse strain containing null alleleles of the *Idua* gene generated by gene targeting. One objective of this investigation was the characterization of murine iduronidase deficiency relative to human iduronidase deficiency, which presents as a spectrum of disease with variable organ system involvement and disease course. Another objective was the use of the mouse model to better characterize the progression of iduronidase deficiency in different organ systems. This might provide a greater understanding of MPS I symptom development, and generate markers of disease useful in therapy assessment. Unexpected findings in murine iduronidase deficiency include life into adulthood, abnormalities in the bone growth plate and diaphysis at an early age, and progressive Purkinje cell loss.

At birth, iduronidase-deficient mice do not have a clinically detectable phenotype, similar to all forms of human MPS I. By four weeks of age, facial dysmorphology is detectable, and progressive facial coarseness then develops as a result of both craniofacial dysostosis as well as abnormalities of subcutaneous tissues. We have noted that the clinical feature of craniofacial dysmorphism is detectable earlier and is more obvious in male compared to female mice, but after 16 weeks of age this gender difference is less apparent. As the early facial dysmorphic features likely relate to craniofacial dysostosis, these observations may indicate that hormonal influences or different GAG catabolic requirements between the sexes may modulate the clinical features of facial dysostosis. This sex based difference in the early clinical features of the *Idua* -/- mouse has not been reported in human, canine, or feline forms of the disease, however the murine MPS VI

model shows gender differences with female mice dying relatively earlier than males (Birkenmeier *et al.*, 1989). Rapidly progressive facial "coarseness" seen in this murine MPS I model is in keeping with severe MPS I, Hurlers syndrome, in humans.

Young MPS I mice are robust with no mortality occurring until approximately 30 weeks of age. Most deaths of affected mice occur between 50 and 70 weeks of age with no affected animals living more than 85 weeks. Males do not live past 70 weeks with females persisting slightly longer but not living past 82 weeks. This is in contrast to the normal littermates representative of the colony, in which only 5% have died by 90 weeks of age and 90% are still living by 2 years of age. The normal life span for unaffected animals in this colony is likely to be approximately 2.5 to 3 years. Therefore the MPS I mice have a significantly shortened life span but do persist to maturity. This is in contrast to the MPS VII murine model where the average life span of male and female mice is reported to be 24 weeks and 20 weeks respectively (Birkenmeier *et al.*, 1989). Although the *Idua* -/- mice seem to die at a later point in life than humans with Hurler syndrome, they clearly have a shortened life span. This attenuation in the phenotype may reflect species differences in rates of GAG storage in various tissues, differences in the secondary effects of GAG storage or may also reflect the lack of significant environmental exposures experienced by the rodent colony. Alternatively, the delayed mortality in *Idua* -/- mice relative to MPS I H in humans may indicate that it is the absolute rate of substrate accumulation relative to chronological time rather than relative to life parameters such as sexual maturity which is important.

Hurler and Scheie syndromes in humans are differentiated on the basis of age of onset and rate of progression of disease, with Hurler syndrome showing early onset and

rapid progression. We show early onset of disease and rapid progression in addition to complex neuropathology in murine MPSI and, therefore, although *Idua* -/- mice live to 'adulthood' their phenotype resembles more closely that of severe MPS I in humans. Persistence to sexual maturity is also noted in the *Idua* -/- dog and cat naturally occurring models, although the true life span of the affected animals has not been accurately determined (Shull *et al.*, 1982, Haskins *et al.*, 1979).

The severe dysostosis multiplex and progressive neurological dysfunction that occur in MPS I constitute the most debilitating aspect of this group of disorders. Skeletal manifestations of disease are apparent by 4 weeks of age in *Idua* -/- mice, including radiographic evidence of aberrant bone modeling in the cranium, the vertebrae, and the ribs. As the mice age, progressive skeletal abnormalities are noted with the development of kyphosis, wide oar shaped ribs, shortened and thickened long bones and severe dysostosis of the facial bones. Histological analysis of the bone reveals aberrant growth plate development and maturation as well as abnormalities of early cortical bone structure. There are striking differences in the extent and degree of growth plate pathology at different developmental time points. At 6 weeks of age the growth plate is widened with increased area of the resting, proliferative, hypertrophic, and spongiosa zones. This widening appears to be caused not only by increases in the volume of the individual chondrocytes but by increased chondrocyte numbers in the growth plate stacks. The columnar organization of the growth plate is still apparent although elongated. The increased area of the zone of provisional calcification and primary spongiosa indicate that at this age the growth plate may be generating cartilage at an increased rate compared with normal, or has difficulty degrading the cartilage produced.

At 6 weeks of age the primary spongiosa is increased in thickness, and there are severe abnormalities in the primary ossification of cartilage in this layer. This is seen as islands of unossified cartilage persisting between osteocytes. There appears to be an increase in volume of this partially ossified material resulting in the loss of well-defined narrow trabeculae as is seen in the control animals at this age.

These abnormalities in the young proximal tibial growth plate of *Idua* -/- mice suggest pathways involving the formation and remodeling of cartilage and subsequent ossification are altered as a result of the accumulation of the substrates of IDUA, namely heparan and dermatan sulfate. The ordered nature of bone matrix is critical for proper bone growth and integrity. This is well exemplified in osteogenesis imperfecta, where mutations of type II collagen resulting in either structurally abnormal collagens or reduced type II collagen production have devastating effects on the strength and shape of bone (Byers *et al.*, 1995).

The early findings within the growth plates of our mice are contrasted by the findings at later ages when the columnar organization of the plate is disrupted and the trabeculae are thin in comparison to controls. The abnormalities observed in the growth plate and diaphysis in older *Idua* -/- mice are similar to the findings described in the cat models of MPS I and MPS VI, and the mouse models of MPS VI and MPS VII (Haskins *et al.*, 1983, Abreu *et al.*, 1995, Evers *et al.*, 1996, Birkenmeier *et al.*, 1989). Recently, a role for dermatan sulfate in the regulation of elastic fibre assembly has been established, with excessive dermatan sulfate inhibiting the formation of mature extracellular elastin (Hinek and Wilson, 2000). Furthermore, it was shown that extracellular elastin regulates the proliferation of fibroblasts, with excess dermatan sulfate, as occurs with IDUA

deficiency, leading to excess fibroblast division. Together these observations may in part explain abnormalities of the bone and connective tissue observed with IDUA deficiency, and highlight the diverse pathways by which accumulation of heparan and or dermatan sulfate can influence normal development.

Early in the disease course Purkinje cell numbers and morphology appear normal in the *Idua* -/- mice. Obvious lysosomal accumulation is noted within the Purkinje cells by 8 weeks of age with evidence of detectable loss of Purkinje cells by 19 weeks of age. Although similar degrees of lysosomal storage within cortical neurons was detected, obvious neuronal cell loss elsewhere within the CNS was not readily apparent, though detailed cell counting studies have not been undertaken. Despite the fact that Purkinje cell depletion is noted, mice showed no obvious evidence of ataxia. This may reflect the presence of severe skeletal disease which limits the mobility of the mice. Neuronal cell dysmorphology and cell loss including Purkinje cell loss have been noted in a mouse model for another lysosomal storage disorder, aspartylglycoasminuria (AGU), resulting from deficiency of glycosylasparaginase. At a young age, mice deficient in glycosylasparaginase demonstrate many pathological changes observed in human AGU patients (Kaartinen *et al.*, 1996). After 10 months of age, the general condition of AGU mice deteriorates gradually and includes progressive motoric impairment, impaired bladder function, and early death. Pathological abnormalities were detected in the central nervous system including widespread lysosomal hypertrophy, with especially severe neuronal vacoulation in the lateral thalamic nuclei and deep cerebellar nuclei. Mice of 20 months of age demonstrated clear neuronal loss including extensive loss of Purkinje cells, and widespread gliosis. Impaired bladder function was noted in older mice, and is

speculated to be secondary to involvement of the central nervous system (Ganzalez-Gomez *et al.*, 1998). In addition to the widespread central nervous system disease including neuronal vacoulation, dysmorphology, and cell loss observed in the mouse models of both MPS I and AGU, adult MPS I mice likewise develop impaired bladder function.

In the severe form of human MPS I, developmental delay is usually noted by 2 years of age followed by progressive deterioration, with patients eventually performing in the moderate to severely retarded range (Colville and Bax, 1996). The mechanisms and processes leading to mental deterioration in human MPS I are not well understood, however, progressive morphological neuronal abnormalities including hillcock enlargements, ectopic dendritogenesis as well as neuronal sclerosis have been reported (Walkley *et al.*, 1988, Ferrer *et al.*, 1988, Dekaban *et al.*, 1976, Dekaben *et al.,* 1977). We report here evidence of secondary accumulation of brain gangliosides in murine MPS I. This secondary accumulation of gangliosides has previously been noted in human and canine iduronidase deficiency as well as other storage disorders unrelated to primary defects of glycosphingolipid metabolism (Constantopoulos and Dekaban 1978, Constantopoulos *et al.*, 1985). The role that ganglioside accumulation may play in the pathogenesis of MPS disorders is unknown but may actually be a central one. The murine models for Tay-Sachs and Sandhoff disease have indicated that GM_2, and likely other gangliosides, may be causally related to apoptotic neuronal cell death (Huang *et al.*, 1997). In addition, GM_2 has been postulated to underlie the generation of ectopic dendrites in pyramidal neurons in both Tay-Sachs as well as other generalized lysosomal storage (Walkley, 1995).

Recently, a novel approach for the therapy of gangliosidoses has been developed which involves the introduction of specific inhibitors of glycosphingolipid biosynthesis (N-Butyldeoxynojirimycin), thereby limiting the accumulation of gangliosides by limiting their initial synthesis. This approach has proven successful in limiting GM_2 accumulation in a murine model of Tay-Sachs disease (Platt *et al.*, 1997). What role this form of therapy may have in storage disorders which result in secondary accumulation of glycosphingolipids remains to be determined.

The severe dysostosis multiplex and progressive neurological dysfunction that occurs in MPS I constitute the most debilitating features of this group of disorders, and both features do not respond well to bone marrow transplantation. The limited response noted for these two tissues likely reflects the presence of early irreversible pathology and/or lack of delivery of adequate enzyme levels to relevant cell types. Purkinje cell loss represents an obviously irreversible feature of disease progression, however our observation that Purkinje cell loss as well as other neurological manifestations of murine MPS I are delayed relative to skeletal and visceral manifestations, and are not present until murine adulthood, suggests that there may exist a post-natal window of opportunity for therapeutic intervention towards prevention of CNS pathology. Long term analysis of genotypically defined MPS IH patients has demonstrated that BMT can stabilize neuronal degeneration particularly when performed early in the course of disease (Hopwood *et al.*, 1993). BMT in human MPS I results in transient improvement in growth of the appendicular skeleton, but has little effect on the long term skeletal complications of disease. Similarly, enzyme replacement therapy (ERT) has not proven effective in correcting dysostosis in the MPS I dog model or the MPS VI cat model although early

BMT in the canine model has shown evidence of mild skeletal improvement (Kakkis *et al.*, 1995, Crawley *et al.*, 1996, Shull *et al.*, 1988). The combination of early enzyme replacement followed by BMT in the MPS VII mouse model has resulted in a dramatic skeletal response as well as evidence of effects on neuronal storage (Sands *et al.*, 1997). The presence of complex skeletal pathology in *Idua* -/- mice as young as 6 weeks of age suggests significant skeletal structural abnormalities are present before, and probably contribute to, the severe dysostosis which becomes apparent later in life. Irreversible features of skeletal pathology may include the presence of aberrant matrix and/or finite windows early in development for normal bone growth.

Alternatively, the limited efficacy of BMT and ERT may be the result of inadequate delivery of therapeutic enzyme to specific, crucial cellular targets. Chondrocytes, for example, exist within a matrix that is resistant to transport of large molecules. In addition, MPS associated accumulation of GAG in the extracellular space may further impede delivery of corrective agents through, for example, congested cartilage and thickened membranes. Thus early intervention may preclude the development of irreversible features, and additionally may have greater access to some cellular targets as GAG accumulation has not yet further limited delivery of corrective agents.

Characterization of murine MPS I has demonstrated the presence of early, widespread lysosomal distention, early and severe dysostosis multiplex, excretion of excessive glycosaminoglycans in urine, a shortened life span, and complex neuropathology including neuronal and glial cell lysosomal distention, excessive CNS accumulation of gangliosides GM_2 and GM_3, and progressive Purkinje cell loss in the

cerebellum. This phenotype is consistent with severe MPS I, Hurler syndrome, in all respects except that the *Idua* -/- mouse lives into adulthood while Hurler syndrome is typified by death in the first decade. As mentioned, the application of life span parameters of human MPS I for placement in the spectrum of MPS I phenotypes may not be applicable to murine MPS I. It is clear that the murine model of MPS I is representative of all major features of Hurler syndrome including those for which current therapies are inadequate. The similarities in the clinical course seen in these mice to the severe form of human MPS I indicates that this is likely to be a very powerful model for the study of disease pathophysiology and therapeutic development. The neuropathology and skeletal pathology noted in this model indicates that complex primary and secondary factors are likely to be involved in the evolving clinical phenotype. The rodent model will thus be invaluable in determining the importance of these secondary factors and what role they may play in the human disorder.

Chapter 4: Pronuclear and embryonic stem cell attempts at generation of murine transgenic lines with ubiquitous or myeloid specific expression of human IDUA

4.1. Introduction

This chapter describes attempts to generate models of therapy for MPS I. While many approaches to therapy for MPS I have been attempted, no cure for MPS I exists. One of the most important findings relevant to the design of therapies for MPS is the finding that co-culturing MPS I cells *in vitro* with cells with a related but clinically distinguishable disease, MPS II, results in "correction" of the glycosaminoglycan accumulation (Fratantoni *et al.*, 1968). It was further suggested that the accumulated GAG resulted from deficiency of specific factors required for GAG degradation, and that these factors most likely were enzymes (Fratantoni *et al.*, 1969). This demonstrated that the lysosomal accumulation of GAGs could be reversed once established, and suggested the presence of a transport mechanism capable of internalizing and delivering exogenously produced enzyme to the lysosome. This is in contrast with many disorders in which corrective factors must be produced internally for proper subcellular localization and function to occur. Also relevant is the observation that patients with very small amounts of IDUA activity undergo a dramatically milder course of disease than patients with no detectable enzyme activity (Scott *et al.*, 1993). This indicates that a small increase in enzyme activity may have a large impact on disease progression. Finally, the progressive nature of MPS I favors early intervention as some disease symptoms may not respond to therapy introduced later in the course of disease.

Allogeneic bone marrow transplantation (BMT) has been used extensively with partial success for MPS I and other lysosomal storage disorders as a source of corrective enzyme activity (Peters *et al.*, 1996, Field *et al.*, 1994, Hopwood *et al.*, 1993). BMT is effective in normalizing serum IDUA activity levels, reducing urinary excretion of

glycosaminoglycans, decreasing hepatosplenomegaly, and results in a general improvement of somatic features of MPS I. While dramatically improving quality of life, BMT has less impact on the neurological and skeletal complications of MPS I (Shapiro *et al.*, 1995, Field *et al.*, 1994). Enzyme replacement therapy (ERT), in which patients are infused with purified protein enzyme, may offer an alternative to BMT for MPS I and, in early limited trials, appears to improve many clinical manifestations of the disease, but like BMT is believed to have limited potential for improving neurological and skeletal symptom development (Kakkis *et al.*, 2001, Wraith JE, 2001, Brooks, 2002).

The restricted benefits obtained with ERT and BMT most likely result from insufficient delivery of therapeutic enzyme to critical tissues or disease irreversibility. Entry through the blood brain barrier requires recognition by a specific transporter; none exists for IDUA. This prevents neurological delivery of IDUA from the circulatory system to the central nervous system. This barrier results in minimal delivery of enzyme upon systemic infusion in ERT, and the limited cellular interaction that occurs between somatic tissues including donor BMT derived cells and the CNS limits benefits from macrophage and other cell based delivery of IDUA. Bone and cartilage cells are entrapped in a matrix which would be predicted to physically exclude enzyme from cells which require enzyme activity for normal development (Torzilli *et al.*, 1997). An additional factor limiting organ improvement may be the development of irreversible complications of MPS I, established before, and nonresponsive to, therapeutic intervention. For example, the recent finding that dermatan sulfate, one of two GAGs accumulated in MPS I, inhibits the formation of elastic fibers, a vital component of extracellular matrix and bone, illustrates a potential mechanism where matrix generated

during enzyme deficiency may be fundamentally altered such that even after enzyme replacement, normal development is impaired (Hinek and Wilson, 2000). As described in chapter 3, MPS I mice show alterations in cortical bone organization and retention of cartilage in growth plate spongiosa. The ability for correction of these pathological states is unknown. The purkinje cell loss and disorder we have observed in adult MPS I mice would also be examples of irreversible damage. Irreversible symptoms might also arise if crucial developmental milestones pass before critical levels of enzyme activity are introduced to required tissues. It remains to be determined to what degree the neurological and skeletal complications of MPS I can be improved with therapy, and what specific cellular targets result in improvement in these critical systems.

It is evident that therapy offers the most benefit when performed early in the progression of MPS I (Hopwood *et al.*, 1993). Examination of a MPS I-H fetus, gestational age 20 weeks, whose sibling had died of confirmed MPS I-H at age 8, revealed intracellular vacoulation in tissues including dermis, mitral valve, dura mater, lymphoid and haemopoietic cells, and connective tissue, and zebra bodies were detected in spinal cord, while no vacoulation was detected in tissues including cerebral cortex, and cerebellum (Crow *et al.*, 1983). These findings, and the possibility that some pathological features of MPS I are irreversible once established (Russell *et al.*, 1998), highlight the need for early intervention for MPS I, especially severe MPS I. The extension of this finding is interest in *in utero* therapy, where possible, such as *in utero* bone marrow transplantion for MPS I (Flake and Zanjani, 1999).

To address the potential of therapeutic intervention for prevention of MPS I symptom development I have sought to generate two transgenic mouse models. One

model would express human IDUA only in a subset of HSC derived cells, in a background of IDUA deficiency when crossed into the MPS I mouse model. This genetic model of *in utero* BMT would allow assessment of the maximum benefit of early BMT directed therapies while avoiding the limitations and barriers to physical BMT transplantation *in utero*. Secondly, I wanted to generate a mouse line that expresses IDUA in all tissues from an early stage of development. This mouse could be used as a donor source in transplantation experiments with MPS I mice, and would determine if expression of IDUA during development causes disease.

4.1.1 A model of *in utero* bone marrow transplantation

The myeloid specific CD11B-IDUA transgenic was designed to determine the therapeutic benefit of early bone marrow cell derived IDUA expression on MPS I. Because of barriers to literal *in utero* transplantation, a genetic approach was employed that would express IDUA in a subset of cells derived from marrow cells. The CD11b gene encodes the alpha chain of the Mac-1 integrin, which is preferentially expressed in myeloid cells such as neutrophils, monocytes and macrophages (Shelley and Arnaout, 1991, Hickstein *et al.*, 1992). This expression profile is consistent with the desired expression of IDUA in a model of *in utero* BMT, as most of the benefit derived from BMT for MPS I is thought to be from monocytes and macrophages. A number of transgenic mice have been generated expressing reporter genes using the CD11b promoter. While a larger 1.7 kb promoter region was shown to drive high level transgene expression preferentially in mature monocytes, macrophages, and neutrophils, but not in myeloid precursors (Dziennis *et al.*, 1995), smaller regions of the putative CD11b promoter (1.5 kb to 0.1 kb) generated less predictable transgene expression, with

significant expression in lymphocytes or no transgene expression at all (Back *et al.*, 1995). Expression with the 1.7 kb promoter region was determined to persist into adulthood at high levels. This construct included the distal exons and polyadenylation sequence of the human growth hormone gene to increase transgene expression. I used this proven CD11b construct to generate the CD11b-IDUA construct pictured in figure 4.4. As the open reading frame of the human *IDUA* gene spans approximately 20 kilobases, I chose to use a cDNA encoding human IDUA, a kind gift from Dr. John Hopwood, which is only 2 kilobases in length therefore facilitating cloning of the final CD11b-IDUA construct. In addition, this IDUA cDNA has been expressed in cell culture and confirmed to encode functional IDUA enzyme activity (Scott *et al.*, 1991).

Constructs were also generated to express either the beta-galactosidase gene or the enhanced green fluorescent gene also from the CD11b promoter construct. It was hoped that reporter gene expression would allow cells expressing the transgenes to be identified.

It should be kept in mind that this proposed model would differ from actual *in utero* transplantation in a number of important ways. The CD11b promoter would not direct transgene expression in lymphoid cells, and thus not all cell types that express IDUA in a transplant recipient receiving BMT would be expressing IDUA in this transgenic model. Another significant difference relates to the timing and distribution of cells expressing IDUA. The introduction of IDUA would occur later in development with *in utero* BMT therapy, as donor cells must engraft, expand, and colonize existing organs whereas the transgenic model would be expected to express IDUA earlier, as mature myeloid cells are generated. As *in utero* transplantation does not involve ablation of host

tissues, engraftment levels are low with all recipients having chimeric bone marrow. Thus only a fraction of marrow derived cells would express the therapeutic enzyme, while the proposed transgenic model would be expected to show expression in all cells in which the CD11b promoter is functional. For example, analysis of macrophages in a successfully engrafted patient who had received *in utero* BMT would contain a mix of normal (donor) and diseased (recipient) macrophages, while all macrophages in the transgenic model would be expected to express IDUA.

Finally, the CD11b promoter drives expression at a higher level than normally occurs from the IDUA gene promoter, where IDUA expression levels are difficult to detect by standard northern blot analysis, while the CD11b transcript is readily detectable (Scott *et al.*, 1992). Taken together these differences suggest the transgenic model driven by the myeloid specific CD11b promoter would be likely to express higher levels of therapeutic IDUA enzyme than with *in utero* transplantation of normal donor cells, thus determining the maximum potential of the myeloid cell lineages as a vehicle for therapy for MPS I. Complications of MPS I not improved despite high level myeloid expression of IDUA in this transgenic model would suggest autologous HSC and other hemopoietic targeted approaches will not represent a cure for these features of MPS I.

4.1.2 Widespread high level IDUA expression

The generation of a mouse line that expresses high levels of human IDUA in all tissues was undertaken for two reasons. Most importantly, I wished to develop a strain of mice expressing active human IDUA, as well as a reporter gene, for use as a donor strain in transplantation experiments with MPS I mice. The second objective of this project was to determine the outcome of high level, widespread IDUA expression on development.

IDUA is normally expressed at very low levels and the consequences of abnormally high levels of IDUA activity are unknown.

Expression of lysosomal enzymes could disrupt development in a number of ways. Transport of many lysosomal enzymes, including IDUA, to the lysosomal compartment requires receptor mediated recognition of mannose-6-phosphate residues found on numerous lysosomal proteins (Von Figura and Hasilik, 1986). Overproduction of any protein which is recognized by this receptor may disrupt lysosomal transport, and might be expected to result in insufficient delivery of lysosomal enzymes to the lysosome, as well as the presence of lysosomal proteins in inappropriate organelles and the extracellular space. Surprisingly, it has been shown that phenotypic correction in MPS I fibroblasts, as assayed *in vitro* by reduction in the accumulation of ^{35}S-labeled glycosaminoglycan, occurs to a greater extent with low level overexpression of IDUA than with higher levels of overexpression. In the same study, a relationship was found between the level of overexpression of IDUA and the secretion of other lysosomal enzymes, also recognized by the mannose-6-phosphate receptor (M-6-P receptor), to the extracellular space, consistent with altered lysosomal targeting (Anson *et al.*, 1992). This suggests that a threshold level for therapeutic expression may exist and that expression above the threshold reduces therapeutic efficacy, raising interesting questions regarding optimum therapy strategies for MPS I.

A number of transgenic mouse lines overexpressing lysosomal enzymes that are recognized by the M-6-P receptor have been reported, with no obvious phenotype (Kyle *et al.*, 1990, Kase *et al.*, 1998). This indicates overexpression of mannose-6-phosphate expressing protein is tolerated. Another mechanism by which overexpression of IDUA

could affect development is the IDUA mediated cleavage of substrates not targeted for lysosomal destruction. As heparan and dermatan sulfate containing GAGs have many functions including being components of extracellular matrix as well as playing a role in receptor-ligand interactions, inappropriate degradation of these IDUA substrates might be expected to lead to disease.

To generate a model with widespread high level IDUA expression constructs were engineered including reporter cassettes to permit identification of transgene expressing cells and organs.

4.1.3 The use of the human IDUA cDNA

To avoid possible regulatory alteration of *Sat-1* resulting from antisense interactions of the complementary murine *Idua* and *Sat-1* regions, and to determine if the human form of IDUA can rescue murine IDUA deficiency, the human rather than murine IDUA cDNA was used for expression of IDUA enzyme. The human IDUA cDNA was provided by John Hopwood, Women's and Children's Hospital, Adelaide Australia. The human IDUA cDNA is a compact 2155 basepairs long and consists primarily of open reading frame, as shown in figure 1.4. The 141 basepair overlap region between exon II of the human IDUA cDNA and a portion of the 3' untranslated region of *Sat-1* is still partially homologous, however, as shown in Figure 4.1, exon II of the human IDUA cDNA has 26 basepairs of disparity with murine *Idua* exon II. No stretch of perfect homology extends beyond 17 basepairs. It is hoped that the differences between the transgenic human IDUA cDNA, and the endogenous murine *Sat-1* gene, will limit alterations to endogenous *Sat-1* expression. Transgenic expression of an antisense mRNA

can diminish endogenous gene function as demonstrated by a number of groups (Manshouri, *et al.*, 1997, Chen *et al.*, 1997).

The human IDUA cDNA is well characterized (Scott *et al.*, 1991) and has been used in many studies. The human IDUA cDNA has been overexpressed in CHO cells (Kakkis *et al.*, 1993) for ERT trials and X-ray crystallography (Kakkis *et al.*, 1994, Unger *et al.*, 1994). It has also been used in retroviral vectors to correct storage in MPS-1 fibroblasts as a prelude to gene therapy experiments (Anson *et al.*, 1992). Enzyme replacement trials using recombinant human IDUA has been performed in the canine model of MPS I (Shull *et al.*, 1994), mouse (Clarke, unpublished results) and humans (Kakkis, 2001), with evidence of therapeutic improvement of lysosomal GAG accumulation. Thus this cDNA is well established and contains all elements required for the production of enzymatically active and properly targeted therapeutic human IDUA enzyme.

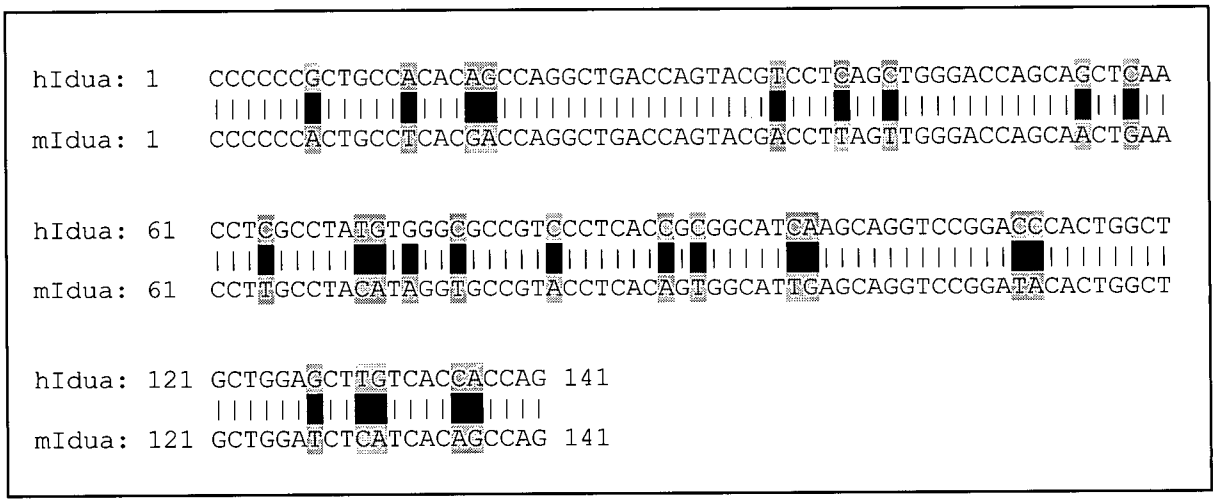

Figure 4.1: Identity between human and murine Idua exon II.

In both species, the 141 basepair exon II of the *Idua* gene overlaps with a portion of 3' untranslated sequence of the *Sat-1* gene. Shaded areas indicate regions of disparity between human and murine *Idua* sequences, and therefore represent regions of nonidentity between the endogenous murine *Sat-1* transcript and expressed human *Idua* transcripts. A total of 26 basepairs differ between the respective cDNAs, scattered throughout the 141 basepair overlap region. The largest consecutive region of identity between the two species is 17 nucleotides long, containing 11/17 (65%) GC content. Thus transgenic expression of the human IDUA cDNA in mouse is less likely to influence murine SAT-1 expression as a result of antisense interactions compared with expression of the murine IDUA cDNA. Blast2 from NCBI was used to generate this figure.

4.1.4 The generation of transgenic mice

Transgenic mice are usually generated by pronuclear injection of fertilized eggs as depicted in figure 4.2. Injected eggs are implanted into surrogate mothers for delivery of founder mice, which are then assessed for transgene presence, and expression pattern. Introduction of DNA by this route leads to random integration of usually multiple head to tail vector copies. While offering rapid production of founder transgenic mice, this approach has a number of consequences including the inability to study transgenes with a

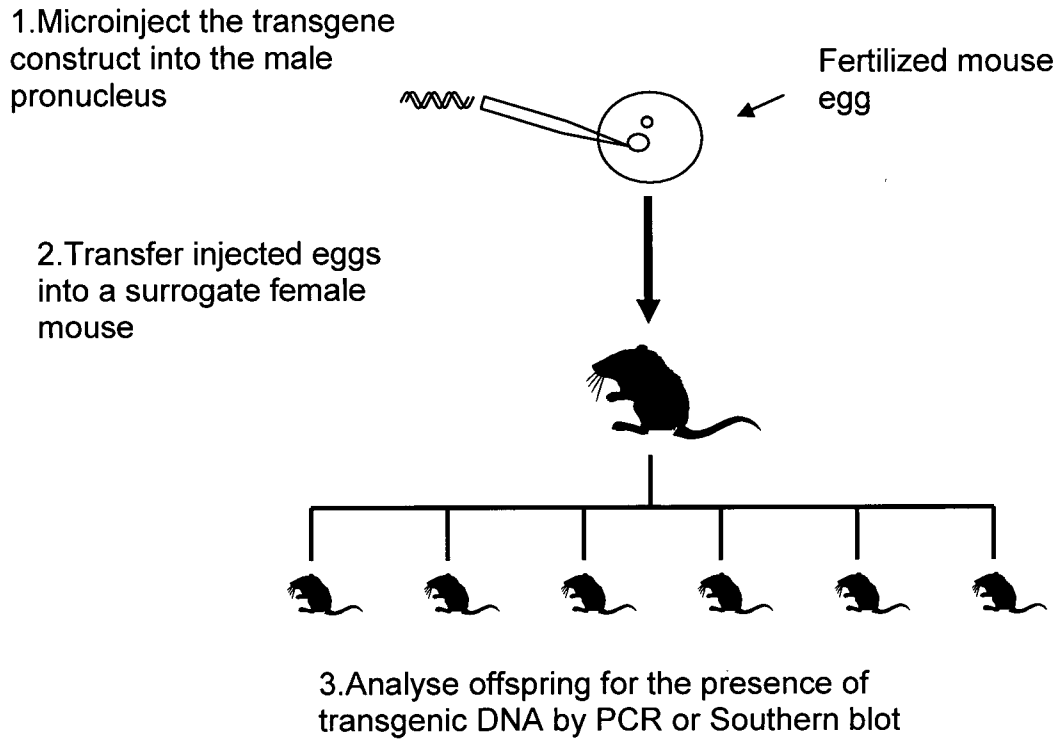

Figure 4.2: Pronuclear injection approach to the generation of transgenic mice
DNA is injected directly into the pronucleus of a fertilized mouse egg. In contrast with the ES approach, analysis for transgene presence and expression occurs in founder mice rather than at the level of the cell.

trans-dominant lethal phenotype, and the cost of producing many founder mice of which a minority contain the transgene and express the transgene in a desired pattern. An alternative approach uses embryonic stem (ES) cells to generate transgenic mice, depicted in figure 4.3. This approach involves introduction of DNA into ES cells, followed by selection for unique clonal populations encoding resistance to an antibiotic. This dramatically enriches for clones that have integrated, and express, construct encoded transgenes, a selection step not available with the pronuclear approach.

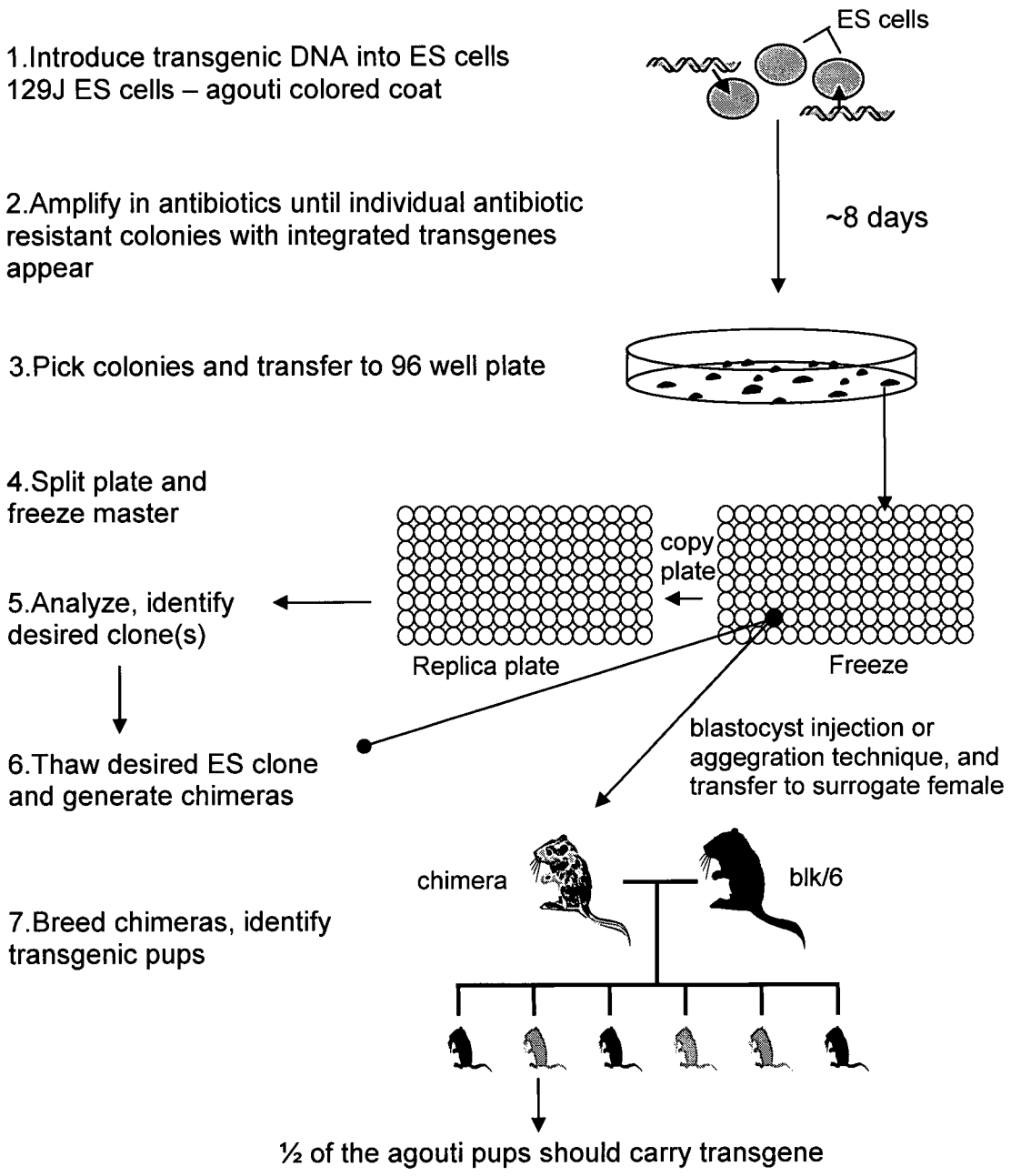

Figure 4.3: Embryonic stem cell approach for the generation of transgenic mice
The major advantage of the ES approach is step 5, having the opportunity to analyze ES clones to identify clones with desired integration events and, where possible, transgene expression. Injection of desired ES cells into blastocysts generates chimeras that may allow for analysis of otherwise lethal phenotypes, another advantage of the ES approach.

As ES clones can be amplified *in vitro*, samples can be taken for analysis while viable cells capable of germline transmission are maintained in culture or frozen. Analysis for molecular characteristics of transgene integration such as copy number and number of independent integration sites can be performed, as well as analysis of transgene expression, if the promoter of the transgene is active in ES cells.

A further advantage of the ES approach is the production of chimeras which include variable amounts of transgenic ES cells and normal blastocyst tissue and may allow escape from lethal developmental bottlenecks, allowing transgene assessment. The Lobe group has used the ES approach to generate reporter mice capable of ubiquitous reporter gene expression (Lobe *et al.*, 1999). By analyzing the expression of a reporter gene in ES cells, clones were identified with superior expression characteristics that were used in the production of transgenic mice more likely to have the potential for ubiquitous transgene expression in adulthood.

In attempts to generate both the myeloid specific and the ubiquitous IDUA expressing IDUA models described above, pronuclear microinjection of DNA transgene constructs, expected to achieve stable chromosomal integration at levels ranging from 10-40% of the resulting mice, was performed. The absence of transgene bearing offspring for either construct after repeated microinjection attempts led to the use of the embryonic stem cell approach to the generation of transgenic mice.

The ES cell approach allows for selection of lines with rare chromosomal integration events and, when promoter elements active in ES cells are involved, partial expression analysis of the introduced transgene construct at the level of the ES cell, before mice are generated. This may identify ES lines more likely to produce desired

expression patterns in adult mice and lines less likely to suffer transgene silencing. In addition, in situations where transgene expression results in embryonic lethality, chimeras produced with the ES approach may allow deduction of the effects of transgene expression, whereas microinjection may fail to generate any offspring for analysis.

Male R1 embryonic stem cells derived from the agouti 129 J murine strain, proven to be capable of germline transmission of genetic alterations, were used throughout this work. However, after successful ES cell manipulation, defined as demonstration of transgene integration and, where possible, transgene expression, no germline chimeras carrying the integrated transgene constructs were generated for either myeloid specific or widespread human IDUA expression. This could be the result of chance, or could result from a dominant-negative effect of transgene expression, *i.e.* human IDUA. It was then decided to employ the conditional IDUA expression approach described in Chapter 5, which would allow for control of tissue specificity and the onset of transgenic IDUA expression.

4.2 Results

4.2.1 Pronuclear injection approach for the generation of myeloid specific, and ubiquitous, IDUA expressing transgenic mice

Constructs for myeloid specific transgene expression were designed as shown in fig 4.4.

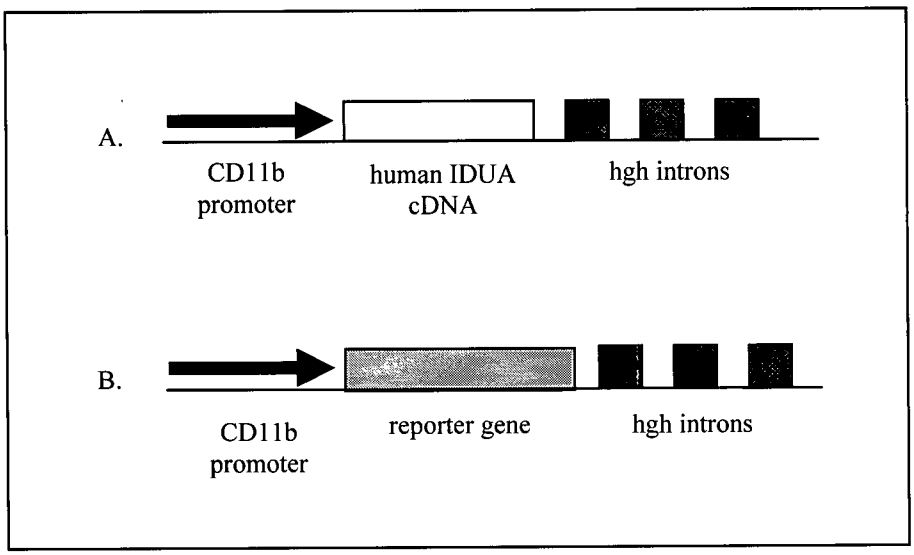

Figure 4.4 Transgenic construct for myeloid specific expression

A. The CD11b-IDUA construct. The 1.8 kilobase upstream region of the CD11b gene containing elements to drive myeloid specific expression, followed by the 2.1 kilobase human IDUA cDNA, with distal noncoding introns of the human growth hormone gene to increase expression levels. B. Reporter construct. Reporter constructs based on the same expression platform as CD11b-IDUA were generated with either the beta-galactosidase gene or the enhanced green fluorescent gene. Hgh introns are human growth hormone regions that provide splicing to the transcript.

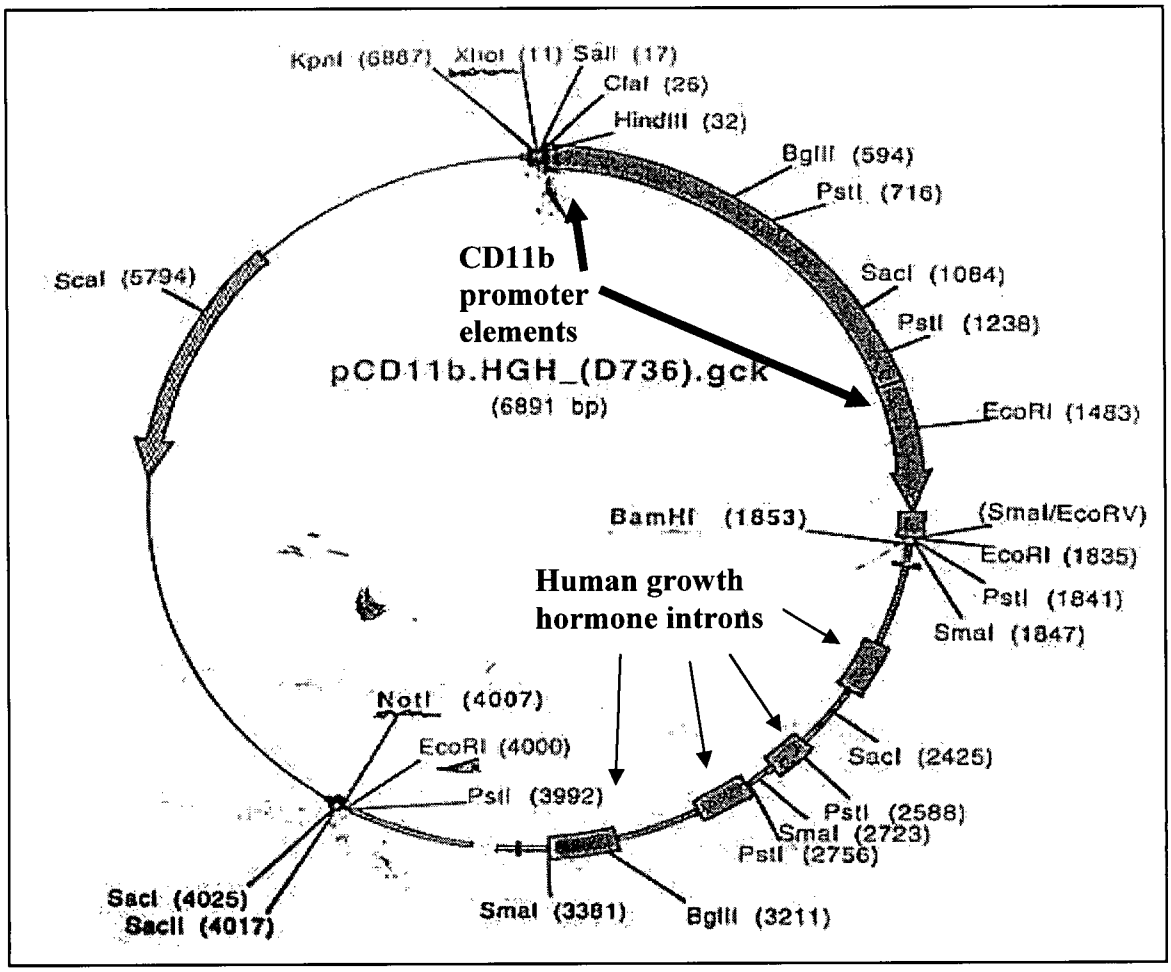

Figure 4.5: A map of the backbone CD11b-hgh vector for myeloid transgene expression

A 1.8 kb fragment (bp 1 to 1853) of the CD11b promoter is followed by a unique BamHI restriction site for insertion of gene of interest, followed by a 2.2 kb genomic region of human growth hormone gene including non coding exons for splicing induced transcript stability. Removal of non desired sequences by restriction with Xho I (at position 11 bp) and Not 1 (position 4007 bp after addition of human IDUA cDNA. Map and vector from Scott Pownall and Frank Jirik.

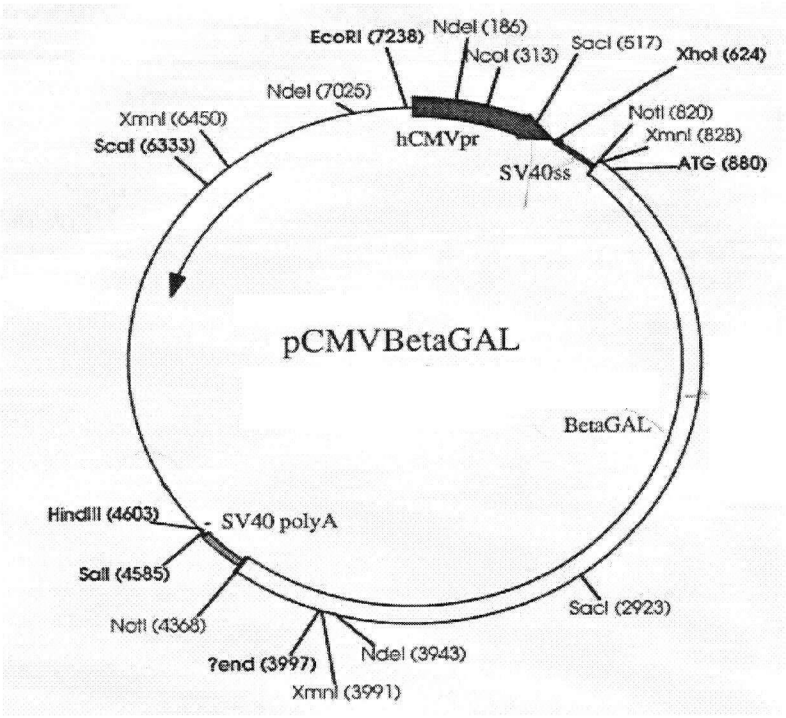

Figure 4.6: Plasmid containing Beta-galactosidase reporter gene

A 3.5 kb Not I/Not I fragment containing the beta-galactosidase reporter was excised for cloning into the CD11B construct as shown in Fig X. Plasmid and map from Grant McGregor.

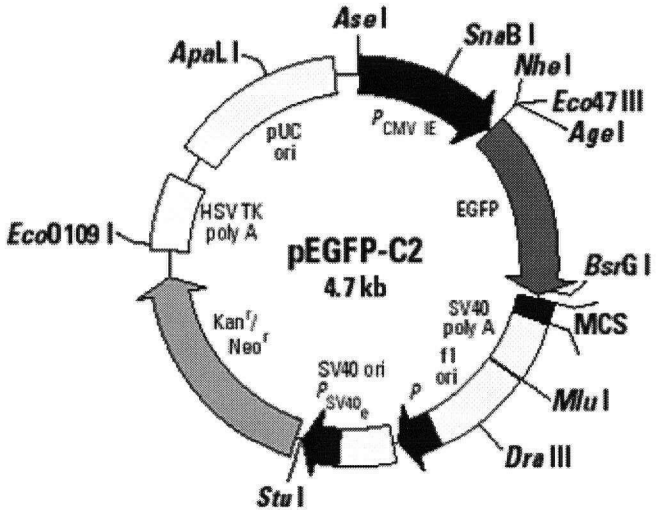

Figure 4.7: The pEGFP-C2 plasmid for expression of enhanced green flourescent protein

This vector was used as a source for the CMV promoter (fragment Ase I to Nhe I, 600 bp) to drive high level widespread expression of the human IDUA cDNA, as a source of the EGFP reporter for use in the CD11B construct (fragment Nhe I to BsrGI, 720 bp) and as a source for a high level widespread EGFP expressing reporter gene (fragment Ase I to Mlu I, 1600 bp). Vector from Clontech.

Pronuclear microinjection of both CD11b constructs was performed at the Centre for Molecular Medicine and Therapeutics. Microinjection of 408 fertilized eggs lead to the birth of 18 mice. Samples of these mice were taken and PCR and southern analysis were preformed to identify transgene positive founders, as shown in figure 4.8.

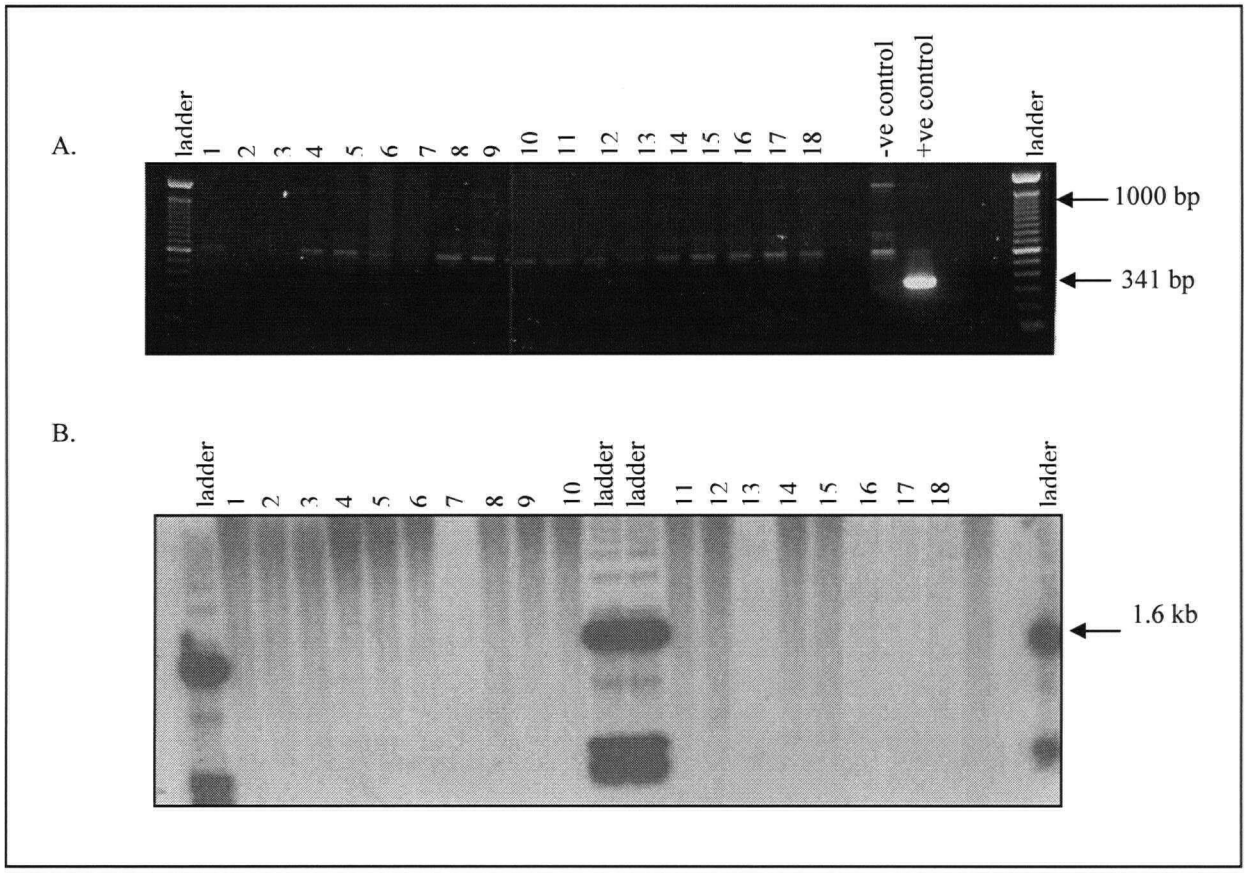

Figure 4.8: Analysis of 18 samples from co-microinjection of CD11b-IDUA and CD11b-LacZ constructs

A. PCR on DNA extracted from tail. PCR primers specific for the human IDUA gene were used in exon I, HID1F, and on the opposite strand in exon IV, HID4R, which produces a PCR band of 341 basepairs. Lanes 1-18, F1 tail samples, lane 19 negative control, lane 20 non transgenic tail sample, lane 21 positive control 1/1000 dilution of human IDUA cDNA (original=0.2 ug/ul). No transgene positive samples were identified. The band observed in most lanes including the nontransgenic control is a nonspecific amplification product. B. Southern blot analysis of EcoRI/Not I digests of the same 11 samples probed with the human IDUA 2.1 kb cDNA. A 1.6 kb band is expected in transgene positve samples. No positives were identified.

Another round of microinjection was performed with the CD11b-IDUA construct and a CD11b-EGFP construct. The EGFP reporter gene was chosen as it was considered to have some benefits not shared with the beta-galactosidase reporter gene. Injection of approximately 350 eggs produced 11 mice. Analysis of DNA samples is shown in figure 4.9.

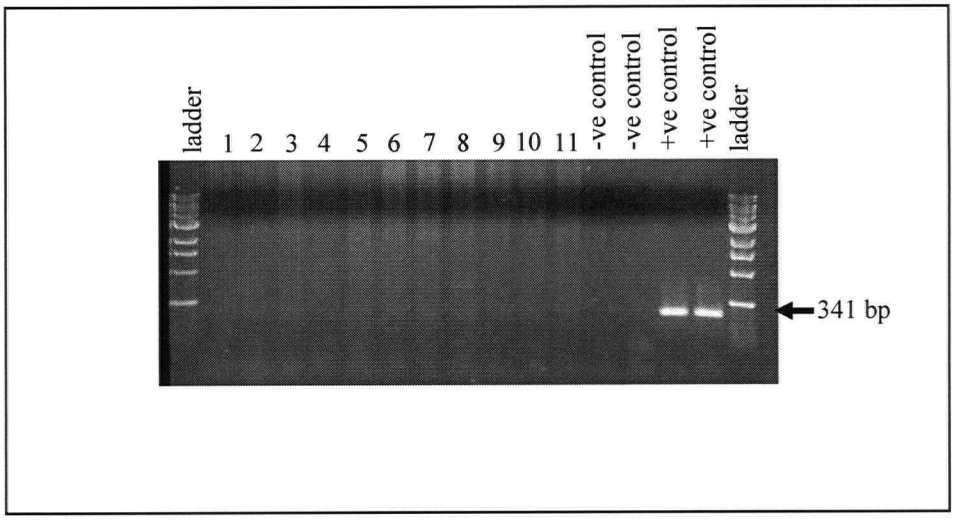

Figure 4.9: Analysis of 11 samples from co-microinjection of CD11b-IDUA and CD11b-EGFP contructs

PCR using human IDUA cDNA specific primers HID1F and HID4R designed to generate a 341 basepair PCR product. No positives were identified while positive control lanes with diluted human IDUA cDNA plasmid are positive.

No transgene positive founders were identified by either PCR, or Southern blot analysis (data not shown). Simultaneously, I attempted to generate transgenic mice with ubiquitous human IDUA expression. A construct for this purpose is shown in figure 4.10.

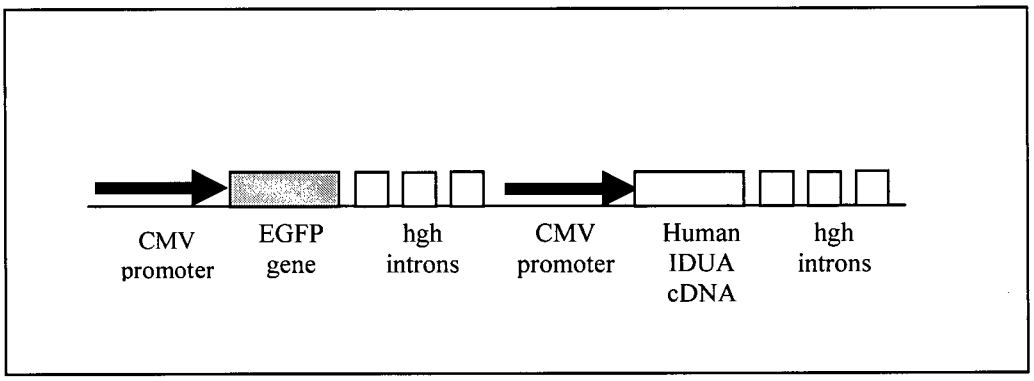

Figure 4.10: Ubiquitous Transgene Construct CMV-IDUA

This construct uses the CMV IE promoter taken from a Clontech mammalian expression platform (figure 4.7) and has been demonstrated to result in high level widespread expression including virtually all mammalian cell types. Both the human IDUA cDNA and the EGFP reporter gene are under the regulation of the CMV IE promoter and both genes in the construct have distal elements of the human growth hormone gene to increase expression levels. Pronuclear injection of the isolated construct was performed on approximately 350 eggs, and 12 mice were produced. PCR and Southern analysis was performed as shown in figure 4.11.

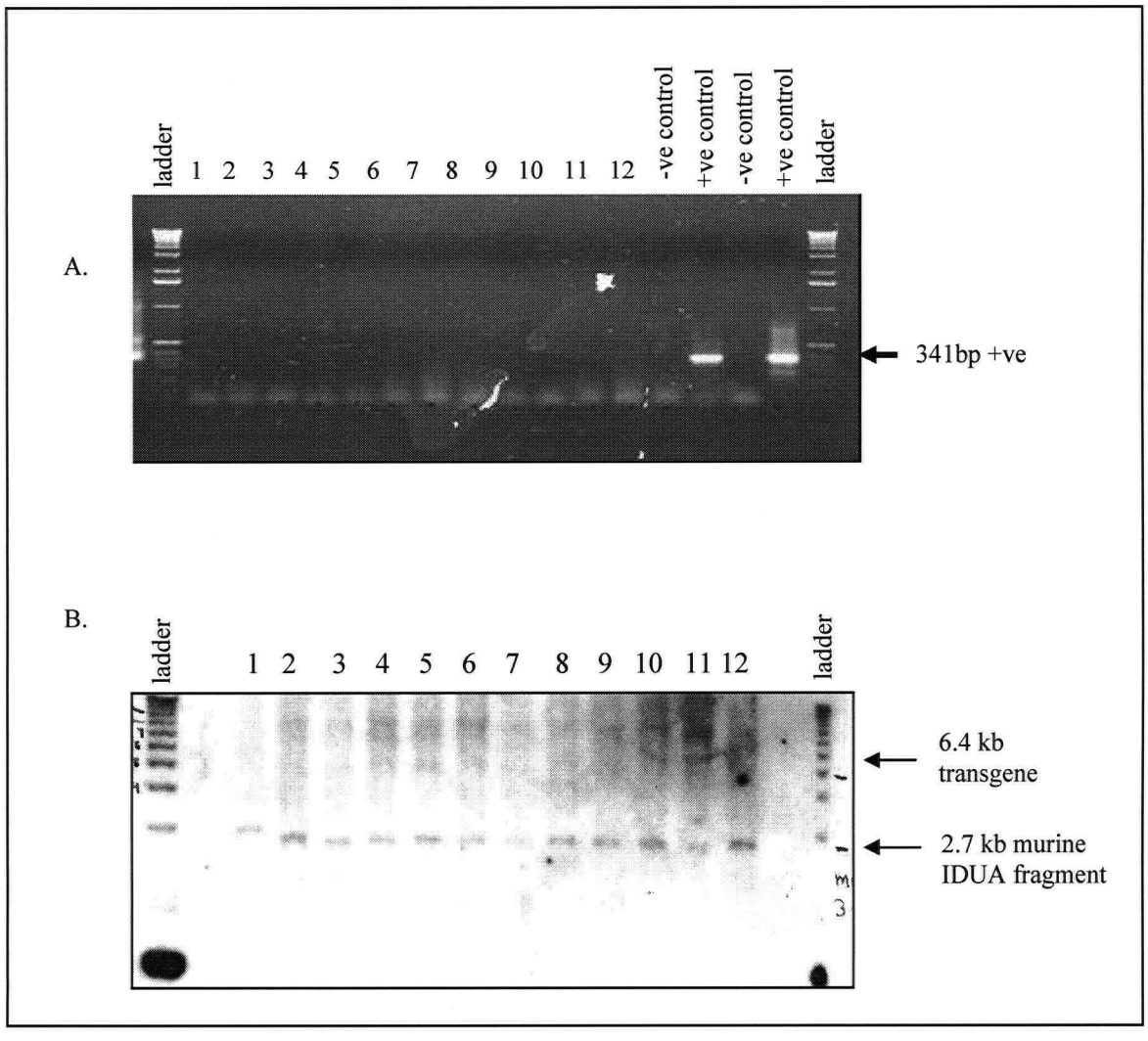

Fig 4.11: Analysis of samples from microinjection of ubiquitous IDUA construct CMV-IDUA

A. Nested PCR on 12 samples from CMV-IDUA injection. 1st PCR with human IDUA cDNA specific primers in exon 3 and 7 followed by second round of PCR using nested primers in exons 4 and 6. No positives identified. Positive control sample IDUA cDNA is positive in both rounds. B. Hind III digested Southern of DNA samples expected to produce a band of 6.4 kb in transgene positive samples. Note band in all lanes including nontransgenic lane which is a 2.7 kb Hind III fragment from the murine IDUA locus with homology to the human IDUA cDNA probe used and which represents an internal probe control. No transgene positive mice were identified. The cause of the shift of the 2.7 kb band in lane 1 is unknown.

As summarized in Table 4.1, pronuclear injection of over 1000 eggs with two different constructs produced only 41 mice, less than expected. Of these, no transgene positive mice were identified.

Construct microinjected	Number of eggs injected	Number of mice produced	Transgene positive	Expected (10-40%)
CD11b-IDUA CD11b-LacZ	408	18	0	1-7
CD11b-IDUA CD11b-EGFP	~350	11	0	1-4
CMV-IDUA CMV-EGFP	~350	12	0	1-5
Totals:	~1100	41	0	4-16

Table 4.1: Summary of Pronuclear Microinjection attempts at generation of transgenic lines

Constructs microinjected and resulting mice. No transgene positive were identified.

Historically, pronuclear microinjection produces transgene positive offspring in 10-40% of offspring, which with the 41 mice produced here would be 4-16 positive mice. An embryonic stem cell approach was then used as it was believed possible barriers to transgene positive offspring might be overcome.

4.2.2 Embryonic stem cell approach for the generation of myeloid specific and ubiquitous IDUA expression

The ES approach was undertaken after the failure to produce transgene positive offspring by pronuclear microinjection. The CD11b-IDUA construct was cloned into a neomycin encoding cassette to confer antibiotic selection after introduction into ES cells. Co-electroporation of DNA constructs lacking selection cassettes with selection cassette containing constructs has been reported to lead to a high level of co-integration. It was decided not to add a selection cassette to the CD11b-LacZ reporter construct but rather to

screen ES clones resistant to Neo, and presumed to contain the CD11B-IDUA construct, for integration of the LacZ construct.

The CMV-IDUA construct previously described and intended for ubiquitous IDUA expression, as well as EGFP reporter expression, was cloned into the Flox vector shown in figure 4.12. The Flox vector was used as it provided convenient cloning sites and includes a neomycin resistance cassette.

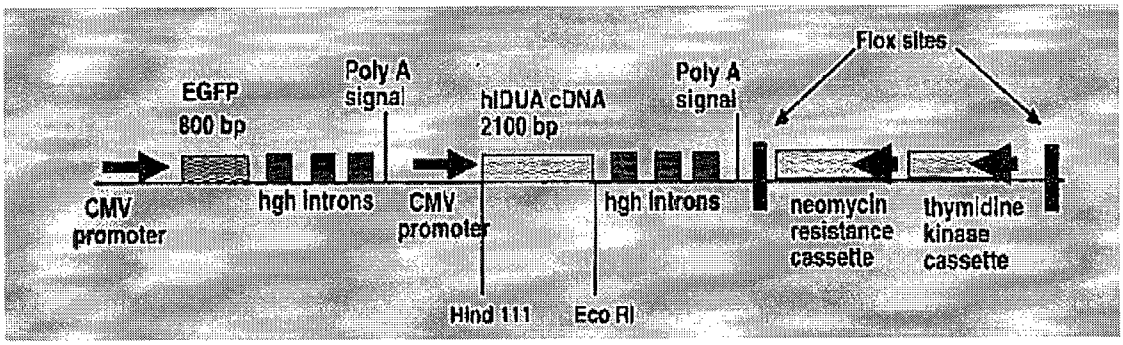

Figure 4.12: pFLOX-CMV-IDUA-EGFP

A construct designed for ubiquitous expression of human IDUA and the EGFP reporter, and allowing for neomycin selection in ES cells.

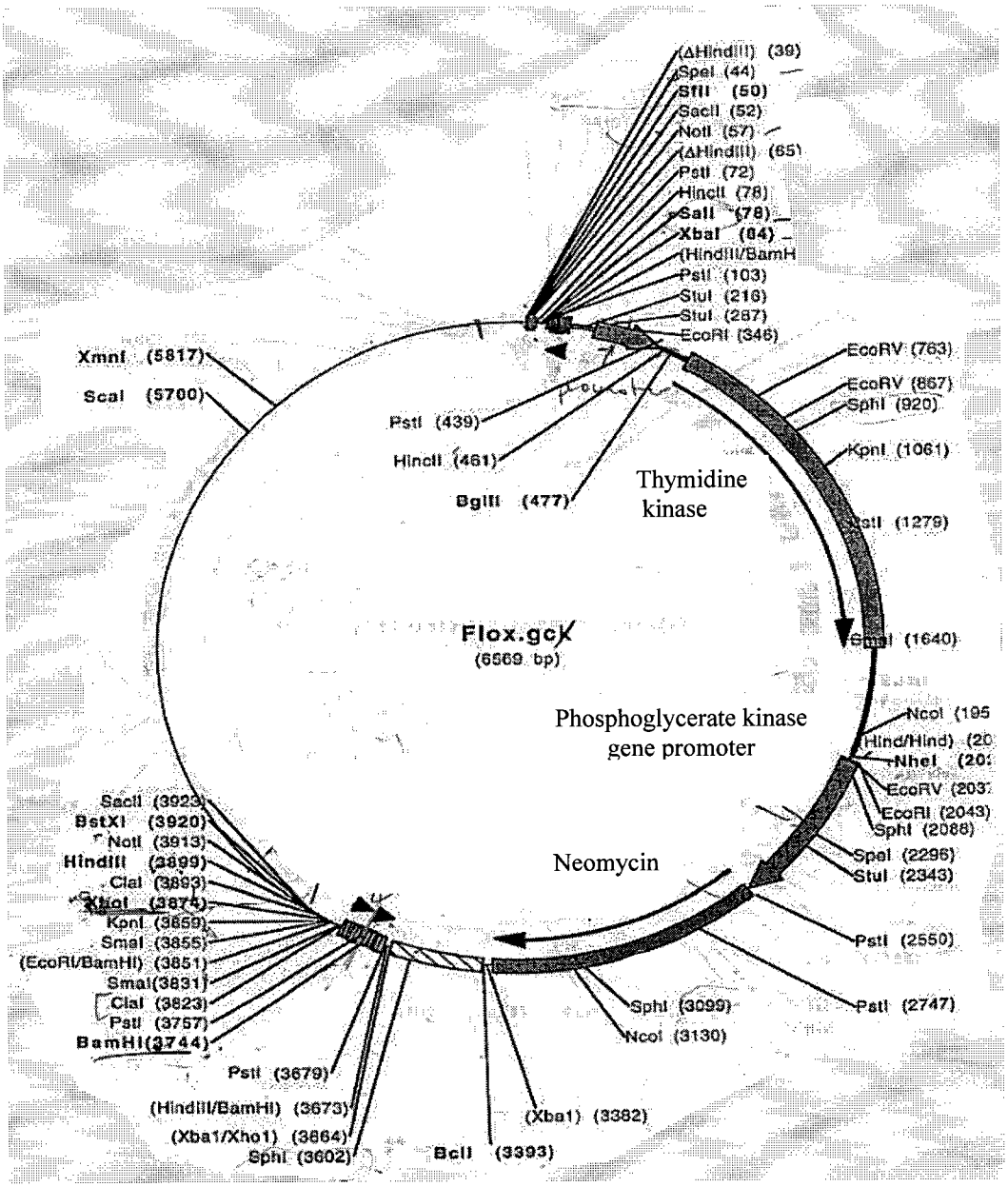

Figure 4.13: The Flox vector used for ES selection of the ubiquitous IDUA and EGFP expressing construct used previously for pronuclear injection

The lox sites (►) are not utilized in this construct. This construct was used as a convenient source of the Neomycin resistance gene, driven by the mouse phosphoglycerate kinase gene promoter. Vector from Scott Pownall.

A second construct intended for ubiquitous IDUA expression, pCAGGs-IDUA, which was considered likely to generate higher levels of transgene expression than the pFlox-CMV-IDUA-EGFP construct, was designed as shown in fig 4.14.

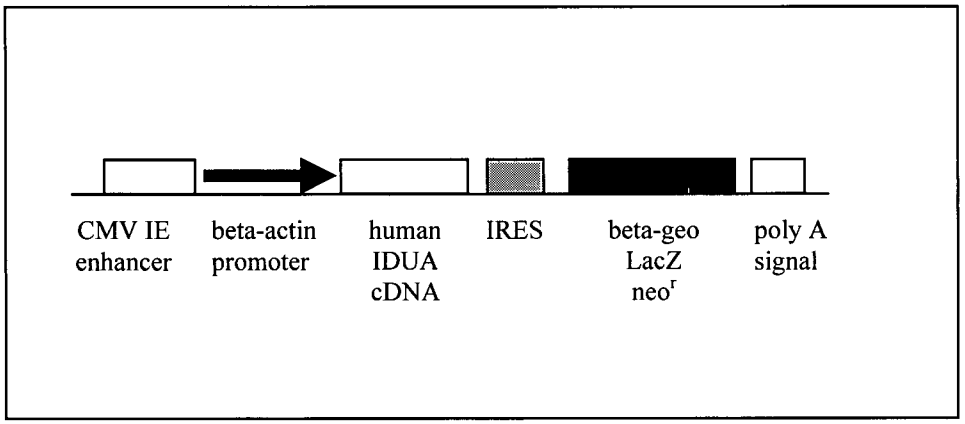

Figure 4.14: Ubiquitous Transgene Construct pCAGGs-IDUA
pCAGGs-IDUA based on the pCAGGs high level mammalian expression vector. The CMV immediate early enhancer element is used with the chicken beta-actin promoter to direct expression of the human IDUA cDNA. An internal ribososme entry site (IRES) allows for expression of a downstream beta-geo fusion gene encoding the beta galactosidase reporter and neomycin resistance genes. A consensus polyadenylation signal completes the construct.

The pCAGGs vector (figure 4.15) (Niwa *et al.*, 1991) was chosen as it has been shown to drive high level expression in eukaryotic cells. In addition, as this vector drives expression in ES cells, replica plates of ES cells could be analyzed for reporter gene expression (LacZ) as well as IDUA enzyme activity.

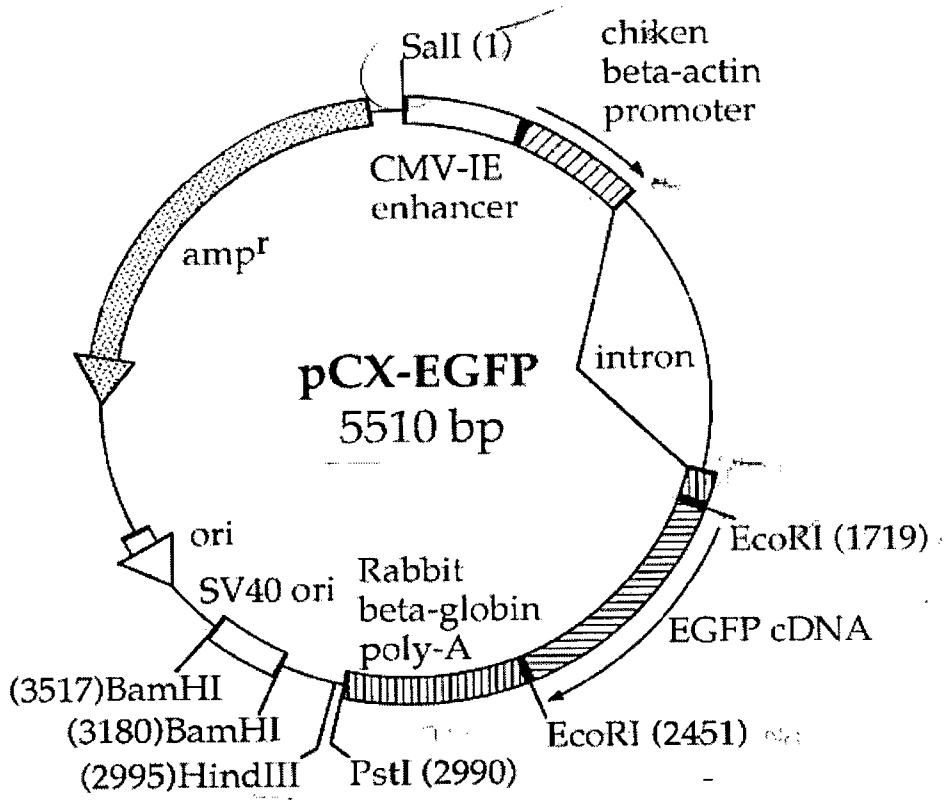

Figure 4.15: pCAGGs vector for high level eukaryotic expression

The pictured vector is pCAGGs with the addition of the EGFP reporter gene. pCAGGs features a proven ubiquitously strong promoter based on the chicken beta-actin promoter demonstrated to drive expression in a wide variety of cells, as well as the CMV-IE enhancer. Other features of this vector include the rabbit beta-globin gene polyadenylation sequence for efficient post transcriptional processing. Vector and map from Dr. Jun-ichi Miyazaki. (Niwa *et al.*, 1991).

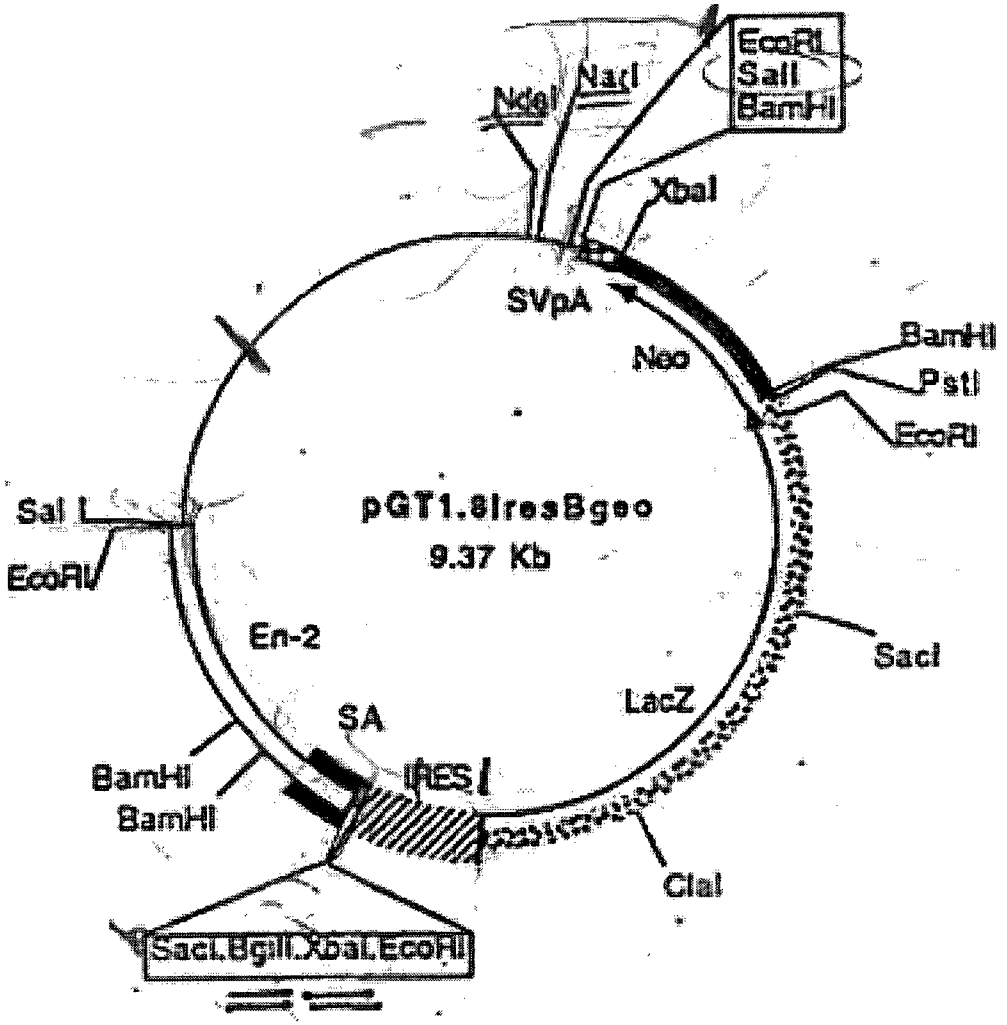

Figure 4.16: The pGT1.8IresBgeo vector

The pGT1.8IresBgeo plasmid features the beta-geo fusion gene for expression of neomycin resistance and beta-galactosidase, and an upstream IRES (internal ribosome entry sequence). The 4.5 kb Xba I/Xba I fragment containing the IRES sequence and beta-geo was removed for addition to pCAGGs. Transgenes cloned upstream of the IRES are expressed along with beta-geo as a dicistronic single transcript. Vector from Scott Pownall (Mountford *et al.*, 1994).

4.2.3 ES lines generated

The CD11b-IDUA transgene construct was successfully introduced into ES cells and independent clones were generated after growth in selective media. In order to

identify clones with co-integration of the CD11b-LacZ, which does not include a selection cassette, Southern blot analysis was performed as shown in figure 4.17. 7 of 14 ES clones that had survived antibiotic selection and therefore had integrated the CD11b-IDUA-Neo construct were found to have integrated the CD11b-LacZ reporter construct.

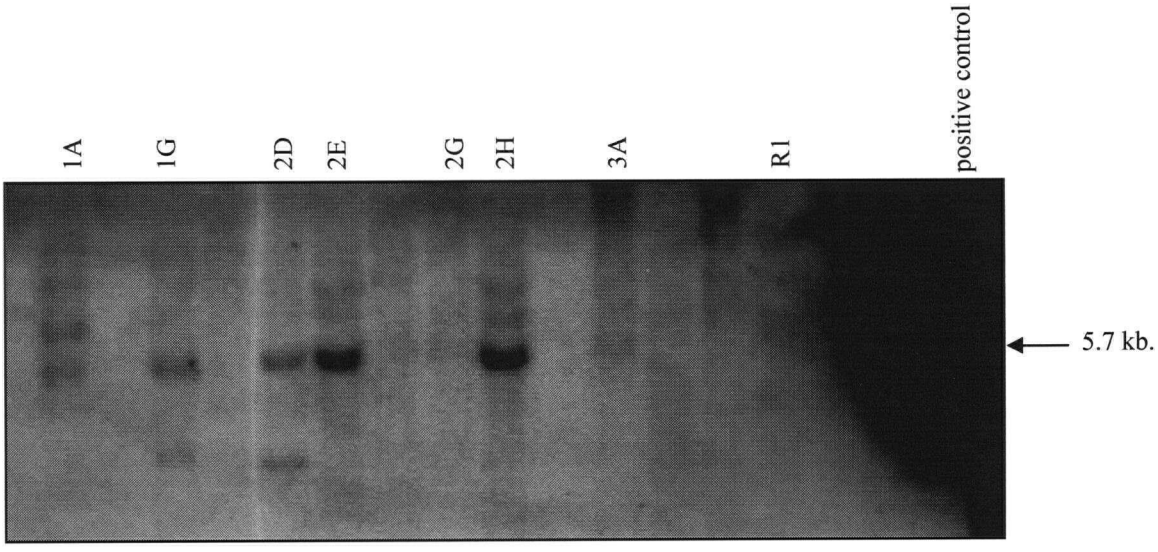

Figure 4.17: CD11b-LacZ reporter construct integrates into ES clones after co-electroporation with the CD11b-IDUA-Neo construct

EcoR1 Southern blot probed with LacZ fragment. Positive bands expected at 5.7 kb. 5 of 14 clones have co-integrated the CD11b-LacZ construct.

ES cells that had been electroporated with the pCAGGs-IDUA construct were screened initially for reporter gene expression by staining for beta-galactosidase activity. Clones showed a wide range of beta-galactosidase intensity shown representatively in figure 4.18.

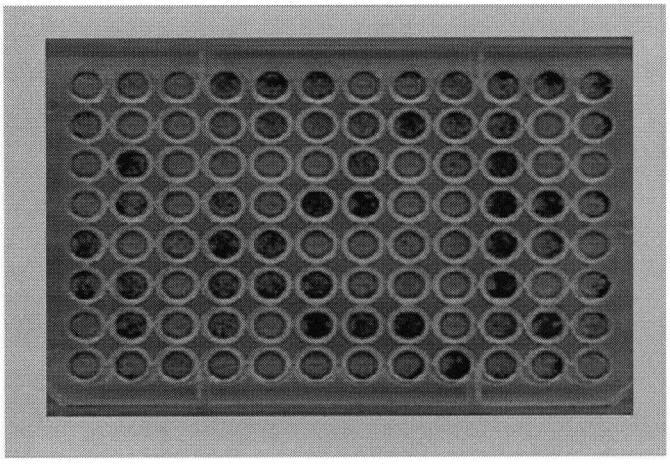

Figure 4.18: Representation of ES clones screened for beta-galactosidase staining intensity

ES clones grown to confluency in 96 well plates were fixed and stained for beta-galactosidase activity.

Reporter gene expression, indicative of the expression of IDUA expressed on the same transgene polycistronic mRNA, was highly variable between different ES clones. The nature of this variability included differences in staining intensity between different clones, and also differences in staining intensity amongst clonal cells within a single well. Clones with high level, consistent beta-galactosidase staining were chosen. A second screen was performed determining approximate IDUA enzyme specific activity levels, normalized to total protein content. pCAGGs-IDUA ES clones were determined to show high levels over non-transfected control ES cells and ES clones transfected with the CD11b-IDUA construct (data not shown). A high degree of correlation was found between the intensity of beta-galactosidase expression and IDUA enzyme specific activity level.

Blastocyst injection of engineered ES lines

Multiple blastocyst injections of various constructs was performed as shown in Table 4.2

Construct	Clone ID	Number of blastocysts injected	Chimeras produced	Percent chimersim
pCAGGs-IDUA				
	2C	~26	2	5%, 5%
	1G	11	0	-
	2D	14	0	-
	12B	~26	1	60%, but female
CD11B-IDUA and CD11b-LacZ				
	2E	~13	1	5%
	2H	~13	2	5%, 5%
Totals:	6	~100	6	low

Table 4.2: Blastocyst injection of engineered ES clones produces only low level chimeras

A total of 103 blastocysts were injected with 6 different characterized ES lines transgene positive for the CD11b constructs or the pCAGGs-IDUA construct. 3 chimeras were produced for each type of transgene. All chimeras were very low level with the exception of a female chimera generated from line pCAGGs-IDUA 12B. However the R1 ES line used is male indicating this chimera could not be capable of germline transgene transmission.

4.3 Discussion

No chimeras capable of germline transmission of either the CD11b-IDUA or the pCAGGs-IDUA transgene constructs were generated after injection of 100 blastocysts. Only low level (5%) chimeras were produced in only 5 chimeras generated, with the exception of a higher level (60%) but female chimera. The reason for the low number of chimeras produced, and the low level of chimerism observed, is unknown. Possibilities for this outcome include alterations to the ES clones rendering them limited in their ability to constitute adult tissues, a constant concern with ES cell culture. Technical barriers could also play a part. Alternatively, the inability to generate high level chimeras and germline transmission after numerous attempts could reflect a biological effect of transgene expression. In order to generate mouse lines which could express transgenic human IDUA, I chose to use a conditional transgene expression approach which would allow control of the timing, and location, of transgene expression. This is described in chapter 5.

Chapter 5: Conditional transgenic expression of human alpha-L-iduronidase in a murine model to establish effective and tolerable limits for gene therapy for MPS I

5.1 Introduction

This chapter describes the successful generation of two murine lines of a conditional transgenic mouse with the potential for expression of human IDUA enzyme. These lines are designed to model, in conjunction with the IDUA deficient mouse line described in Chapter 3, gene therapy approaches for MPS I. As described in Chapter 4, numerous attempts to generate murine strains over-expressing IDUA, from the human IDUA cDNA, were not successful. As pronuclear injection leads to variable levels of transgene positive founder mice and is dependant on operator skill and experience, it is possible that by chance no transgene constructs were integrated into injected nuclei. It is also possible that screening of founder mice could have missed transgene positive founders.

An approach using embryonic stem cells, in which engineered, partially defined cells are used in the generation of chimeric mice, was then employed as this might allow for development of transgene carrying chimeras, and allows for repeated attempts with clonal cells. However only low level chimeras were generated and no germ line transmissable mice were identified. This suggests that the expression of the transgene, human IDUA, might be deleterious to normal development. To explore this possibility, and towards generation of IDUA expressing mice for use in transplantation and as models of gene therapy, a conditional transgene system was employed. This approach would allow selective IDUA transgene expression avoiding developmental transgene induced bottlenecks, should they exist. With this conditional system, transgenic expression of IDUA can be regulated both spatially and temporally, and is controlled by Cre mediated recombination. The therapeutic benefit of selective IDUA expression could

be assessed with strategic breeding into the IDUA deficient MPS I mouse model, and a mouse line expressing Cre recombinase. Thus the two objectives of Chapter 4, the generation of a model of *in utero* bone transplantation, and the generation of a model with widespread or ubiquitous expression, could be achieved with a single initial transgenic mouse. In addition, the same mouse could be crossed with other Cre expressing mice testing IDUA specific expression in virtually every tissue imaginable to address the outcome of specific reconstitution on murine MPS I.

5.1.1 Conditional transgene regulation systems

The inability to generate transgenic mice lines expressing human IDUA, either ubiquitously, or in marrow derived cells, raised the possibility that IDUA overexpression impaired development. In order to create a mouse that had the potential for IDUA expression but was initially carrying a silent version of the IDUA transgene, a conditional transgenic approach was used that would allow regulation of the activation of IDUA transgene expression and hopefully avoid possible developmental bottlenecks. Conditional control of transgene expression allows for regulation of the location and timing of transgene expression. Conditional control is required when one wants to study the function of a gene which is deleterious to normal development, as could be the case with IDUA expression, and to address the biological functions of a gene product in a specific environment, the main objective of the generation of transgenic lines expressing IDUA. Specifically, crossing of selectively activated IDUA expressing lines into the *Idua* -/- deficient background by transplantation, or mating, to address the benefit of cell specific IDUA reconstitution on the phenotype of murine MPS I. Conditional control ideally involves low or zero basal transgene expression when "off", and high levels of

gene expression when "on". The conditional system should be specific to the transgene and not alter general metabolism.

Two fundamentally different approaches to conditional gene regulation have been established. Both approaches are based on two components: an effector transgene that acts on a target transgene, in a so called binary transgene system. These systems involve mating an effector line with a line carrying the target transgene, producing double transgenic offspring with the potential for target transgene expression. In one approach, exemplified by the TetR transactivator system, the effector transgene encodes a transactivator which transactivates transcription of the target transgene (Gossen and Bujard, 1992). Introduction of doxycycline (dox) or other inducer regulates the binding of the transactivator to the operator of the system, allowing for regulation of gene expression including gene activation or repression. The TetR transactivator approach has been used successfully *in vivo* to regulate genes in a variety of ways. In the second approach, the effector transgene encodes a recombinase such as Cre or FLP that specifically rearranges target sequences to regulate gene expression. The differences between these approaches make them suited for different situations.

Transcriptional transactivation has two main advantages over recombination based regulation. First, expression of the target gene is reversible, allowing for the transient expression of a transgene. Second, variable levels of target transgene expression can be obtained by regulating inducer concentration. However, transactivation suffers from variable levels of background expression, reducing their utility for the regulation of deleterious transgenes. Recombination based regulation, with its irreversibility, is suited for tissue specific knockouts, for cell-lineage analysis, and for permanent gene activation.

My objective was to generate a mouse line in which IDUA expression could be induced in specific tissues and at specific times. The irreversibility of the recombination approach was acceptable, and an important benefit of the recombination approach is the non-existent basal expression before recombination. Most importantly, many mice strains expressing tissue specific Cre recombinase have been generated, providing a wide selection of activating mice, as shown in table 5.1.

Expression pattern	Promoter	Reference
ubiquitous early	PGK	Lallemand *et al.*, 1998
myeloid cells	endogenous M lysozyme	Clausen *et al.*, 1999
liver	albumin	Postic *et al.*, 1999
chondrocytes	collagen type II	Sakai *et al.*, 2001
smooth muscle	smooth muscle myosin heavy chain	Xin *et al.*, 2002
mid/hindbrain	En2	Zinyk *et al.*, 1998
pancreatic beta-cells	Ins2	Herrera *et al.*, 2000

Table 5.1: Representative Cre expressing mice

This allows for analysis of expression in many different tissues at various stages of development. As shown in table 5.1, a mouse strain expressing Cre in myeloid cells, similar to the expression pattern of the CD11b promoter and useful for assessment of the potential of bone marrow transplantation for MPS I, has been generated and confirmed to express Cre preferentially in myeloid lineage cells (Clausen *et al.*, 1999). Also characterized and potentially useful are mice strains expressing Cre in liver,

chondrocytes, or ubiquitously (Postic *et al.*, 1999, Sakai *et al.*, 2001, Lallemand *et al.*, 1998).

With suitable recombination sites and other DNA elements, a single transgenic line could be designed with ubiquitous potential for expression of human IDUA, regulated by the expression pattern of Cre. This one line would then be used to address a number of biological questions through differential Cre mediated activation, including acting as a source of expressing cells for transplantation experiments into the *Idua* -/- mouse line, as a genetic model of tissue specific IDUA expression for breeding experiments with the *Idua* -/- line, and to determine the phenotype of IDUA expression during development.

Two recombinases have been used for genomic manipulations in mammalian cells, Cre from bacteriophage P1 (Sauer and Henderson, 1989) and FLP from *Saccharomyces cerivisiae* (O'Gorman *et al.*, 1991). The availability of different Cre expressing mice as activators makes the Cre/LoxP system of recombination more suitable to this project and will be discussed further. The Cre recombinase of P1 bacteriophage is a 38 kD protein that belongs to the integrase family of site-specific recombinases. As depicted in figure 5.1, Cre recombinase mediates recombination between two of its recognition sites, loxP sites, which consists of a 34 basepair (bp) consensus DNA recognition sequence consisting of a core sequence of 8 bp and two 13 bp flanking palindromic sequences (Hamilton and Abremski, 1984). The asymmetric core sequence defines an orientation to the loxP site, and regions flanked by two loxP sites with the same orientation undergo deletion of the flanked region upon Cre mediated recombination while loxP sites facing each other lead to inversion of the intervening

region. The function of Cre in the bacteriophage P1 life cycle is to ensure the phage genome exists as a monomeric plasmid within the bacteriophage, E. coli, as concatomers of the phage genome could result in loss of the phage genome upon cell replication. The Cre recombinase is also active in mammalian cells (Sauer and Henderson, 1988), and *in vivo* in transgenic mice (Lasko *et al.*, 1992), including in postmitotic cells like neurons and T cells (Gorman and Bullock, 2000). It is important that the Cre recombinase not result in long term instability in the mouse genome for it to be useful in transgenic studies. A random occurrence of a specific 34 bp sequence requires a 1×10^{18} bp length of DNA, while the entire mammalian genome is only 3×10^{9} bp, making it unlikely the 34 bp loxP site would be encountered in the mammalian genome (Nagy 2000).

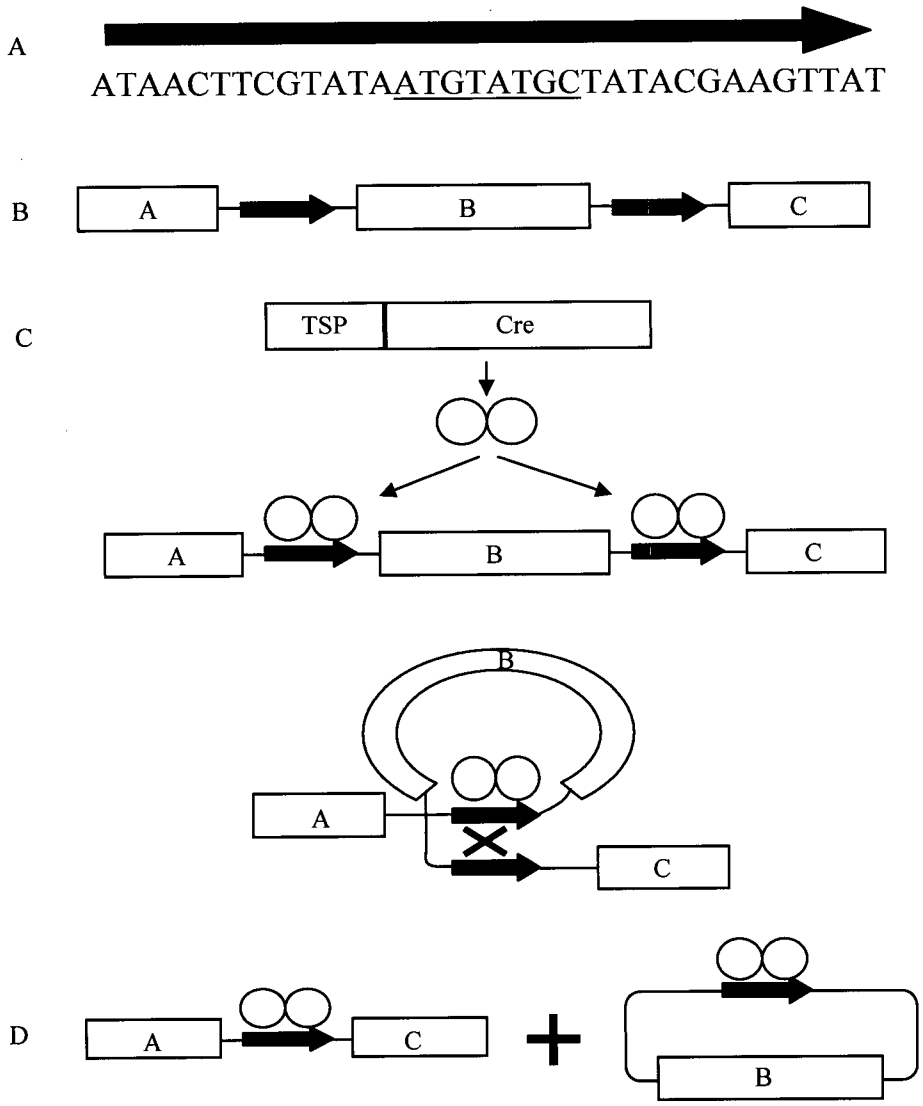

Figure 5.1: Cre/loxP recombination

A) The 34 bp loxP site (black arrow, underlying sequence), consists of an 8 bp directional core element (underlined) flanked by two palindromic 13 bp sequences. B) A representative target region, which has been engineered to include two loxP sites (black arrows) flanking a region for potential removal. C) Introduction of Cre recombinase which, as dimers, binds to the loxP sites and mediates recombination between them. D) The products of recombination are the original target region minus the region flanked by loxP sites and an independent DNA element containing the flanked region, which is degraded. For tissue specific knockouts, region B represents an exon of a gene flanked by loxP sites located in adjacent introns. For conditional gene activation described in this project, region B represents a strong transcription stop signal (polyadenylation signal) removal of which allows expression of region C, the human IDUA cDNA transgene. The specificity of the promoter driving Cre dictates the activation of expression of human IDUA. TSP=tissue specific promoter.

The Cre/loxP system has been used to mediate recombination *in vitro* and *in vivo* that include the activation or inactivation of a gene (Lewandoski, 2001), translocations (Medberry *et al.*, 1995), and inversions (Molete *et al.*, 2001). This level of regulation of control can be combined with the transactivator control elements described earlier to further control the onset and location of transgene expression.

For the purpose of this study, conditional gene activation was desired such that Cre recombination would allow expression of human IDUA. A construct with most of the desired elements had already been described, which when used with an ES cell approach, generated mouse lines suitable for the analysis of Cre expressing mice. These reporter mice lines, Z/AP and Z/EG, are designed such that Cre mediated recombination causes a switch from the expression of the lacZ gene to alkaline phosphatase or green fluorescent protein, respectively (Lobe *et al.*, 1999, and Novak *et al.*, 2000). These reporter mice lines are crossed into lines expressing Cre recombinase for determination of the Cre promoter expression pattern. With the addition of an internal ribosome entry site (IRES) allowing for the production of dicistronic transcripts (Mountford *et al.*, 1994), the transcription of the IDUA transgene could be linked to the expression of a reporter in a system allowing for tissue specific expression of human IDUA and monitoring of the state of IDUA expression with a dual reporter system indicating both on and off states of IDUA expression. As depicted in figure 5.1, by flanking a stop signal, in the form of a polyadenylation signal, with loxP sites, the expression of downstream elements can be regulated by the specific expression of Cre recombinase. This forms the basis of the successful generation of a conditional transgenic mouse line with the potential for tissue specific expression of human IDUA.

5.1.3 Experimental Approach

The embryonic stem cell approach to the generation of transgenic mice offers the advantage of selecting cell clones with rare, desired expression characteristics at the level of cell culture. As discussed previously, the generation of transgenic mice with specific expression patterns can be problematic with the traditional pronuclear approach. Critical to this project was the ability to express human IDUA, as well as a reporter gene, in as many or ideally all tissues of developing and adult mice. As demonstrated by Lobe *et al.*, examination of the transgene expression characteristics of embryonic stem cells allows for the isolation of clones more likely to give desired long term transgene expression when used to produce transgenic mouse lines (Lobe *et al.*, 1999). By using a promoter active in embryonic stem cells, directing the expression of a reporter gene, individual clones with high or low level transgene expression can be identified. Furthermore, clonal populations with consistent expression patterns can be identified. While it might be expected that all genetically identical cells in a clonal population would express transgenes in the same manner, in practice, and as described in chapter 4, this is not the case. In fact identical insertions can lead to differences in transgene expression within genetically identical, clonal populations of cells. This could be due to integration into a region subject to variable expression, such as a cell cycle related gene, and indicates that the promoter elements used in this study are not sufficient to insulate expression of the transgene construct from regional transcription influences. Given this, those integrations that give strong, consistent (*i.e.* all cells in the population) are chosen for the generation of mouse lines. The embryonic stem cell approach also allows for the molecular analysis

of clones; that is, representative cells can be genetically analyzed while clonal cells are still available for mouse generation.

Relevant to the use of the Cre/Lox system is the number and pattern of transgene integrations, as well as the number of integration sites throughout the genome, that are present in a clone that is transgene positive as identified by antibiotic selection and or reporter gene expression. As tandem integrations, or independent integrations in the same cell but on different chromosomes, can result in undesired recombination events between lox sites or breeding difficulties, Southern blot analysis of clones can be performed to identify clones with single site, single number transgene construct integrations. It is also possible to prematurely recombine representative samples of cell clones to confirm that a clone has the ability to express the recombined transgenes, in this case human IDUA and human alkaline phosphatase. Figure 5.2 is a schematic of the selection and screens that were initially planned for the identification of desired embryonic stem cell clones.

Antibiotic resistance is encoded by the transgene construct, so that huge enrichment for clones with integrated constructs occurs after 8 days of growth in selection media. Lac Z expression is analyzed in clones for intensity, as well as consistency. Single integrations at a single locus are desired, to simplify later recombination and transmission. The ability of clones to undergo successful recombination can be assessed via transfection of Cre plasmid, and scored by staining for alk phos expression and/or IDUA activity. Together, these screens are intended to enrich for rare integration events promoting long term transgene expression even in differentiated cells types.

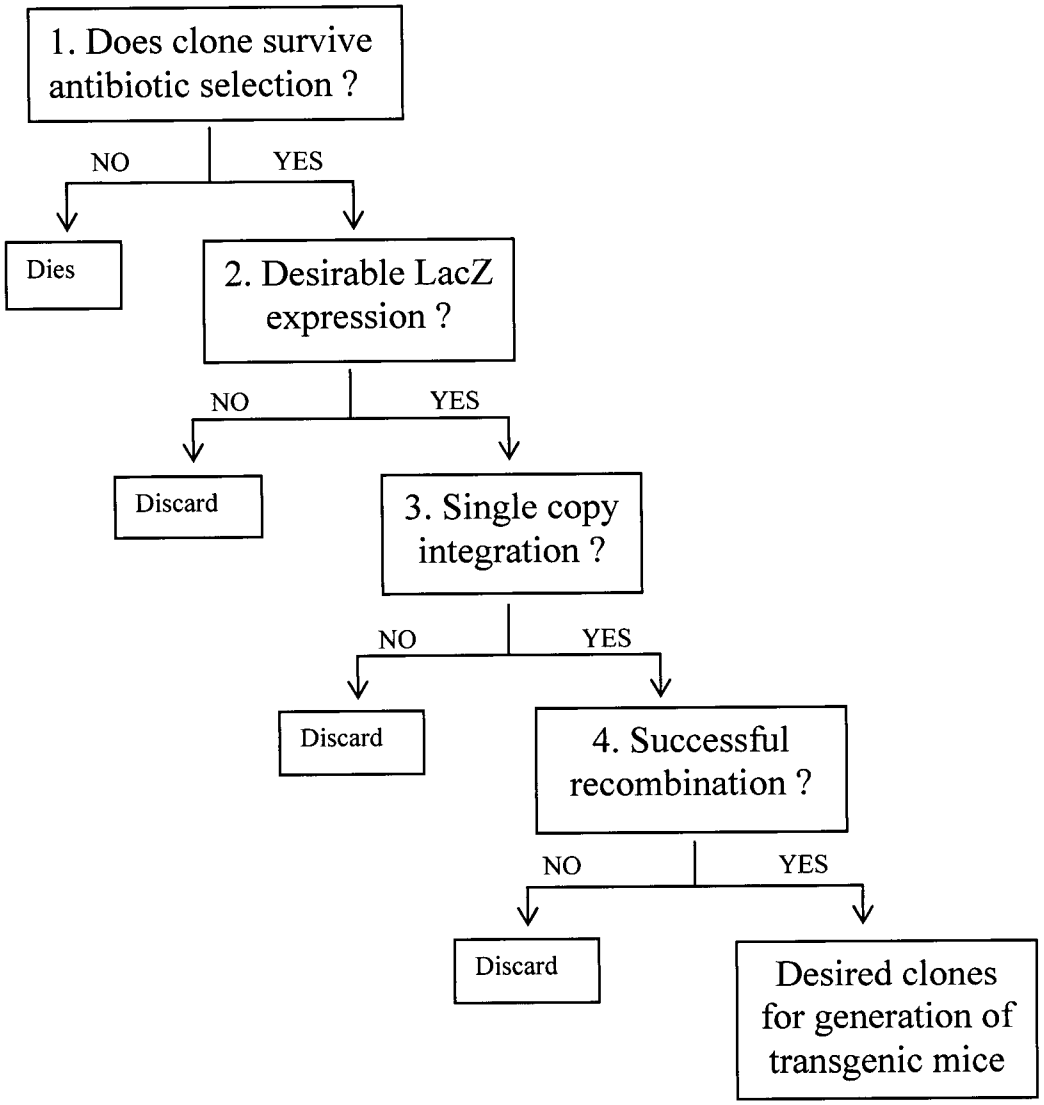

Figure 5.2: Schematic of the selection and screening for desirable ES clones

Rather than clone the desired elements for conditional Cre-mediated regulation and a reporter system for use in ES cells, I chose to use the proven Z/AP based constructs generated by Dr. Corrinne Lobe (Lobe *et al.*, 1999). The parent vector pCCALL2-IRES-hAP/cg is described in figure 5.3. This vector uses recombination to remove transcription stop signals that otherwise prevent expression of downstream genes. Driving expression of this construct are the same elements found in pCCAG, the CMV enhancer

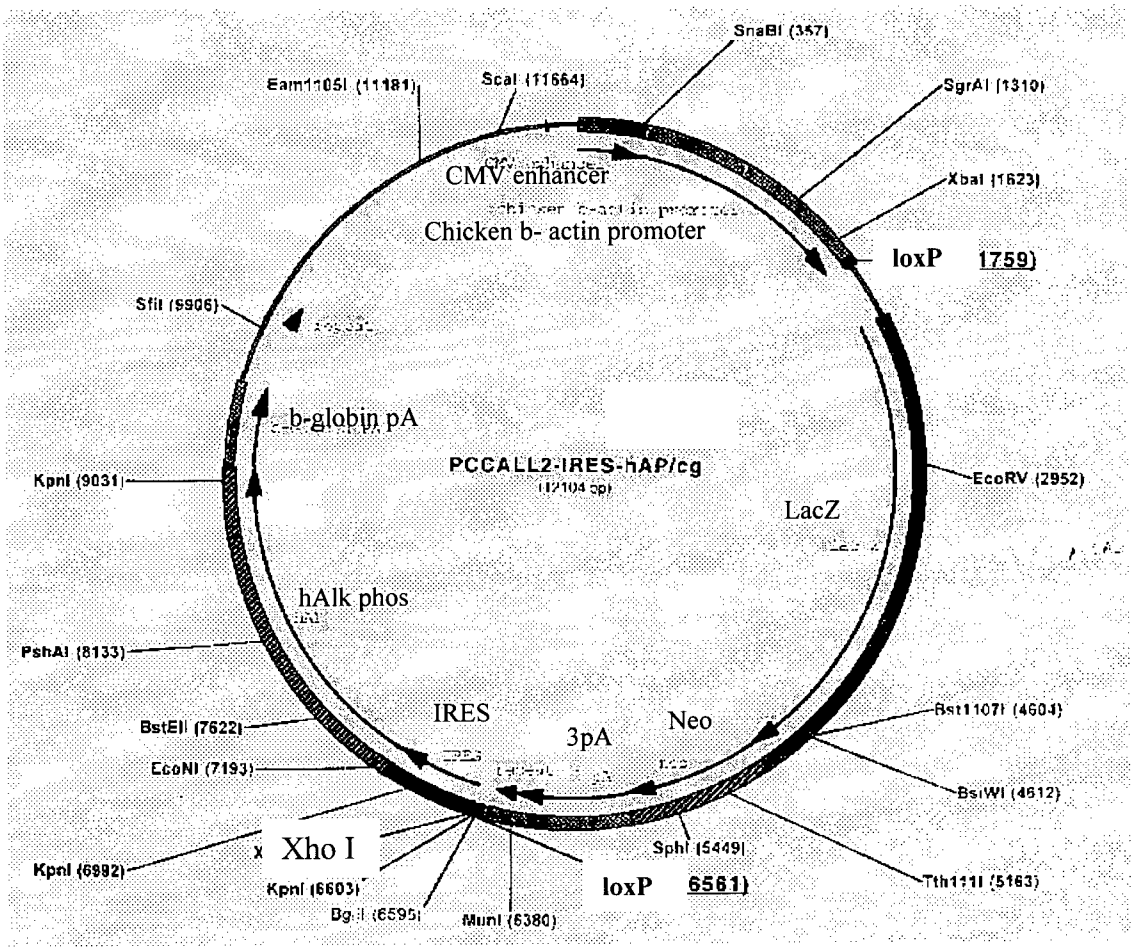

Figure 5.3: pCCALL2-IRES-hAP/cg parent construct

The CMV enhancer coupled with the chicken beta-actin promoter drive expression of downstream elements. Flanked by loxP recombination sites is the beta-geo fusion gene encoding beta-galactosidase reporter expression (LacZ) and neomycin resistance (Neo), allowing for positive selection and transgene expression analysis in ES culture. Also flanked by the loxP sites are 3 strong polyadenylation signals (3pA) which prevent further transcription, preventing expression of any introduced transgenes and the second reporter gene, human alkaline phosphatase (hAlk phos). Introduction of Cre removes the loxP flanked beta-geo and the 3pA, allowing for expression of introduced transgenes and the hAlk phos reporter. From Dr. Corrinne Lobe (Lobe *et al.*, 1999).

and the promoter from the chicken b-actin gene. LoxP sites flank the beta-geo fusion gene, encoding beta-galactosidase and neomycin resistance, and three polyadenylation

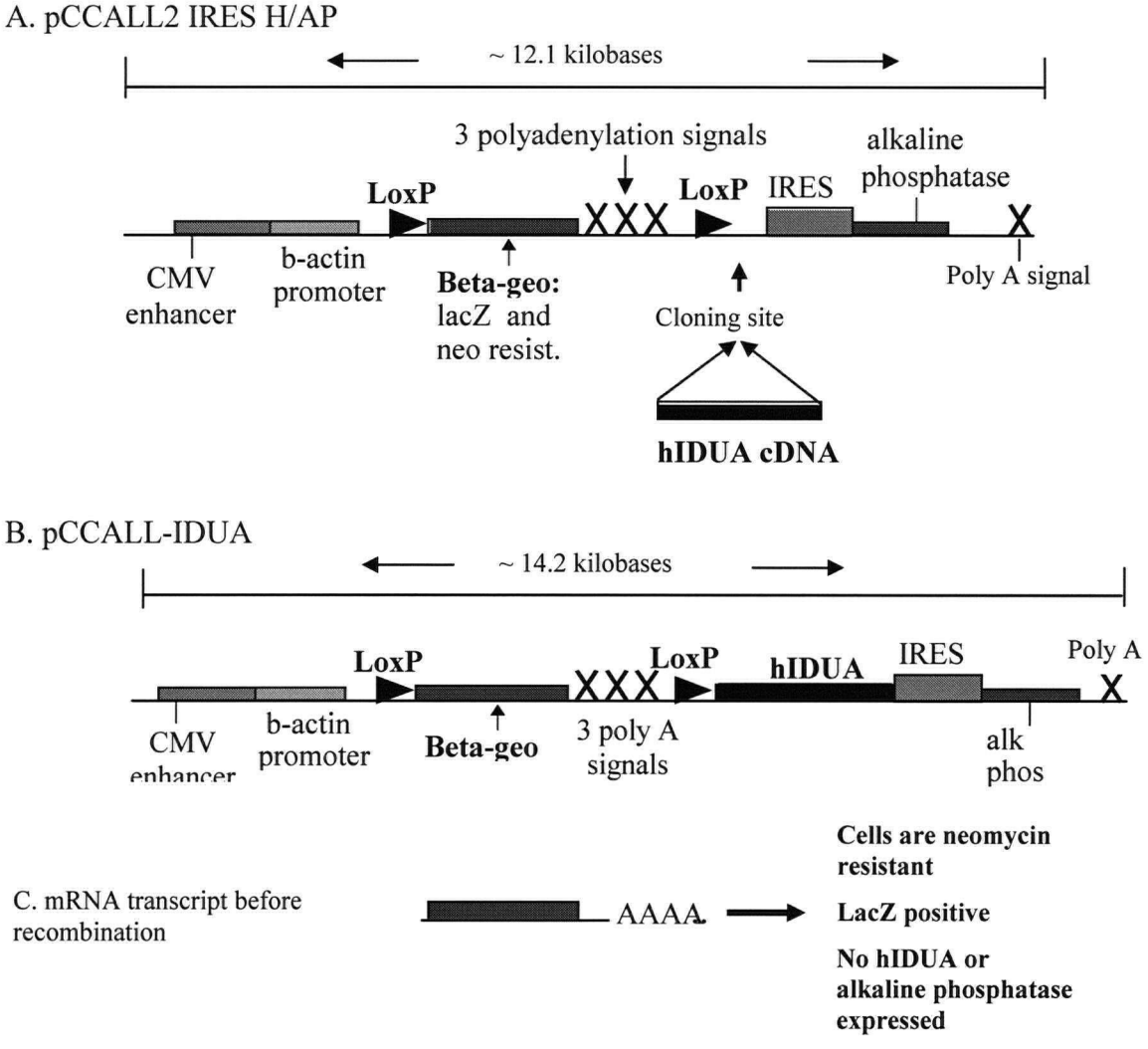

Figure 5.4: Schematic of the pCCALL-IDUA construct

This construct is designed to allow conditional expression of human IDUA as well as reporter genes indicating state of recombination. A. Expression of the construct is driven by the pCCAG promoter, which consists of the CMV enhancer and chicken beta-actin promoter. Immediately downstream lies one of two loxP sites, then a selection and reporter gene cassette followed by three copies of the SV40 polyadenylation signal, and the second flanking loxP site. The flanking loxP sites are used for Cre mediated recombination, leading to removal of the beta-geo selection cassette and the polyadenylation sequences, allowing for expression of a transgene and the human placental alkaline phosphatase reporter gene. B. The 2.1 kb human IDUA cDNA with polyadenylation sequence removed was added to pCCALL2 to make pCCALL-IDUA. C. The initial mRNA transcript before Cre mediated recombination. No human IDUA or alkaline phosphatase are expressed. LoxP=loxP 34 bp recombination site with indicated orientation, beta-geo=beta-galactosidase and neomycin fusion gene, alk phos=human alkaline phosphate gene, IRES=internal ribosome entry site.

signals. A unique cloning site follows the LoxP site, allowing addition of genes of interest. Next, an IRES, or internal ribosome entry sequence, allows linked transcription of genes of interest and the alkaline phosphatase reporter gene. A rabbit polyadenylation signal completes the construct.

A schematic of the construct, including the addition of the human IDUA cDNA, is shown in figure 5.4. As shown, the unrecombined construct pCCALL-IDUA should express beta-geo, allowing for LacZ reporter analysis, but no human IDUA, as the 3 polyadenylation sites are intact. Figure 5.5 describes the recombined transgene construct, with removal of the beta-geo cassette and 3 polyadenylation signals, leading to loss of LacZ expression and allowing for expression of downstream human IDUA and the human alkaline phosphatase reporter gene. Using the pCal-IDUA construct, I hoped to generate a conditional Cre-regulated transgenic mouse line with the potential to express human IDUA.

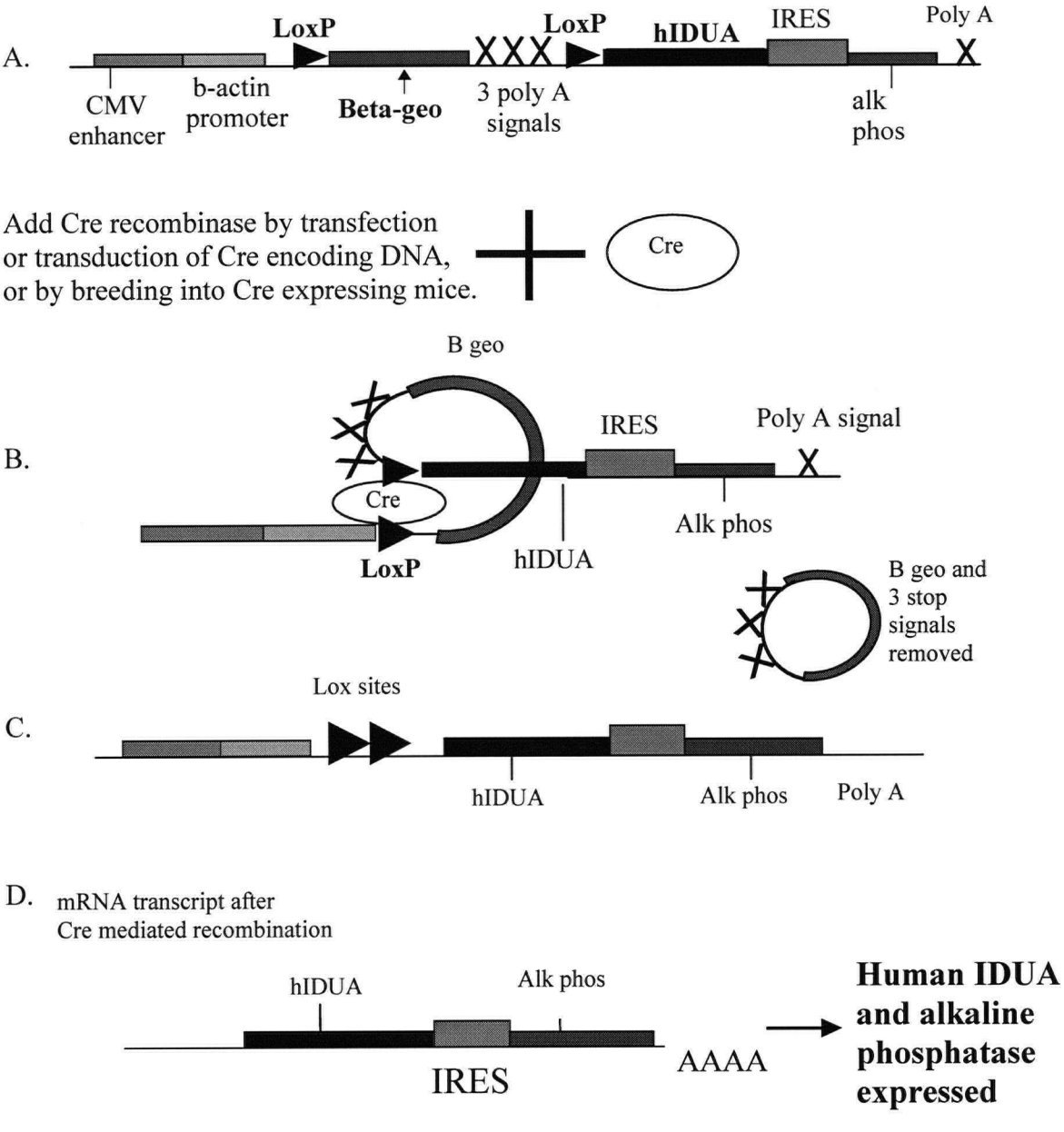

Figure 5.5: Recombination and the expression of human IDUA

A) the unrecombined construct expressing beta geo. B) With the addition of Cre recombinase, recombination occurs between the two loxP sites and the beta geo cassette and the 3 polyadenylation signals are lost. C) The recombined allele, which after removal and degradation of the region encoding the beta-geo fusion gene and 3 strong polyadenylation signals which functioned as a block to downstream transcription. D) After recombination the construct expresses human IDUA and the alkaline phosphatase reporter gene from a single transcript. LoxP=loxp 34 bp site for recombination, IRES=internal ribosome entry site.

5.2 Results

The pCCALL2-IRES-hAP/cg parent construct was obtained in plasmid form from Dr. Corrinne Lobe (Lobe *et al.*, 1999). Numerous individual transformed colonies were used to seed individual large volume cultures and large scale plasmid isolations were performed. As shown in firgure 5.6, restriction digestion with Pst 1 and Bam HI enzymes, both multiple cutters in the pCCALL2-IRES-hAP/cg construct, determined that all individual clones appeared identical with no evidence for rearrangement.

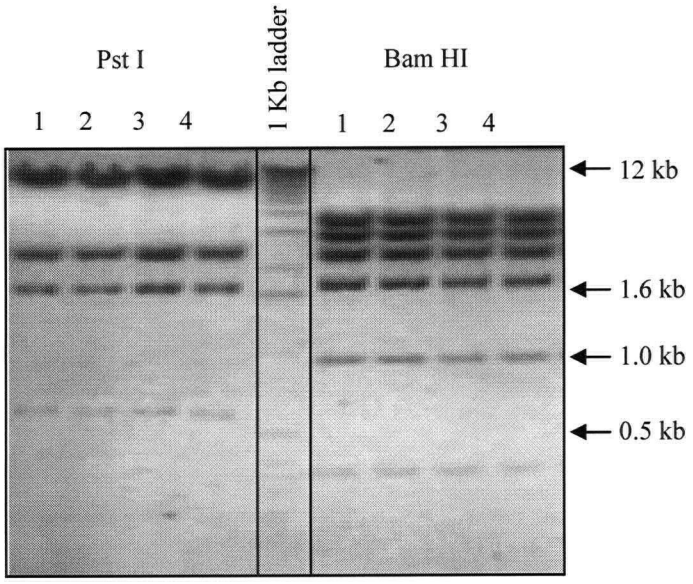

Figure 5.6: Rearrangement check on pCCALL2 construct.
Pst I and Bam HI restriction enzymes were used to confirm that the amplified primary construct was not rearranged after transfection and large scale plasmid isolation. All 4 clones tested produced bands as predicted confirming no rearrangements had occurred. Ladder sizes are shown on the far right.

The introduction of the human IDUA cDNA was simple as a unique Xho 1 site is present in the pCCALL2-IRES-hAP/cg construct directly upstream of the internal ribosome entry site (IRES). A blunted form of the human IDUA cDNA with no polyadenylation signal

was introduced to the Xho 1 opened, blunted pCCALL2-IRES-hAP/cg construct, and transformed cultures were screened for the IDUA cDNA by PCR as shown in figure 5.7.

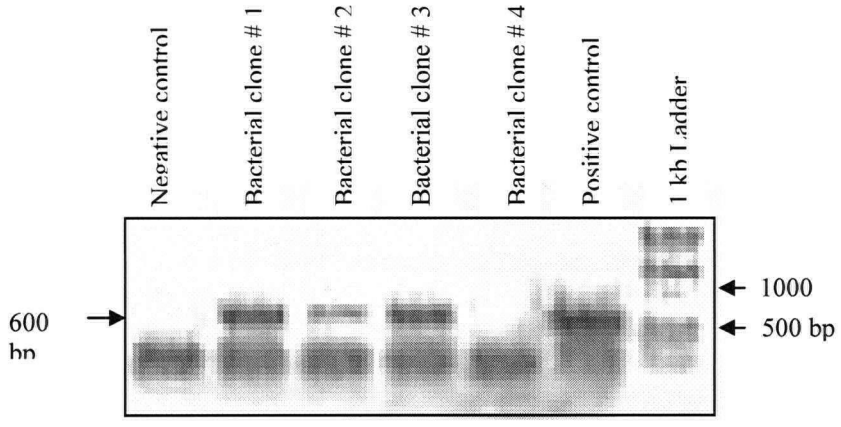

Figure 5.7: PCR detection of bacterial clones containing pCCALL2 ligated with the human IDUA cDNA.

A positive PCR result using primers in exon 3 and 7 of the human IDUA cDNA is expected to produce a band of 600 bp. 3 of 4 clones tested were determined to contain the IDUA cDNA, however orientation is unknown.

To determine the orientation of the IDUA cDNA, a Pst 1 digestion was performed on 8 PCR positive clones, as shown in figure 5.8. Clones 1 and 2 appeared to have the IDUA insert in the correct orientation. Further restriction analysis was performed with Apa 1, Hinc II, and Sph I, as shown in figure 5.9. While clones 1 and 2 generate all the predicted bands for a properly oriented clone with a human IDUA cDNA insert upon restriction, clones 3 and 4, with incorrect orientation, and no insert, respectively, clearly do not.

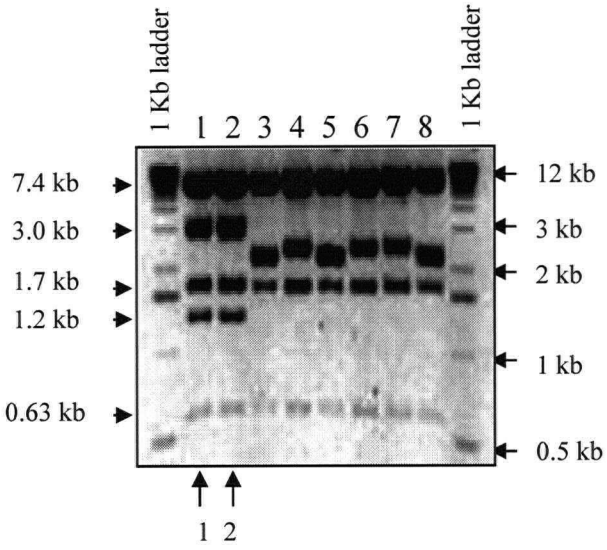

Figure 5.8: Pst I restriction digest of plasmid from ligation of pCCALL2 construct with human IDUA cDNA to determine orientation.

IDUA cDNA containing bacterial clones were identified by PCR specific to the IDUA cDNA. Desired orientation of the cDNA within the construct was predicted based on sequence information to produce fragments after Pst I digestion of 7400 bp, 3000 bp, 1700 bp, 1200 bp, 630 bp, and 188 bp. Reverse orientation of the IDUA cDNA was predicted to produce fragments of 7400 bp, 2100 bp, 2055 bp, 1700bp, 630 bp, and 188 bp. Lanes 1 and 2 contain clones with apparent correct orientation. Lanes 3 to 8 have inserts in the incorrect orientation.

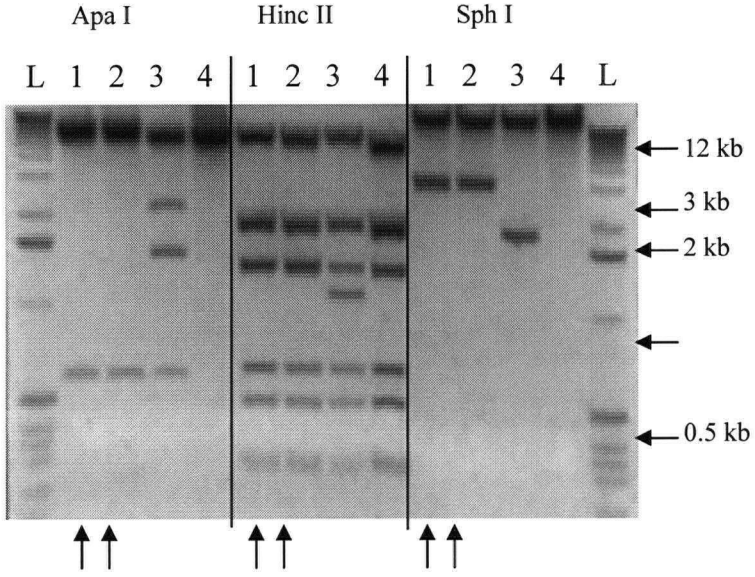

Figure 5.9: Restriction digestion to identify clones with correctly inserted and unrearranged hIDUA cDNA into pCCALL2.

Clones 1 and 2 show predicted correct restriction fragments after Apa I, Hinc II, and Sph I restriction digestion. L= 1kb ladder.

The final pCCALL-IDUA clone, after restriction analysis was amplified and a large scale plasmid isolation was performed. A final check of the pCCALL-IDUA plasmid was performed with Apa 1, Hinc II, Pst I, and SpH1, as shown in figure 5.10, and no rearrangements were detected.

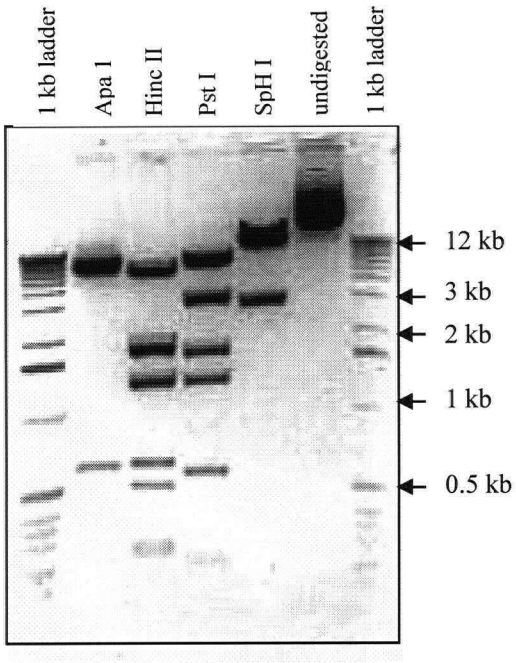

Figure 5.10: Analysis of large scale plasmid isolation of pCCALL-IDUA. Restriction digestion was performed to confirm the amplified construct contained no rearrangements. Digestion with Apa I, Hinc II, Pst I, and Sph I restriction enzymes produced bands of predicted size.

The pCCALL-IDUA plasmid was electroporated into ES cultures, cells were plated at very low density to promote the formation of individual clones from single cells, and neomycin selection was carried out for 8 days. Individual clones were then picked and transferred to 96 well plates for propagation, further analysis, and freezing. A replica plate of the cells was analysed for LacZ expression from the beta-geo fusion gene. Figure

5.11 represents the variable nature of LacZ expression observed between different ES clones.

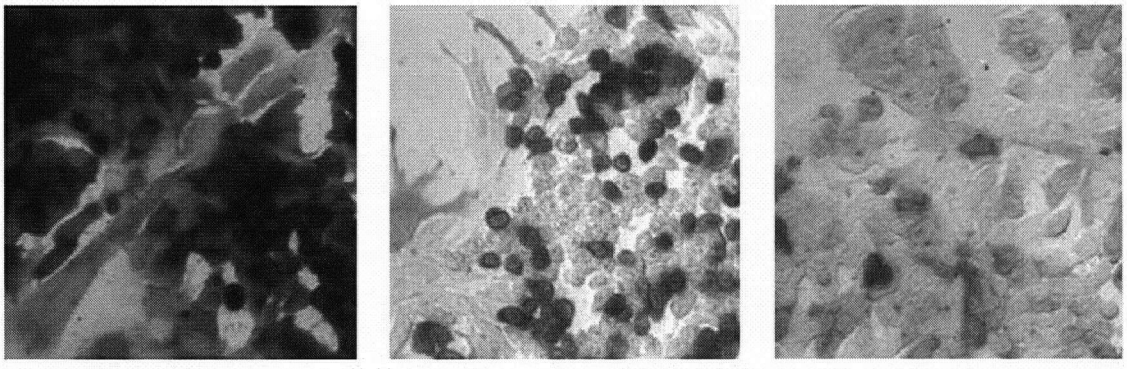

2-6B 4-3E 4-7A

Figure 5.11: LacZ staining of ES colonies demonstrating expression variability.

As I found with the transgenic ES approach in chapter 4, genetically identical ES cells derived from single, transgene containing cells, and therefore clones, express variable levels of the beta-galactosidase reporter gene. This is exemplified in figure 5.11. Clone 2-6B shows strong consistent staining. Clone 4-3E is an example of a clonal population of cells expressing highly variable staining between individual cells, with some cells showing no or little staining while adjacent cells stain strongly. Clone 4-7A demonstrates a weak, but consistent staining clone. This visual screen allows detection of clones hopefully more likely to express transgenes in a consistent manner after differentiation into different cell types in adult mice, and may differentiate clones with high (dark) transgene expression from clones with low (light) transgene expression. Note clones contain multiple cells types including persistent ES cells (small and round) and fibroblast type cells (large and flat). Clones with dark, and consistent, staining were identified, consolidated to new 96 well plates, and amplified.

Next, clones with suitable LacZ staining characteristics were analysed by Southern blotting to identify clones with single integrations of the pCCALL-IDUA construct.

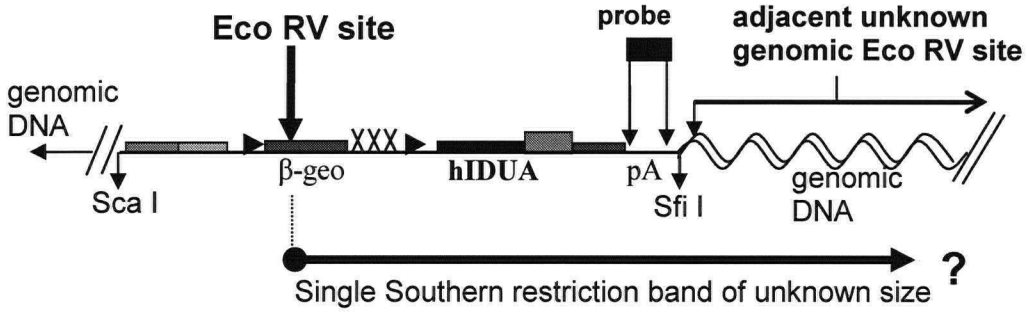

Figure 5.12: Southern blot identification of ES clones containing single copy integrations of pCCALL-IDUA.
X or pA=polyadenylation site, β-geo= beta-galactosidase and neomycin fusion protein.

It is important to identify single copy integrates as multiple adjacent integrations may show aberrant Cre mediated recombination events. As depicted in figure 5.12, an enzyme (EcoRV) cutting once within the pCCALL-IDUA construct was used such that single copy integrations would generate a single Southern band, of unknown size and dependant on a restriction site in adjacent genomic DNA, after probing with a portion of the construct as shown. Multiple tandem copy integrations will produce at least 2 bands after Southern analysis, including one band made up entirely of repeated construct DNA, expected to be approximately 14.0 kb in size for a head to tail integration, and one terminal band including adjacent chromosomal DNA. These clones are avoided. Figure 5.13 shows the results of Southern analysis of transgene expressing ES clones.

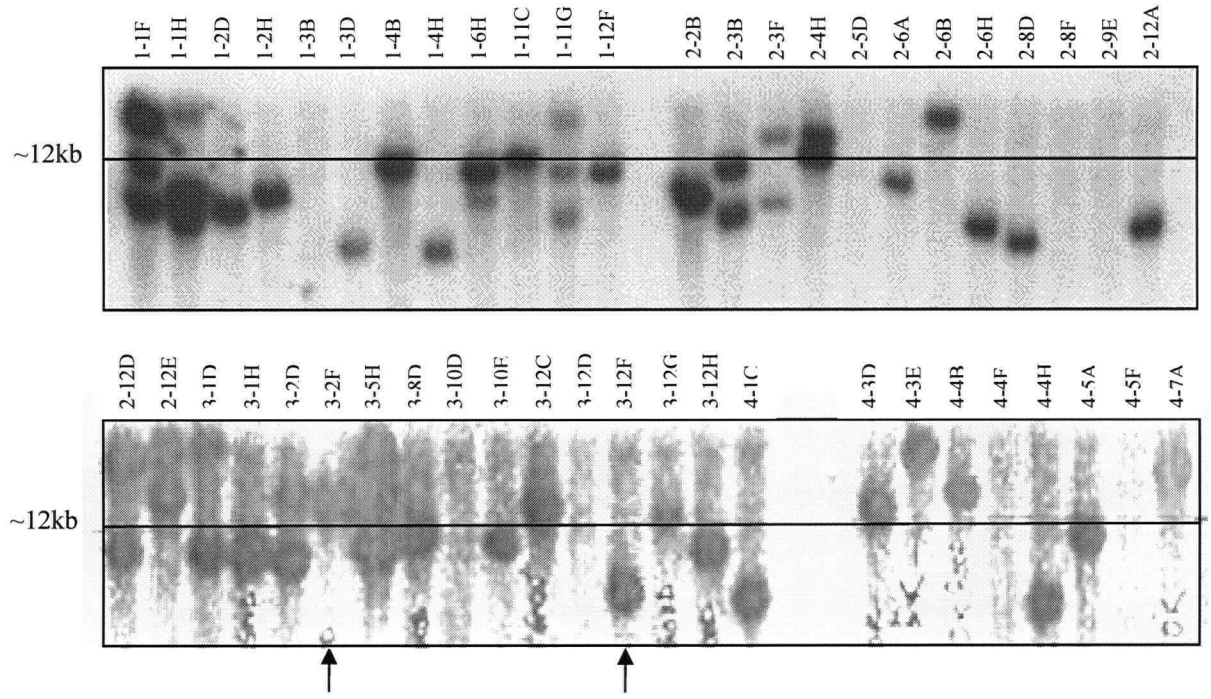

Figure 5.13: Southern blot analysis of 48 ES clones with good reporter gene expression for single copy integrates.

After EcoRV digestion, DNA from ES clones was probed with a fragment of the pCCALL-IDUA construct. ES clones with single copy, single locus integrations will produce single bands of unknown size.

Lane 1-1F, at the upper left hand corner of figure 5.13, clearly shows multiple bands and is thus to be avoided. Lane 1-2H is an example of a suitable clone. Arrows identify ES clones 3-2F and 3-12F, eventually to become mouse lines after fulfilling further expression criteria. A line indicates the approximate position of the 12 kb band of the 1 kb ladder. Clones with bands slightly larger than the 12 kb size were avoided even with single bands as a repeat band of 14 kb size could be superimposed upon the unique band. 20 of 48 assessed clones were found to have multiple integrations, partial integrations, or unexplainable or ambiguous integrations, and were discarded. It is clear upon examination of figure 5.13 that the clones 3-2F and 3-12F, which finally produced

germline chimeras, are different clones. During picking of ES clones, cross contamination of clones can occur as fragments of a picked clone drift and are included with other clones. During propagation, one clone may outgrow co-cultured cells leading to single clones with multiple representation in final amplified clone lines. In figure 5.13, clone 3-2F produces a much larger restriction fragment as detected by Southern blot analysis than clone 3-12F. This indicates that although the clones were picked in close succession and possibly from the same plate, creating the potential for cross contamination, these clones sharing exceptional LacZ expression characteristics represent unique and distinct clones.

After Southern analysis, clones that proved to have suitable LacZ expression and contained single copy integrations were expanded for further analysis and to create low passage number freezes suitable for chimera production. After the expansion, samples of each clone were re-stained for LacZ to determine the stability of transgene expression over time. Of the top 12 clones after initial LacZ staining, single copy analysis, and expansion, 6 clones were found to have changed their LacZ staining properties. Clones were transfected with Cre plasmid using lipofectamine to determine if they could recombine and express the human alkaline phosphatase portion of the construct. Figure 5.14 demonstrates the result of a partial Cre transfection, and demonstrates the binary nature of recombinational activation. Approximately 80% of clones analyzed showed evidence of successful recombination.

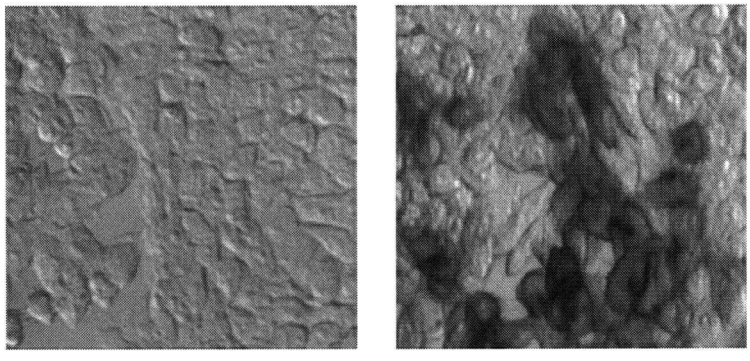

Figure 5.14: Alkaline phosphatase staining of ES cells containing single copy integrations of pCCALL-IDUA.

On the left, ES cells unable to express Alk phos after being transduced with activating CRE plasmid. On the right, a clone with individual alk phos positive ES cells can be seen. The absolute nature of reporter gene expression, either on or completely off, is exemplified by the individual strongly expressing cells surrounded by cells that have not undergone Cre mediated recombination.

More than 50 ES clones, initially identified for having superior LacZ staining, were analyzed for single copy integrations, alkaline phosphatase expression after recombination, and persistence of transgene expression with LacZ after amplification. A final ranking of the top 9 clones was generated, shown in table 5.1. Not all clones with excellent LacZ staining characteristics were suitable for transgenic mouse generation, for example clone 2-6H, with the best overall staining, was not capable of recombination in the presence of Cre, and would therefore never be able to express human IDUA in adult mice. Shaded lanes mark the 2 ES clones, 3-2F and 3-12F, that became mouse lines.

Clone ID	Percent Confluence	Percent LacZ positive	Consistency LacZ intensity	Southern single copy	Alk phos expression	Percent Persistent LacZ staining, ranking	Clone ID	**Overall rating**
1-2D	100	95	variable	yes	**negative**	90, 5	1-2D	
1-2H	100	92	good	yes	positive	90, 6	1-2H	**4**
1-3D	75	90	variable	yes	positive		1-3D	
1-4H	75	85	variable	yes	positive		1-4H	
2-6A	50	90	excellent	**unsure**	positive	80, 8	2-6A	**6**
2-6B	10	90	excellent	yes	positive	95, 2	2-6B	**1**
2-6H	10	100	excellent	yes	**negative**	100,1	2-6H	
2-8D	100	90	variable	yes	positive		2-8D	
2-12A	20	95	good	yes	positive	90, 4	2-12A	**3**
3-1H	50	90	good	**no**	positive		3-1H	
3-2F	20	98	excellent	yes	positive	95, 3	3-2F	**2**
3-8D	10	98	good	**no**	**no cells**		3-8D	
3-12F	80	90	excellent	yes	positive	80, 7	3-12F	**5**
3-12G	20	80	good	**no**	positive		3-12G	
3-12H	60	80	excellent	**no**	positive		3-12H	
4-1C	100	90	good	yes	**negative**		4-1C	
4-3D	50	80	good	**no**	positive		4-3D	
4-3E	80	90	excellent	yes	positive	80, 9	4-3E	**7**
4-4B	70	90	excellent	yes	positive	75, 10	4-4B	**8**
4-4H	20	90	good	yes	**negative**	70, 11	4-4H	
4-5A	80	80	good	**no**	positive		4-5A	
4-7A	50	85	excellent	yes	positive	70, 12	4-7A	**9**

Table 5.2: Summary of ES clone analysis

The 20 most suitable lines as determined by LacZ staining were ranked for overall suitability. A final ranking of the top 9 clones for the generation of transgenic mice was determined, far right. Clones 3-2F, and 3-12F, successfully used to generate transgenic mouse lines, are shaded.

The pCAL-IDUA mouse lines.

Two distinct ES clones have been used to generate mouse lines: line 3-12F was generated by blastocyst injection of ES cells, and 3-2F generated by the aggregation technique. Both lines were produced using the R1 ES line derived from a (129/Svcp x 129/SvJ) F1 embryo.

For the 3-2F line, CD1 blastocysts were used for the generation of chimeras. The experiments using with the 3-2F pCal-IDUA line were performed by Dr. Corrinne Lobe and staff. The CD1 mouse strain is useful as they have red eyes and high level chimeras can be identified by their black eyes, encoded by the 129J agouti line, and eye color is evident right from birth in contrast with coat color selection used in the traditional 129J agouti-C57BL/6 black system. Suitable ES lines with desired expression characteristics were thawed and aggregated with eight-cell stage CD1 mouse embryos (2.5 days post coitus), then transferred to pseudo-pregnant recipients to produce chimeric mice (Nagy, 1997). Male chimeras were mated with CD1 females to identify germ-line transmitters. Pups were genotyped by staining ear clips for lacZ expression (Lobe *et al.*, 1999). The offspring generated from this mating are exprected to be 50% CD1/50% 129Svcp/J (R1 ES cells). An inbred line was also generated, which involved breeding the 3-2F chimeras with 129 SVEV line. Finally, the 3-2F line was mated with mice expressing pCX-NLS-Cre (Mar and Nagy, unpublished), a ubiquitously expressing Cre mouse line with zygote expression of Cre. This system includes a Cre recombinase equipped with a nuclear localization signal expressed by the exceptionally strong CMV enhancer/chicken beta-actin promoter combination pCAGG (Niwa *et al.*, 1991).

These mice generated from the 3-2F ES line await further characterization, however, no obvious phenotype was observed in litters expected to contain double transgenic pups that should express human IDUA.

Line 3-12F was produced using ES cells and 3.5 day postcoitis blastocysts from C57BL/6 mice at the Centre for Molecular Medicine and Therapeutics under the supervision of Diana Carlson. Chimeras positive for LacZ staining were then bred with C57BL/6 mice producing a F1 that included pups positive for LacZ staining which are a combination of 129J agouti and C57BL/6. The Cre line used for ubiquitous activation of the 3-12F pCal IDUA line is Jackson stock # TgN (hCMV-Cre) 140 Sau homozygotes. This strain contains a Cre recombinase gene under the control of a human cytomegalovirus minimal promoter. This promoter directs widespread transcription such that Cre recombinase is expressed in all tissues. This includes the germline tissues and gametes, allowing for recombination in fertilized zygotes such that every cell of the developing mouse contains a recombined, activated cell expressing IDUA.

Figure 5.15 shows the generation of mouse lines from the pCal-IDUA 3-12F ES clone. After ES injection into blastocyts, and implantation into surrogate mothers, 7 pups were born, 4 of which had an agouti coat and therefore were constituted by the 129 J ES cells. 3 of the 4 were male, consistent with the male gender of the 129 J ES line, while one of the chimeras was female and therefore unlikely to be capable of germline transmission of the transgene. All 4 agouti pups were positive for LacZ expression, indicating the pCal-IDUA construct was successfully expressed. Two independent chimeras successfully transmitted the transgene to offspring when bred into the bl/6 strain. Transgene bearing offspring from the bl/6 and chimera, identified by LacZ

staining, were then bred into the CMV-Cre mouse line. As the CMV-Cre mice are homozygous for the CMV-Cre transgene, half the offspring were expected to be double transgenic, that is containing both the pCal-IDUA transgene as well as the CMV-Cre transgene. These double transgenic mice were expected to express human IDUA, the human alkaline phosphate reporter, and to no longer express the LacZ reporter gene.

Initial analysis of ear notch samples indicates the recombination is not complete in any of the double transgenic pups, with samples staining for both LacZ and alk phos. These double transgenic mice have no obvious phenotype and await further characterization.

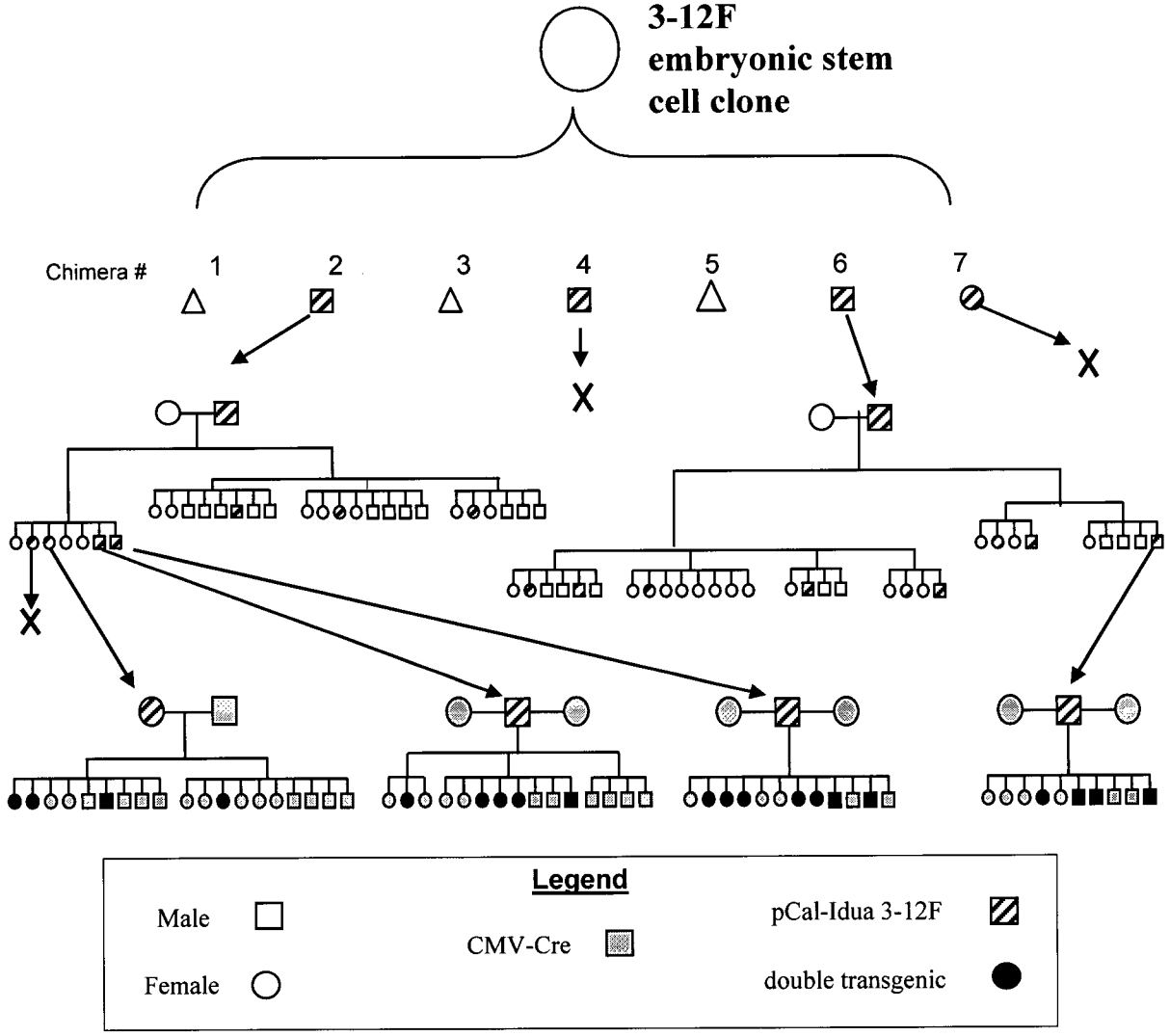

Figure 5.15: Overall Pedigree

Mouse lines generated from the pCal-IDUA 3-12F embryonic stem cell clone. Chimeras were bred with bl/6 mice to produce a stable mouse strain. Offspring of the bl/6 and chimera mating were then bred with CMV-Cre mice to produce double transgenic offspring that should express human IDUA and alkaline phosphatase in a widespread fashion from an early stage of development. These double transgenic offspring are viable, and express human IDUA and the alkaline phosphatase reporter gene.

5.3 Discussion

This chapter describes the successful generation of the pCal-IDUA lines, transgenic mouse lines with the potential to express human IDUA. I employed a conditional transgenic system involving Cre-mediated activation, and an approach involving embryonic stem cells, to generate mice in which the expression of human IDUA could be regulated both spatially and temporally.

The Cre-Lox recombination system has now been used successfully for many different manipulations of the mouse genome (Nagy, 2000). The absolute nature of transgene expression afforded by the Cre-Lox system was especially useful for this work, where it is important to be able to completely regulate IDUA expression, especially in the un-recombined, "IDUA off" state. In addition, the availability of well characterized mouse strains expressing tissue specific-Cre will allow many specific questions about therapeutic intervention for MPS I to be addressed with the pCal-IDUA strains.

The embryonic stem cell approach to the generation of transgenic mice proved useful for this work and produced lines with the potential for adult transgene expression. The small number of ES clones deemed suitable for the generation of transgenic lines after multiple screens, less than 5 % of ES clones, highlights the advantage of this approach, which allows for the identification of rare integrates permissive to long term, ubiquitous expression. In practice, only 6 of 400 ES clones were deemed to be highly desirable for mouse line production after 5 criteria were met, as shown in figure 5.16. Approximately 10 % of picked ES clones showed initial desirable LacZ staining qualities. Of 48 clones assessed for single copy integrations, only 50 % showed a clearly desired result. Repeated LacZ staining after 3 further passages (approximately 7 to 10

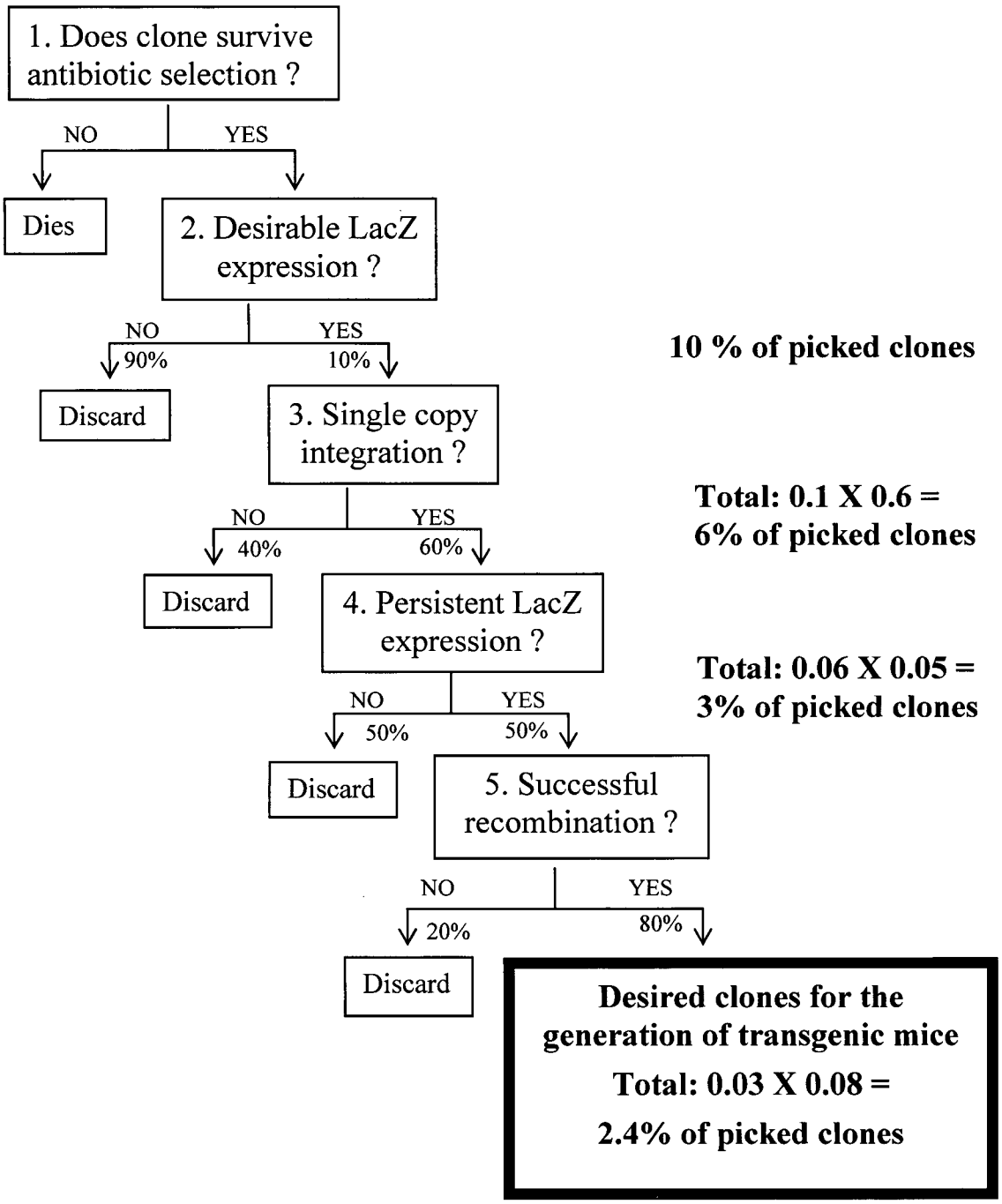

Figure 5.16: Schematic of the selection and screen for desired ES clones

The percentage of cells discarded and saved is shown for each screening level. On the right, the remaining percentage of ES clones deemed suitable at that level of screening. After numerous screens less than 5 % of randomly picked ES clones surviving antibiotic selection are deemed suitable for the generation of transgenic mice.

days of continuous culture) showed 50 % of clones under consideration had profoundly changed LacZ staining characteristics. The majority of clones tested, 80%, showed recombination potential as determined by alkaline phosphatase staining. Overall, less than 5% of clones surviving antibiotic selection were deemed suitable for injection into blastocysts towards the generation of transgenic mouse lines. As pronuclear injection tends to produce greater numbers of multiple integrations, it is clear that generating mice with ubiquitous expression potential by pronuclear injection might require the production and screening of hundreds of mice.

Clearly the elements included in this transgenic construct are not sufficient to insulate the construct from regional influences. In fact, clones with truly superior transgene expression may not only benefit from integration into a permissive site but, in fact, a site subject to regional enhancers. Thus the analysis of transgene expression at both the ES and adult tissue level could be useful in the identification of regions in the genome suitable for long term high level transgene expression. These regions could be useful in the generation of transgenic organisms, or in gene therapy approaches.

Initial results from studies with the pCal-IDUA lines indicate that, when at least one of the pCal-IDUA transgenic lines is bred into a ubiquitous activator Cre line, some of the double transgenic offspring undergo recombination resulting in expression of both human IDUA and the reporter alkaline phosphatase. These pCal-IDUA lines can be used to express human IDUA specifically in a wide variety of tissues, by mating with mice expressing Cre in a tissue specific manner. Thus both the objectives of chapter 4, namely the generation of transgenic lines with marrow cell derived IDUA expression, and ubiquitous IDUA expression, can be realized.

Transgenic lines expressing human IDUA in marrow derived cells, when crossed into the IDUA deficient mouse line, will be useful in determining the maximum possible therapeutic benefit of expression from this cell lineage, and this compound transgenic-knockout will represent a genetic model of *in utero* bone marrow transplantation.

The generation of a mouse line that expresses high levels of human IDUA in all tissues was undertaken for two reasons. Most importantly, I wished to develop a strain of mice expressing active human IDUA, as well as a reporter gene, for use as a donor strain in transplantation experiments with MPS I mice. The second objective of this project was to determine the outcome of high level, widespread IDUA expression on development. IDUA is normally expressed at very low levels and the consequences of abnormally high levels of IDUA activity are unknown. The initial results described here indicate that at least mosaic expression of human IDUA is tolerated during development and is not associated with any obvious phenotype.

Chapter 6: Summary and conclusions

6.1 Characterization of the long term pathophysiology of murine MPS I

Currently, there are no effective therapeutics that alter all of the features of lysosomal storage disorders. As such, severe MPS I is not presently curable, although bone marrow transplantation and enzyme replacement therapy offer partial amelioration of some disease symptoms. The means by which iduronidase deficiency, and the resulting accumulation of heparan and dermatan sulfate, leads to the detectable clinical abnormalities in MPS I are not fully understood. It remains to be determined which features of MPS I are irreversible and which features can be improved, with therapy. In addition, the identification of the specific cellular targets and critical time points for successful therapeutic intervention are unknown. The generation of a mouse model of MPS I has allowed for specific questions about the progression of symptom development to be addressed in a manner not possible in human MPS I patients.

Important findings described in this thesis include the presence of early pathology in reticuloendothelial cells, growth plates of bones, the presence of secondary accumulations of substrates not directly linked to IDUA deficiency in brain, and the presence of neurologic disease including dysmorphology of Purkinje cells in the cerebellum. Long term characterization of murine MPS I suggests this animal model represents severe human MPS I, or Hurler syndrome, as there is obvious involvement of the neurologic and skeletal systems, despite the fact that the murine model lives into adulthood.

The observations in this rodent model are important as they confirm the utility of the IDUA deficient mouse, and provide a better understanding of the pathology occurring over time in tissues not yet responsive to therapy. Finally, characterization of these

features of murine IDUA deficiency has identified numerous markers of MPS I progression that will be useful in the assessment of therapies for IDUA deficiency.

6.2 Future work:

The MPS I mouse provides a convenient model for the detailed examination of IDUA deficiency and represents a useful model for generalized lysosomal storage disorders. Future studies on this mouse model will likely focus on further understanding the neurologic and skeletal features of MPS I. Perhaps more important, even without delineating the underlying causes of these MPS I features, this animal model should prove useful in the assessment of therapeutics for MPS diseases.

6.3: Generation of transgenic murine strains expressing human IDUA.

The objective of this project was to generate transgenic mouse lines expressing human IDUA. After numerous attempts to produce transgenic mice expressing human IDUA using both pronuclear injection as well as embryonic stem cell approaches, with traditional, non-regulated promoters, no transgenic mice were generated. This led to the use of a conditional system, in which the expression of human IDUA is regulated by the introduction of Cre recombinase. Using Cre mediated recombination, and a dual reporter system, two transgenic mouse lines have been developed which have the potential to express human IDUA in a cell specific manner. By utilizing the ever expanding library of mice expressing Cre recombinase in specific tissues, the effects of specific reconstitution of IDUA, in a background of IDUA deficiency, can be determined. These mice strains will help identify where, and when, therapeutic IDUA is most effective in preventing or correcting specific features of IDUA deficiency. In addition, the compatibility of

expression of human IDUA with normal cell metabolism, and animal development, can be determined.

There are many stages in the cellular maturation of a lysosomal enzyme that might be overwhelmed during high level transgenic expression. Correct post translational modification, endosomal compartment transport, and generalized lysosomal function could be altered when one lysosomal enzyme is inappropriately expressed. Many transgenic cell lines or mouse strains have been generated that express predominantly human lysosomal enzymes. Kyle *et al.* generated a mouse line expressing the human GUS enzyme, deficient in MPS VII. The GUS enzyme is targeted to the lysosome via the mannose-6-phosphate (M6P) receptor, as is IDUA. They demonstrated complete correction of the murine MPS VII phenotype when the transgenic line expressing human GUS was crossed into the GUS -/- MPS VII mouse line (Kyle *et al.*, 1990). Mice hemizygous for the human genomic transgene expressed 10 fold higher levels of GUS activity in most tissues and did not produce any detectable negative phenotype. This confirmed that human GUS is enzymatically functional and is properly targeted in murine cells, can correct murine MPS VII, and is well tolerated even at high levels of expression.

Expression of alpha-galactosidase A at high levels in Chinese hamster ovary (CHO) cells results in its intracellular aggregation, crystallization in lysosomes, and selective secretion (Ioannou *et al.*, 1992). It may be that certain enzymes have a tendency for aggregation and that overexpression of these enzymes creates an environment for aggregate formation. A transgenic mouse line overexpressing human alpha-galactosidase between 20 and 10,000 fold had no obvious phenotype resulting from overexpression (Kase *et al.*, 1998) and no detected aggregate formation.

Human IDUA has been overexpressed in cell culture using Chinese hamster ovary (CHO) to levels 3000 to 7000 fold above normal (Kakkis *et al.*, 1993). Surprisingly, the activity and distribution of 5 other lysosomal enzymes were not significantly affected even at this high level of overexpression. No aggregations were noted.

This ability for overexpression of an enzyme bearing the M6P phosphate residue for lysosomal targeting without disturbing general lysosomal targeting may be limited to certain cell types. Retroviral transduction of human MPS I fibroblasts with 3 constructs expressing varying levels of human IDUA produced surprising results that are relevant to this current thesis; including the induction of a novel disease state (Anson *et al.*, 1992). The 3 constructs differed in the regulatory elements driving expression of human Idua cDNA, with the first, pLIdSN, using the 5' viral long repeat (LTR), the second, pLNCId, uses the cytomegalovirus (CMV) immediate early promoter, while in the third, pLNTid, the CMV promoter is replaced with a fragment of the mouse CD45 gene. The three constructs, LNCId, LIdSN, and LNTId, were found to express 250X, 150X, and 10X normal levels of IDUA activity in MPS I human fibroblasts. While all three constructs corrected the enzymatic defect in MPS I fibroblasts, only the construct with the lowest level of expression (10X, LNTId) was successful in fully correcting the GAG storage of the MPS I fibroblasts. Increasing overexpression of IDUA resulted in reduced therapeutic benefit as assessed by intracellular accumulation of ^{35}sulphate labeled GAG. In addition, the levels of other lysosomal enzymes were determined to be lowered in lysosomes, but increased in the cell media, indicating the lysosomal enzymes were secreted rather than delivered to the lysosome (Anson *et al.*, 1992). The pattern of decreased lysosomal enzymes in the lysosome but increased extracellular concentrations of lysosomal

enzymes is found in I cell disease, which results in increased secretion of mannose-6-phosphate-dependent lysosomal enzymes as the enzyme mediating addition of terminal mannose phosphate residues is deficient. With overexpression of the mannose-6-phosphate bearing IDUA in this study, the MPR receptor mediated delivery of lysosomal enzymes is thought to be disrupted, leading to misrouting of lysosomal enzymes to the secretion pathway and ultimately the extracellular space.

The consequences of this misrouting of lysosomal enzymes, should it occur *in vivo*, are unknown. The catalytic activity of lysosomal enzymes at the near neutral pH of the extracellular space has not been investigated but with sufficient enzyme even low levels of activity might result in inappropriate degradation of enzyme substrates. These results indicate the level of IDUA expression occurring in gene therapy may need to be limited for optimal correction of lysosomal storage of GAGs, and suggest that excessive levels of IDUA expression, as could occur for some cell types after gene therapy, may not be therapeutic.

Macrophage specific transgenic overexpression of human protective protein/cathepsin A (PPCA) was partially corrective for a murine model of galactosialidosis (PPCA-/-), a visceral and neurodegenerative disease resulting from deficiency of PPCA. Correction of visceral storage and partial correction or delay of onset of neuronal storage was achieved with either bone marrow transplantation of transgenic marrow overexpressing PPCA from a macrophage specific promoter element into the PPCA-/- mouse, or with breeding of the same macrophage specific PPCA transgenic line into PPCA-/- mice (Hahn *et al.*, 1998). Some neuronal cells, including Purkinje cells, continued to show storage and died with both therapy approaches. This

indicates that, at least with the levels of transgene expression achieved in this study, marrow derived cells including macrophages may not be able to fully correct neuronal lysosomal storage and pathology.

Some cell types may be better targets for the therapeutic overexpression of a lysosomal enzyme than others. Pompe disease includes severe metabolic myopathy and cardiomyopathy and therefore muscle would seem a logical choice for expression of the therapeutic lysosomal enzyme alpha-glucosidase (GAA) deficient in this disorder. Using knockout mice with this disease, and transgenic lines containing the cDNA for the human enzyme under muscle or liver specific promoters controlled by tetracycline, Raben *et al.* demonstrated that the liver provided enzyme far more efficiently than muscle tissue. The achievement of therapeutic levels with skeletal muscle expression required the entire muscle mass to produce high levels of enzyme of which little found its way to the plasma, whereas liver, comprising less than 5% of body weight, secreted 100 fold more enzyme, all of which was in the active 110 kDa precursor form (Raben *et al.*, 2001). In a transgenic line with very high expression of GAA in skeletal muscle it was shown excessive levels of GAA are not well tolerated, with virtually every cell containing small lysosomes with PAS-positive storage material.

It is clear that the transport systems for delivery of exogenous lysosomal enzymes, using the mannose-6-phosphate receptors, allows rescue of animal models of lysosomal storage disease with gene products of human versions of the lysosomal enzymes. Overexpression of lysosomal enzymes has been associated with numerous phenomenon including aggregation of transgenic proteins, secretion of transgenic as well

as native lysosomal enzymes, and deficiency of intralysosomal-lysosomal enzymes leading to lysosomal disease in cell culture.

Surprisingly, transgenic mouse lines overexpressing lysosomal enzymes have for the most part not exhibited obvious clinical or pathological phenotypes, with the exception of lysosomal storage disease in mice overexpressing GAA enzyme in muscle. The phenotype of the overexpression of IDUA on normal cell metabolism is relevant to gene therapy approaches for MPS I. Only by overexpressing IDUA in all tissues, during development, can the safety of such approaches be determined. In addition, cell specific reconstitution of IDUA activity in a background of IDUA deficiency may identify cell types required for efficient correction of MPS I complications.

It has been determined that expression of human IDUA in normal mice, at the levels obtained with these transgenic strains, does not induce obvious disease. The dual reporter expression system which indicates the state of Cre mediated recombination, and therefore human IDUA expression, has proven functional and the expression of human IDUA has been confirmed.

The generation of a conditional system for the expression of human IDUA in mice will provide a versatile tool for the study of the effects of gene therapy for MPS I. In addition to genetic crosses into the IDUA deficient strain to address the benefit of IDUA expression in specific tissues at defined time points, these transgenic mice lines can provide a source of human IDUA expressing cells for use in transplantation studies. Since these transgenic mice express a reporter gene as well as human IDUA, this system provides ease of monitoring of transgene expression and the tracking of transgenic cells in recipients. Finally, the phenotype of transgenic human IDUA expression, if any, can

be determined. It is hoped that these mouse strains will be useful in determining levels, locations, and time points important to the efficacy and safety of gene therapy for MPS I.

6.4 Future work

Much remains to be learned from the conditional transgenic lines produced during this thesis work. Most importantly; crosses into the IDUA deficient murine line and lines expressing Cre recombinase need to be comprehensively analyzed. In particular, detailed evaluation of human specific IDUA activity after Cre recombination, in various mouse tissues by immunocapture is critical. The complexity of this analysis and the considerable time required for breeding into various Cre expressing lines as well as the murine IDUA deficient line precluded inclusion into this thesis project. It is hoped these transgenic murine lines will lead to a better understanding of the tissue specific elements and expression patterns that are required to effectively cure MPS I.

References

Abreu S, Hayden J, Berthold P, Shapiro IM, Decker S, Patterson D, Haskins M (1995) Growth plate pathology in feline mucopolysaccharidosis VI. Calcif Tissue Int 57: 185-190.

Anson DS, Bielicki J, and Hopwood JJ (1992) Correction of Mucopolysaccharidosis Type I fibroblasts by retroviral-mediated transfer of the human alpha-L-iduronidase gene. Hum Gene Therapy 3: 371-379.

Aronovich EL, Pan D, Whitley CB (1996) Molecular genetic defect underlying alpha-L-iduronidase pseudodeficiency. Am J Hum Genet 58: 75-85.

Back A, East K, Hickstein D (1995) Leukocyte integrin CD11b promoter directs expression in lymphocytes and granulocytes in transgenic mice. Blood 85: 1017-24.

Barton NW, Brady RO, Dambrosia JM, Di Bisceglie AM, Doppelt SH, Hill SC, Mankin HJ, Murray GJ, Parker RI, Argoff CE (1991) Replacement therapy for inherited enzyme deficiency--macrophage-targeted glucocerebrosidase for Gaucher's disease. N Engl J Med 324: 1464-70.

Barton RW, Neufeld EF (1971) The Hurler corrective factor. Purification and some properties. J Biol Chem 246: 7773-9.

Bastedo L, Sands MS, Lambert DT, Pisa MA, Birkenmeier E, Chang PL (1994) Behavioral consequences of bone marrow transplantation in the treatment of murine mucopolysaccharidosis type VII. J Clin Invest 94: 1180-6.

Bernfield M, Gotte M, Park PW, Reizes O, Fitzgerald ML, Lincecum J, Zako M (1999) Functions of cell surface heparan sulfate proteoglycans. Annu Rev Biochem 68: 729-77.

Birkenmeier EH, Barker JE, Vogler CA, Kyle JW, Sly WS, Gwynn B, Levy B, Pegors C (1991) Increased life span and correction of metabolic defects in murine mucopolysaccharidosis type VII after syngeneic bone marrow transplantation. Blood 78: 3081-92.

Birkenmeier EH, Davisson MT, Beamer WG, Ganschow RE, Vogler CA, Gwynn B, Lyford KA, Maltais LM, Wawrzyniak CJ (1989) Murine mucopolysaccharidosis type VII: characterization of a mouse with ß-glucuronidase deficiency. J Clin Invest 83: 1258-1266.

Bissig M, Hagenbuch B, Stieger B, Koller T, Meier PJ (1994) Functional expression cloning of the canalicular sulfate transport system of rat hepatocytes. J Biol Chem 269: 3017-21.

Bosch A, Perret E, Desmaris N, Trono D, Heard JM (2000) Reversal of pathology in the entire brain of mucopolysaccharidosis type VII mice after lentivirus-mediated gene transfer. Hum Gene Ther 11: 1139-50.

Breider MA, Shull RM, Constantopoulos G (1989) Long-term effects of bone marrow transplantation in dogs with mucopolysaccharidosis I. Am J Pathol 134: 677-92.

Breunig F, Wanner C (2003) Enzyme replacement therapy for Fabry disease: proving the clinical benefit. Nephrol Dial Transplant 18: 7-9.

Brooks DA (2002) Enzyme replacement for MPS I. Hum Gene Ther 3: 371-9.

Byers PH (1995) Disorders of collagen biosynthesis and structure. In: Scriver CR, Beaudet AL, Sly WS, Valle D, eds. The metabolic and molecular bases of inherited disease, 7th edn. New York: McGraw Hill 2427-2839.

Casal ML, Wolfe JH (1998) Variant clinical course of mucopolysaccharidosis type VII in two groups of mice carrying the same mutation. Lab Invest 78: 1575-81.

Casal ML, Wolfe JH (2000) Mucopolysaccharidosis type VII in the developing mouse fetus. Pediatr Res 47: 750-6.

Casal ML, Wolfe JH (2001) *In utero* transplantation of fetal liver cells in the mucopolysaccharidosis type VII mouse results in low-level chimerism, but overexpression of beta-glucuronidase can delay onset of clinical signs. Blood 97: 1625-34.

Chen H, Berard J, Luo H, Landers M, Vinet B, Bradley WE, Wu J (1997) Compromised allograft rejection response in transgenic mice expressing antisense sequences to retinoic acid receptor beta2. J Immunol 159: 623-34.

Clarke LA, Nelson PV, Warrington C, Morris CP, Hopwood JJ, Scott HS (1994) Mutation analysis of 19 North American mucopolysaccharidosis type I patients: identification of two additional frequent mutations. Hum Mutat 3: 275-282.

Clarke LA, Nasir J, Zhang H, McDonald H, Applegarth DA, Hayden MR, Toone J (1994) Murine alpha-L-iduronidase: cDNA isolation and expression. Genomics 24:311-6.

Clarke LA, Russell CS, Pownall S, Warrington CL, Borowski A, Dimmick JE, Toone J, Jirik F (1997) Murine mucopolysaccharidosis type 1: targeted disruption of the murine α-L-iduronidase gene. Hum Mol Gen 64: 503-511.

Clarke LA, Scott HS (1993) Two novel mutations causing mucopolysaccharidosis type I detected by single strand conformational analysis of the α-L-iduronidase gene. Hum Mol Genet 2: 1311-1312.

Clausen BE, Burkhardt C, Reith W, Renkawitz R, Forster I (1999) Conditional gene targeting in macrophages and granulocytes using LysMcre mice. Transgenic Res 8: 265-77.

Cleary MA, Wraith JE (1995) The presenting features of mucopolysaccharidosis type IH (Hurler syndrome). Acta Paediatr 84: 337-339.

Colville GA, Bax MA (1996) Early presentation in the mucopolysaccharide disorders. Child Care Health Dev 22: 31-6.

Constantopoulos G, Dekaban AS (1978) Neurochemistry of the mucopolysaccharidoses: Brain lipids and lysosomal enzymes in patients with four types of mucopolysaccharidosis and in normal controls. J Neurochem 30: 965-973.

Constantopoulos G, Shull RM, Hastings N, Neufeld EF (1985) Neurochemical characterization of canine α-L-iduronidase deficiency disease (model of human mucopolysaccharidosis I). J Neurochem 45: 1213-1217.

Crawley AC, Brooks DA, Muller VJ, Petersen BA, Isaac EL, Bielicki J, King BM, Boulter CD, Moore AJ, Fazzalari NL, Anson DS, Byers S, Hopwood JJ (1996) Enzyme replacement therapy in a feline model of Maroteaux-Lamy syndrome. J Clin Invest 97: 1864-1873.

Crow J, Gibbs DA, Cozens W, Spellacy E, Watts R (1983) Biochemical and histopathological studies on patients with mucopolysaccharidoses, two of whom had been treated with fibroblast transplantation. J Clin Pathol 36:415-430.

Daly TM, Lorenz RG, Sands MS. (2000) Abnormal immune function *in vivo* in a murine model of lysosomal storage disease. Pediatr Res 47: 757-62.

Daly TM, Ohlemiller KK, Roberts MS, Vogler CA, Sands MS (2001) Prevention of systemic clinical disease in MPS VII mice following AAV-mediated neonatal gene transfer. Gene Ther 8: 1291-8.

Daly TM, Vogler C, Levy B, Haskins ME, Sands MS (1999) Neonatal gene transfer leads to widespread correction of pathology in a murine model of lysosomal storage disease. Proc Natl Acad Sci USA 96: 2296-300.

Deguchi Y, Okutsu H, Okura T, Yamada S, Kimura R, Yuge T, Furukawa A, Morimoto K, Tachikawa M, Ohtsuki S, Hosoya K, Terasaki T (2002) Internalization of basic fibroblast growth factor at the mouse blood-brain barrier involves perlecan, a heparan sulfate proteoglycan. J Neurochem 83: 381-9.

Dekaban AS, Constantopoulos G (1977) Mucopolysaccharidosis types I, II, IIIA and V: pathological and biochemical abnormalities in the neural and mesenchymal elements of the brain. Acta Neuropath 39: 1-7.

Dekaban AS, Constantopoulos G, Herman MM, Steusing JK (1976) Mucopolysaccharidosis type V (Scheie syndrome): a postmortem study by multidisciplinary techniques with emphasis on the brain. Arch Pathol Lab Med 100: 237-245.

Dziennis S, Van Etten RA, Pahl S (1995) The CD11b promoter directs high-level expression of reporter genes in macrophages in transgenic mice. Blood 85: 319-29.

Erickson RP (1999) Antisense transgenics in animals. Methods 18:304-310.

Everett LA, Glaser B, Beck JC, Idol JR, Buchs A, Heyman M, Adawi F, Hazani E, Nassir E, Baxevanis AD, Sheffield VC, Green ED (1997) Pendred syndrome is caused by mutations in a putative sulphate transporter gene (PDS). Nat Genet 17: 411-22.

Evers M, Saftig P, Schmidt P, Hafner A, McLoghlin DB, Schmahl W, Hess B, von Figura K, Peters C (1996) Targeted disruption of the arylsulfatase B gene results in mice resembling the phenotype of mucopolysaccharidosis VI. Proc Natl Acad Sci 93: 8214-8219.

Fairbairn LJ, Lashford LS, Spooncer E, McDermott RH, Lebens G, Arrand JE, Arrand JR, Bellantuono I, Holt R, Hatton CE, Cooper A, Besley GT, Wraith JE, Anson DS, Hopwood JJ, Dexter TM (1996) Long-term *in vitro* correction of alpha-L-iduronidase deficiency (Hurler syndrome) in human bone marrow. Proc Natl Acad Sci USA 93: 2025-30.

Ferrer I, Cusi V, Pineda M, Galofre E, Vila J (1988) Focal dendritic swellings in Purkinje cells in mucopolysaccharidoses types I, II and III: a Golgi and ultrastructural study. Neuropath & App Neurobiol 14: 315-323.

Field RE, Buchanan JAF, Copplemans MGJ, Aichroth PM (1994) Bone-marrow transplantation in Hurler's syndrome. J Bone & Joint Surg 76: 975-981.

Flake AW and Zanjani ED (1999) *In utero* hematopoietic stem cell transplantation: ontogenic opportunities and biologic barriers. Blood 94: 2179-91.

Folch J, Lees M, Stanley, GH (1957) A simple method for the isolation and purification of total lipids from animal tissues. J Biol Chem 226: 497-509.

Fratantoni J, Hall CW, Neufeld EF (1968) Hurler and Hunter syndromes: mutual correction of the defect in cultured fibroblasts. Science 162: 570-572.

Fratantoni JC, Hall CW, Neufeld EF (1968) The defect in Hurler's and Hunter's syndromes: faulty degradation of mucopolysaccharide. Proc Nat Acad Sci 60: 699-706.

Gonzalez-Gomez I, Mononen I, Heisterkamp N, Groffen J, Kaartinen V (1998) Progressive neurodegeneration in aspartylglycosaminuria mice. Am J Pathol 153: 1293-300.

Gorlich D, Rapoport TA (1993) Protein translocation into proteoliposomes reconstituted from purified components of the endoplasmic reticulum membrane. Cell 75: 615-30.

Gorman C, Bullock C (2000) Site-specific gene targeting for gene expression in eukaryotes. Curr Opin Biotechnol 11: 455-60.

Gossen M, Bujard H (1992) Tight control of gene expression in mammalian cells by tetracycline-responsive promoters. Proc Natl Acad Sci USA 89: 5547-51.

Groffen AJ, Veerkamp JH, Monnens LA, van den Heuvel LP (1999) Recent insights into the structure and functions of heparan sulfate proteoglycans in the human glomerular basement membrane. Nephrol Dial Transplant 14: 2119-29.

Grosson CL, MacDonald ME, Duyao MP, Ambrose CM, Roffler-Tarlov S, Gusella JF (1994) Synteny conservation of the Huntington's disease gene and surrounding loci on mouse Chromosome 5. Mamm Genome 5: 424-8.

Hahn CN, del Pilar Martin M, Zhou XY, Mann LW, d'Azzo A (1998) Correction of murine galactosialidosis by bone marrow-derived macrophages overexpressing human protective protein/cathepsin A under control of the colony-stimulating factor-1 receptor promoter. Proc Natl Acad Sci USA 95: 14880-5.

Hamilton DL, Abremski K (1984) Site-specific recombination by the bacteriophage P1 lox-Cre system. Cre-mediated synapsis of two lox sites. J Mol Biol 178: 481-6.

Hardouin N, Nagy A (2000) Gene-trap-based target site for cre-mediated transgenic insertion. Genesis 26: 245-52.

Haskins ME, Aguirre GD, Jezyk PF, Desnick RJ, Patterson DF (1983) The pathology of the feline model of mucopolysaccharidosis I. Am J Pathol 112: 27-36.

Haskins ME, Jezyk PF, Desnick RJ, McDonough SK, Patterson DF (1979) Alpha-L-iduronidase deficiency in a cat: a model of mucopolysaccharidosis I. Pediat Res 13: 1294-1297.

Hastbacka J, Superti-Furga A, Wilcox WR, Rimoin DL, Cohn DH, Lander ES (1996) Atelosteogenesis type II is caused by mutations in the diastrophic dysplasia sulfate-transporter gene (DTDST): evidence for a phenotypic series involving three chondrodysplasias. Am J Hum Genet 58: 255-62.

He X, Li CM, Simonaro CM, Wan Q, Haskins ME, Desnick RJ, and Schuchman EH (1999) Identification and characterization of the molecular lesion causing mucopolysaccharidosis type I in cats. Mol Genet Metab 67: 106-12.

Herrera PL (2000) Adult insulin- and glucagon-producing cells differentiate from two independent cell lineages. Devel 127: 2317-22.

Hickstein D, Baker D, Gollahon K, and Back A (1992) Identification of the promoter of the myelomonocytic leukocyte integrin CD11B. Proc Natl Acad Sci 89: 2105-2109.

Hogan B, Beddington R, Costantini F, and Lacy E (1994) Manipulating the mouse embryo. Cold Spring Harbor Laboratory Press, Cold Spring Harbor, NY.

Hopwood JJ and Muller V (1982) Diagnostic enzymology with special reference to a sulfated disaccharide derived from heparin. Clin Sci 62: 193-201.

Hopwood JJ, Muller V, Smithson A, Baggett N (1979) A fluorometric assay using 4-methylumbelliferyl alpha-L-iduronide for the estimation of alpha-L-iduronidase activity and the detection of Hurler and Scheie syndromes. Clin Chim Acta 92: 257-65.

Hopwood JJ, Vellodi A, Scott HS, Morris CP, Litjens T, Clements PR, Brooks DA, Cooper A, Wraith JE (1993) Long-term clinical progress in bone marrow transplanted mucopolysaccharidosis type I patients with a defined genotype. J Inher Metab Dis 16: 1024-1033.

Huang J-Q, Trasler JM, Igdoura S, Michaud J, Hanai N, Gravel RA (1997) Apoptotic cell death in mouse models of GM2 gangliosidosis and observations on human Tay-Sachs and Sandhoff diseases. Hum Mol Gen 6: 1879-1885.

Human Gene Mutation Database, http://uwcmml1s.uwcm.ac.uk/uwcm/mg/search/119327.html

Ioannou YA, BishopDF, Desnick RJ (1992) Overexpression of human alpha-galactosidase A results in its intracellular aggregation, crystallization in lysosomes, and selective secretion. J Cell Biol 119: 1137-50.

Jezyk PF, Haskins ME, Patterson DF, Mellman WJ, Greenstein M (1977) Mucopolysaccharidosis in a cat with arylsulfatase B deficiency: a model of Maroteaux-Lamy syndrome. Science 198: 834-6.

Kaartinen V, Nagy A (2001) Removal of the floxed neo gene from a conditional knockout allele by the adenoviral Cre recombinase *in vivo*. Genesis 31: 126-9.

Kakkis ED (2002) Enzyme replacement therapy for the mucopolysaccharide storage disorders. Expert Opin Investig Drugs 11: 675-85.

Kakkis ED, Matynia A, Jonas AJ, Neufeld EF (1994) Overexpression of the human lysosomal enzyme alpha-L-iduronidase in Chinese hamster ovary cells. Protein Expr Purif 5: 225-32.

Kakkis ED, McEntee MF, Schmidtchen A, Neufeld EF, Ward DA, Compf RE, Kania S, Bedolla C, Chien S-L, Shull RM (1995) Long-term and high-dose trials of enzyme replacement therapy in the canine model of mucopolysaccharidosis I. Biochem Molecular Med 58: 156-167.

Kakkis ED, McEntee MF, Schmidtchen A, Neufeld EF, Ward DA, Gompf RE, Kania S, Bedolla C, Chien SL, Shull RM (1996) Long-term and high-dose trials of enzyme replacement therapy in the canine model of mucopolysaccharidosis I. Biochem Mol Med 58: 156-67.

Kakkis ED, Muenzer J, Tiller GE, Waber L, Belmont J, Passage M, Izykowski B, Phillips J, Doroshow R, Walot I, Hoft R, Neufeld EF (2001) Enzyme-replacement therapy in mucopolysaccharidosis I. New Eng J Med 344: 182-188.

Kakkis ED, Schuchman E, He X, Wan Q, Kania S, Wiemelt S, Hasson CW, O'Malley T, Weil MA, Aguirre GA, Brown DE, Haskins ME (2001) Enzyme replacement therapy in feline mucopolysaccharidosis I. Mol Genet Metab 72: 199-208.

Karniski LP, Lotscher M, Fucentese M, Hilfiker H, Biber J, Murer H (1998) Immunolocalization of sat-1 sulfate/oxalate/bicarbonate anion exchanger in the rat kidney. Am J Physiol 275: F79-87.

Kase R, Shimmoto M, Itoh K, Utsumi K, Kotani M, Taya C, Yonekawa H, Sakuraba H (1998) Immunohistochemical characterization of transgenic mice highly expressing human lysosomal alpha-galactosidase. Biochim Biophys Acta 1406: 260-6.

Keeling KM, Bedwell DM (2002) Clinically relevant aminoglycosides can suppress disease-associated premature stop mutations in the IDUA and P53 cDNAs in a mammalian translation system. J Mol Med 80: 367-76.

Kornfeld S (1987) Trafficking of lysosomal enzymes. FASEB J 1: 462-8.

Kyle JW, Birkenmeier EH, Gwynn B, Vogler C, Hoppe PC, Hoffmann JW, Sly WS (1990) Correction of murine mucopolysaccharidosis VII by a human beta-glucuronidase transgene. Proc Natl Acad Sci USA 87: 3914-8.

Lakso M, Sauer B, Mosinger B Jr, Lee EJ, Manning RW, Yu SH, Mulder KL, Westphal H (1992) Targeted oncogene activation by site-specific recombination in transgenic mice. Proc Natl Acad Sci USA 89: 6232-6.

Lallemand Y, Luria V, Haffner-Krausz R, Lonai P (1998) Maternally expressed PGK-Cre transgene as a tool for early and uniform activation of the Cre site-specific recombinase. Transgenic Res. 7: 105-12.

Lee A, Beck L, Brown RJ, Markovich D (1999) Identification of a mammalian brain sulfate transporter. Biochem Biophys Res Commun 263: 123-9.

Lee A, Beck L, Markovich D (2003) The mouse sulfate anion transporter gene Sat1 (Slc26a1): cloning, tissue distribution, gene structure, functional characterization, and transcriptional regulation thyroid hormone. DNA Cell Biol 22: 19-31.

Lewandoski M (2001) Conditional control of gene expression in the mouse. Nat Rev Genet 2: 743-55.

Lobe CG, Koop KE, Kreppner W, Lomeli H, Gertsenstein M, Nagy A (1999) Z/AP, a double reporter for cre-mediated recombination. Dev Biol 208: 281-92.

Lowry OH, Rosebrough NS, Farr AL, Randall R. (1951) Protein measurement with the folin phenol reagent. J Biol Chem 193: 265-272.

Lowry RB, Applegarth DA, Toone JR, MacDonald E, Thunem NY (1990) An update on the frequency of mucopolysaccharide syndromes in British Columbia. Hum Genet 85: 389-90.

Ludwig T, Eggenshwiler J, Fisher P, D'Ercole AJ, Davenport ML, Efstariadis A (1996) Mouse mutants lacking the type 2 IGF receptor (IGF2R) are rescued from perinatal lethality in Igf2 and Igf1r null backgrounds. Develop Bio 177: 517-535.

Lutzko C, Kruth S, Abrams-Ogg AC, Lau K, Li L, Clark BR, Ruedy C, Nanji S, Foster R, Kohn D, Shull R, Dube ID (1999) Genetically corrected autologous stem cells engraft, but host immune responses limit their utility in canine alpha-L-iduronidase deficiency. Blood 93: 1895-905.

Lutzko C, Meertens L, Li L, Zhao Y, Abrams-Ogg A, Woods JP, Kruth S, Hough MR, Dube ID (2002) Human hematopoietic progenitors engraft in fetal canine recipients and expand with neonatal injection of fibroblasts expressing human hematopoietic cytokines. Exp Hematol 30: 801-8.

Lutzko C, Omori F, Abrams-Ogg AC, Shull R, Li L, Lau K, Ruedy C, Nanji S, Gartley C, Dobson H, Foster R, Kruth S, Dube ID (1999) Gene therapy for canine alpha-L-iduronidase deficiency: *in utero* adoptive transfer of genetically corrected hematopoietic progenitors results in engraftment but not amelioration of disease. Hum Gene Ther 10: 1521-32.

MacDonald ME, Scott HS, Whaley WL, Pohl T, Wasmuth JJ, Lehrach H, Morris CP, Frischauf AM, Hopwood JJ, Gusella JF (1991) Huntington disease-linked locus D4S111 exposed as the alpha-L-iduronidase gene. Somat Cell Mol Genet 17: 21-5.

Manshouri T, Yang Y, Lin H, Stass SA, Glassman AB, Keating MJ, Albitar M (1997) Downregulation of RAR alpha in mice by antisense transgene leads to a compensatory increase in RAR beta and RAR gamma and development of lymphoma. Blood 89: 2507-15.

Markovich D, Bissig M, Sorribas V, Hagenbuch B, Meier PJ, Murer H (1994) Expression of rat renal sulfate transport systems in Xenopus laevis oocytes. Functional characterization and molecular identification. J Biol Chem 269: 3022-6.

McKusick VA, Neufeld EF (1983) The mucopolysaccharide storage disesases. In:Stanbury JB. Wyngaarden JB, Fredrickson DS, Goldstein JL, Brown MS (eds): The Metabolic basis of Inherited disease, 5th Edition. New York: McGraw-Hill, pp 751-777.

Medberry SL, Dale E, Qin M, Ow DW (1995) Intra-chromosomal rearrangements generated by Cre-lox site-specific recombination. Nucleic Acids Res 23: 485-90.

Meertens L, Zhao Y, Rosic-Kablar S, Li L, Chan K, Dobson H, Gartley C, Lutzko C, Hopwood J, Kohn D, Kruth S, Hough MR, Dube ID (2002) *In utero* injection of alpha-L-iduronidase-carrying retrovirus in canine mucopolysaccharidosis type I: infection of multiple tissues and neonatal gene expression. Hum Gene Ther 13: 1809-20.

Moseley RH, Hoglund P, Wu GD, Silberg DG, Haila S, de la Chapelle A, Holmberg C, Kere J (1999) Downregulated in adenoma gene encodes a chloride transporter defective in congenital chloride diarrhea. Am J Physiol 276: G185-92.

Mountford P, Zevnik B, Duwel A, Nichols J, Li M, Dani C, Robertson M, Chambers I, Smith A (1994) Dicistronic targeting constructs: Reporters and modifiers of mammalian gene expression. Proc Natl Acad Sci USA 91: 4303-4307.

Nagy A (1997) Formation of mouse chimeric embryos from ES cells. In: Houdebine LM, editor. Amsterdam: Harwood Academic Publishers, p 167–172.

Nagy A (2000) Cre recombinase: the universal reagent for genome tailoring. Genesis 26: 99-109.

Nagy A, Mar L (2001) Creation and use of a Cre recombinase transgenic database. Methods Mol Biol 158: 95-106.

Nagy A, Rossant J, Nagy R, Abramow-Newerly W, Roder JC (1993) Derivation of completely cell culture-derived mice from early-passage embryonic stem cells. Proc Natl Acad Sci USA 90: 8424-8428.

Nagy A. URL: http://www.mshri.on.ca/develop/nagy/Cre.htm.

Neufeld EF (1991) Lysosomal storage diseases. Ann Rev Biochem 60: 257-280.

Neufeld EF, Muenzer J (1995) The mucopolysaccharidoses. In: Scriver CR, Beaudet AL, Sly WS, Valle D, eds. The metabolic and molecular bases of inherited disease, 7th edn. New York: McGraw Hill: 2427-2839.

Niwa H, Yamamura K, Miyazaki J (1991) Efficient selection for high-expression transfectants with a novel eukaryotic vector. Gene 108: 193-200.

Novak A, Guo C, Yang W, Nagy A, Lobe CG (2000) Z/EG, a double reporter mouse line that expresses enhanced green fluorescent protein upon Cre-mediated excision. Genesis 28: 147-55.

O'Connor LH, Erway LC, Vogler CA, Sly WS, Nicholes A, Grubb J, Holmberg SW, Levy B, Sands MS (1998) Enzyme replacement therapy for murine mucopolysaccharidosis type VII leads to improvements in behavior and auditory function. J Clin Invest 101: 1394-400.

O'Gorman S, Fox DT, Wahl GM (1991) Recombinase-mediated gene activation and site-specific integration in mammalian cells. Science 251: 1351-5.

Pearson AD (1986) Survey of preparative regimens and complications of bone marrow transplantation in patients with lysosomal storage diseases. Birth Defects Orig Artic Ser 22: 153-62.

Peters C, Balthazor M, Shapiro EG, King RJ, Kollman C, Hegland JD, Henslee-Downey H, Trigg ME, Cowan MJ, Sanders J, Bunin N, Weinstein H, Lenarsky C, Falk P, Harris R, Bowen T, Williams TE, Grayson GH, Warkentin P, Sender L, Cool, VA, Crittenden M, Packman S, Kaplan P, Lockman LA, Anderson J, Krivit W, Dunsenbery K, Wagner J (1996) Outcome of Unrelated donor bone marrow transplantation in 40 children with Hurler syndrome. Blood 87: 4894-4902.

Platt FM, Neises GR, Reinkensmeier G, Townsend MJ, Perry VH, Proia RL, Winchester B, Dwek RA, Butters TD (1997) Prevention of lysosomal storage in Tay-Sachs mice treated with N-butyldeoxynojirimycin. Science 276: 428-431.

Poenaru L (1997) First trimester prenatal diagnosis of metabolic diseases. Prenat diagn 7: 333.

Postic C, Shiota M, Niswender KD, Jetton TL, Chen Y, Moates JM, Shelton KD, Lindner J, Cherrington AD, Magnuson MA (1999) Dual roles for glucokinase in glucose homeostasis as determined by liver and pancreatic beta cell-specific gene knock-outs using Cre recombinase. J Biol Chem 274: 305-15.

Raben N, Lu N, Nagaraju K, Rivera Y, Lee A, Yan B, Byrne B, Meikle PJ, Umapathysivam K, Hopwood JJ, Plotz PH (2001) Conditional tissue-specific expression of the acid alpha-glucosidase (GAA) gene in the GAA knockout mice: implications for therapy. Hum Mol Genet 10: 2039-47.

Rauch U, Feng K, Zhou XH (2001) Neurocan: a brain chondroitin sulfate proteoglycan. Cell Mol Life Sci 58: 1842-56.

Regeer RR, Lee A, Markovich D (2003) Characterization of the human sulfate anion transporter (hsat-1) protein and gene (SAT1; SLC26A1). DNA Cell Biol 22: 107-17.

Reuser AJ, Van Den Hout H, Bijvoet AG, Kroos MA, Verbeet MP, Van Der Ploeg AT (2002) Enzyme therapy for Pompe disease: from science to industrial enterprise. Eur J Pediar 161 Suppl 1: S106-11.

Ross CJ, Bastedo L, Maier SA, Sands MS, Chang PL (2000) Treatment of a lysosomal storage disease, mucopolysaccharidosis VII, with microencapsulated recombinant cells. Hum Gene Ther 11: 2117-27.

Ross CJ, Ralph M, Chang PL (2000) Somatic gene therapy for a neurodegenerative disease using microencapsulated recombinant cells. Exp Neurol 166: 276-86.

Roubicek M, Gehler J, Spranger J (1985) The clinical spectrum of alpha-L-iduronidase deficiency. Am J Med Genet 20: 471-481.

Roughley PJ, Lee ER (1994) Cartilage proteoglycans: structure and potential functions. Microsc Res Tech 28: 385-97.

Russell C, Hendson G, Jevon G, Matlock T, Yu J, Aklujkar M, Ng KY, Clarke LA (1998) Murine MPS I: insights into the pathogenesis of Hurler syndrome. Clin Genet 53: 349-61.

Sakai K, Hiripi L, Glumoff V, Brandau O, Eerola R, Vuorio E, Bosze Z, Fassler R, Aszodi A (2001) Stage-and tissue-specific expression of a Col2a1-Cre fusion gene in transgenic mice. Matrix Biol 19: 761-7.

Sands MS, Barker JE, Vogler C, Levy B, Gwynn B, Galvin N, Sly WS, Birkenmeier E (1993) Treatment of murine mucopolysaccharidosis type VII by syngeneic bone marrow transplantation in neonates. Lab Invest 68: 676-86.

Sands MS, Vogler C, Torrey A, Levy B, Gwynn B, Grubb J, Sly WS, Birkenmeier EH (1997) Murine mucopolysaccharidosis type VII: long term therapeutic effects of enzyme replacement and enzyme replacement followed by bone marrow transplantation. J Clin Invest 99: 1596-1605.

Scheie HG, Hambrick GW, Barness LA (1962) A newly recognised forme fruste of Hurler's disease (gargoylism). Amer J Ophathal 53: 753-769.

Scott HS, Anson DA, Orsborn AM, Nelson PV, Clements P, Morris CP and Hopwood JJ (1991) Human alpha-L-idurondidase: cDNA isolation and expression. Proc Natl Acad Sci USA 88: 9695-9699.

Scott HS, Bunge S, Gal A, Clarke LA, Morris CP, Hopwood JJ (1995) Molecular genetics of mucopolysaccharidosis type I: diagnostic, clinical, and biological implications. Hum Mut 6: 288-302.

Scott HS, Gup X-H, Hopwood JJ, Morris CP (1992) Structure and sequence of the human alpha-L-iduronidase gene. Genomics 13: 1311-1313.

Scott HS, Litjens T, Nelson PV, Thompson PR, Brooks DA, Hopwood JJ, Morris CP (1993) Identification of mutations in the alpha-L-iduronidase gene (IDUA) that cause Hurler and Scheie syndromes. Amer J Hum Gen 53: 973-86.

Shapiro EG, Lockman LA, Balthazor M, Krivit W (1995) Neuropsychological outcomes of several storage diseases with and without bone marrow transplantation. J Inher Metab Dis 18: 413-429.

Shapiro EG, Lockman LA, Balthazor M, Krivit W (1995) Neuropsychological outcomes of several storage diseases with and without bone marrow transplantation. J Inherit Metab Dis 18:413-29.

Shelley S, and Arnaout A (1991) The promoter of the CD11B gene directs myeloid-specific and developmentally regulated expression. Proc Natl Acad Sci 88: 10525-10529.

Shull RM, Breider MA, Constantopoulos G (1988) Long-term neurological effects of bone marrow transplantation in a canine lysosomal storage disease. Pedia Res 24: 347-352.

Shull RM, Kakkis ED, McEntee MF, Kania SA, Jonas AJ, Neufeld EF (1994) Enzyme replacement in a canine model of Hurler syndrome. Proc Natl Acad Sci USA 91: 12937-41.

Shull RM, Lu X, McEntee MF, Bright RM, Pepper KA, Kohn DB (1996) Myoblast gene therapy in canine mucopolysaccharidosis. I: Abrogation by an immune response to alpha-L-iduronidase. Hum Gene Ther 7: 1595-603.

Shull RM, Munger RJ, Spellacy E, Hall CW, Constantopoulos G, Neufeld E (1982) Animal model of human disease. Canine α-L-iduronidase deficiency: a model of mucopolysaccharidosis I. Am J Pathol 244-248.

Shull RM, Walker MA (1988) Radiographic findings in a canine model of mucopolysaccharidosis I: changes associated with bone marrow transplantation. Invest Radiol 23: 124-130.

Snyder EY, Taylor RM, Wolfe JH (1995) Neural progenitor cell engraftment corrects lysosomal storage throughout the MPS VII mouse brain. Nature 374: 367-70.

Song HH, Filmus J (2002) The role of glypicans in mammalian development. Biochim Biophys Acta 1573: 241-6.

Soper BW, Lessard MD, Vogler CA, Levy B, Beamer WG, Sly WS, Barker JE (2001) Nonablative neonatal marrow transplantation attenuates functional and physical defects of beta-glucuronidase deficiency. Blood 97: 1498-504.

Southern EM (1975) Detection of specific sequences among DNA fragments separated by gel electrophoresis. J Mol Biol 98: 503-517.

Stevenson RE, Howell RR, McKusick VA, Suskind R, Hanson JW, Elliott DE, Neufeld EF (1976) The iduronidase-deficient mucopolysaccharidoses: clinical and roentgenographic features. Pediatrics 57: 111-122.

Stoltzfus LJ, Sosa-Pineda B, Moskowitz SM, Menon KP, Dlott B, Hooper L, Teplow DB, Shull RM, Neufeld EF (1992) Cloning and characterization of cDNA encoding canine alpha-L-iduronidase. mRNA deficiency in mucopolysaccharidosis I dog. J Biol Chem 267: 6570-5.

Suzuki K (1965) The pattern of mammalian brain gangliosides-II. Evaluation of the extraction procedures, post-mortem changes and the effect of formalin preservation. J Neurochem 12: 629-638.

Taylor RM, Wolfe JH (1997) Decreased lysosomal storage in the adult MPS VII mouse brain in the vicinity of grafts of retroviral vector-corrected fibroblasts secreting high levels of beta-glucuronidase. Nat Med 3: 771-4.

Torzilli PA, Arduino JM, Gregory JD, Bansal M (1997) Effect of proteoglycan removal on solute mobility in articular cartilage. J Biomech 30: 895-902.

Vogler C, Levy B, Galvin NJ, Thorpe C, Sands MS, Barker JE, Baty J, Birkenmeier EH, Sly WS (1999) Enzyme replacement in murine mucopolysaccharidosis type VII: neuronal and glial response to beta-glucuronidase requires early initiation of enzyme replacement therapy. Pediatr Res 45: 838-44.

Vogler C, Sands MS, Levy B, Galvin N, Birkenmeier EH, Sly WS (1996) Enzyme replacement with recombinant beta-glucuronidase in murine mucopolysaccharidosis type VII: impact of therapy during the first six weeks of life on subsequent lysosomal storage, growth, and survival. Pediatr Res 39: 1050-4.

Von Figura K., Hasilik A (1986) Lysosomal enzymes and their receptors. Ann Rev Biochem 55: 167-93.

Walkley SU (1995) Pyramidal neurons with ectopic dendrites in storage diseases exhibit increased GM2 ganglioside immunoreactivity. Neuroscience 68: 1027-1035.

Walkley SU, Haskins ME, Shull RM (1988) Alterations in neuron morphology in mucopolysaccharidosis type I: a Golgi study. Acta Neuropathol 75: 611-620.

Watts WE, Gibbs DA (1986) Lysosomal storage diseases: biochemical and clinical aspects. Taylar and Francis, London pubs 1986.

Whitley, B, Ridnour, MD, Draper, KA, Dutton, CM, Neglia, JP (1989) Diagnostic test for mucopolysaccharidosis I. Direct method for quantifying excessive urinary glycosaminoglycan excretion. Clin Chem 35: 374-379.

Wood SA, Allen ND, Rossant J, Auerbach A, Nagy A (1993) Non-injection methods for the production of embryonic stem cell-embryo chimeras. Nature 365: 87-89.

Wraith JE (2001) Enzyme replacement therapy in mucopolysaccharidosis type I: progress and emerging difficulties. J Inherit Metab Dis 24: 245-50.

Wurst W, Joyner A (1993) Production of targeted embryonic stem cell clones. In Gene Targeting: A Practical Approach. (Ed. A. Joyner), 33-62. IRL Press at Oxford University Press

Xin HB, Deng KY, Rishniw M, Ji G, Kotlikoff MI (2002) Smooth muscle expression of Cre recombinase and eGFP in transgenic mice. Physiol Genomics 10: 211-5.

Zinyk DL, Mercer EH, Harris E, Anderson DJ, Joyner AL (1998) Fate mapping of the mouse midbrain-hindbrain constriction using a site-specific recombination system. Curr Biol 8: 665-8.